FINNISH METEOROLOGICAL INSTITUTE
CONTRIBUTIONS

No. 50

IN SITU OBSERVATIONS OF THE ATMOSPHERES OF TERRESTRIAL PLANETARY BODIES

Ari-Matti Harri

Dissertation for the degree of Doctor of Science in Technology to be presented with due permission of the Department of Electrical and Communications Engineering, Helsinki University of Technology (Espoo, Finland) for public examination and debate in Auditorium S1 at Helsinki University of Technology on the 6th of September, 2005, at 12 o'clock noon.

Finnish Meteorological Institute
Helsinki, 2005

ISBN 951-697-614-X (paperback)
ISBN 951-22-7799-9 (pdf)
ISSN 0782-6117

Yliopistopaino
Helsinki, 2005

Preface

The work presented in this dissertation was performed in the frame of planetary exploration activities of the Space Research Division of the Finnish Meteorological Institute. I would like to express my gratitude to the Director General of the Finnish Meteorological Institute, Prof. Petteri Taalas, and the former Director General Prof. Erkki Jatila, for providing the operational support of an efficient scientific research institute. I am indebted to the head of the Space Research Division, Prof. Tuija Pulkkinen as well as for the former heads of the Division, Prof. Risto Pellinen and Prof. Christian Sucksdorff, for their support and for providing the working infrastructure and the possibility to get involved in the enchanting and challenging environment of international planetary missions.

I have been working on planetary exploration since 1988. Most of that time my focus has been on Mars and Titan, as well as somewhat also on the Venusian atmosphere. At the beginning I had the idea of focusing this thesis on our investigations of the Martian atmosphere and on the Mars-96 Mission. However, the interesting and challenging responsibilities of the Mars-96 mission took all my mental energy, and even more, and the thesis writing never materialized. After I recovered from the shocking failure of Mars-96, I reawakened the idea of writing the thesis based on the investigations of Mars-96 and the NetLander mission that had just recently started. Since 2001 I have gradually gathered together data packages of our scientific instrument projects and missions to construct the pieces that are included in this dissertation. And I have found that worth doing, even if this has been a slow and tedious struggle. It was quite a challenge to weave together investigations that have taken place in the course of about 15 years. Naturally I have given more weight on the recent investigations. The older developments are included in this thesis to shed light on the lessons learned in the course of the various planetary missions and to provide a good contextual frame for the work.

The supervisor of this work, Prof. Turkka Tuomi at the Helsinki University of Technology, deserves my sincere thanks for his support during the lengthy final production phase of this Summary. The work in the physics laboratory student team of Professor Tuomi in 1983-1986 was essential in guiding my ambitions and career toward the world of scientific exploration.

I am grateful to Prof. Hannu Savijärvi at the Helsinki University, who has had a special role in guiding my thinking on the planetary atmospheres and on how to settle the controversies between the scientific requirements and the constraints set by the instrumentation and planetary mission technologies.

I am deeply indebted to the head of Space Research Division, Prof. Tuija Pulkkinen, who played an indispensable role during the final production phase of this dissertation. Her professional advices as well as demanding encouragement were really needed for this thesis work to come true.

During the years of 1994 - 1995 I had the opportunity to work as a consultant for the NASA Jet Propulsion Laboratory (NASA/JPL) for 10 months. This period was a major starting point of this thesis work. I am happy to express my gratitude to the JPL project managers Barbara Brown and Mark Herring for their invaluable support during my stay at JPL.

I want to give special thanks to Dr. David Crisp at the NASA/JPL for sharing his insights on various aspects of planetary exploration and atmospheric science in particular. David has been a key partner both in the atmospheric modeling activity and in the process of developing atmospheric sensor systems for various Martian missions and experiments.

Jouni Polkko has contributed in most significant fashion in the development of instrumentation for our planetary missions. I owe mighty thanks for his insight into Martian instrumentation and sensor system design skills that have enabled so many successful planetary missions, as well as for his sometimes weird sense of humor.

I would like to thank Dr Teemu Mäkinen for contributing significantly to the development of the Pressure Profile Instrument (PPI) for Titan. He was also a key person behind the first analysis of the PPI instrument data. And his devotion to scientific exploration serves as a good example to any planetary explorer. Teemu is also an excellent artist, and his artwork has visualized many planetary mission concepts. A few pieces of his artworks are also used in this Summary.

I wish to thank Asko Lehto for his invaluable contribution and strong dedication to the success of our sensor qualification program. He was the key person behind the development of the sensor test systems and performed most of the long-lasting and tedious test runs.

I would like to express my gratitude to Dr Gilbert Leppelmeier for taking care of a key role in the development process of the flight units for the PPI instrument and for giving cogent advice during the writing process of this thesis. Gilbert also gave valuable comments on the English language of this Summary.

I am grateful to my colleague Dr Tero Siili for the various useful discussions on atmospheric science issues and our planetary missions, as well as on atmospheric observations and modeling tools.

I have had the privilege to collaborate closely with Dr Slava Linkin since 1988, when he was in charge of developing the Small Stations for the Mars-96 mission. Slava with his devotion to science and inspiring personality was one of the leading characters for me to follow in the beginning of my career in the field of planetary exploration.

I am thankful to Dr Bo Fagerström and Dr Timo Siikonen at the Technical University of Helsinki for their indispensable contribution to the aerodynamical calculations during the PPI/HASI instrument development work. I enjoyed their inspiring company and profound dedication to science.

I wish to express my gratitude for the long and highly fruitful collaboration with Hannu Jauhiainen in the Vaisala Inc., Dr Seppo Korpela in the Space Systems Finland Ltd., and Taisto Tuominen in the Patria Space Systems ltd. on the field of developing scientific instruments for space.

I want to thank Professor Hannu Koskinen for his various professional and highly valuable comments on this Summary.

When writing this Summary I was supported by helpful advice from Dr Risto Pirjola, who deserves my sincere thanks. He was also a key person participating in our Mars-96 activity.

I owe special thanks to Prof. James E. Tillman from Washington University for supporting our instrument development projects in a highly beneficial fashion. Jim has participated in our projects to the extent that we consider him being another leg of the FMI team in Seattle.

Many other colleagues of mine have helped me greatly during this thesis process. I owe mighty thanks to Sini Merikallio, who provided invaluable help and guidance with atmospheric modeling tools. Discussions with her were always useful in addition to being fun and relaxing. I am grateful to Petri Makkonen for effective collaboration in the development of the Netlander and MetNet missions, Henrik Kahanpää for his indispensable work on sorting out the calibration coefficients of the PPI readings and Maria Genzer for her system engineering skills and firmness in enforcing the high level design quality standards that are necessarily behind any successful planetary projects. I am thankful to Dr Johanna Tamminen for useful hints on utilizing the LaTex tools and helpful comments on Summary of this thesis, as well as for giving an encouraging example of how too long undone thesis work can eventually be completed. Hanna Lappalainen deserves my sincere thanks for her effective collaboration during the stressful and busy development work of our planetary missions. I am indebted to Lasse Häkkinen and Pasi Soljala for providing highly important support in solving the trouble caused by computers. Also, I would like to thank Dr Antti Pulkkinen, with whom we were mentally beating each other to struggle more and more in weight lifting exercises. Heavy physical training helped me indispensably in keeping the body and mind in balance, especially during the hectic development phases of the NetLander and MetNet missions in 1999-2002.

I wish to thank all the associates and colleagues in the industrial and university teams I have had the pleasure to work with. Thank you for the exciting and enjoyable collaboration in the field of space exploration.

And I would like to thank all my colleagues at the Finnish Meteorological Institute for the numerous helpful discussions as well as for the nice and comfortable working environment.

Finally, I want to give warm hugs to my wife Eeva and my children Annika and Mikael for tolerating me even during the late phases of the writing process, when I was even more absent-minded than I normally am.

Contextual frame and contents

Direct observations of planetary atmospheres are scarce and significantly more data are needed for the understanding of their behavior. The principal theme of this dissertation is the exploration of planetary atmospheres by means of in situ observations, focusing on investigations performed by payloads operating on the planetary surface. The contextual frame includes the whole palette of planetary exploration including definition of scientific objectives, observational strategies, scientific payload and data analysis, as well as development of technological solutions and simulation models for planetary missions. This approach also led to the initiation of the planetary missions MetNet and NetLander to Mars.

This work contributes to both in situ atmospheric observations and atmospheric modeling, which are strongly intertwined. Modeling efforts require observations to give solid background and foundation for the simulations, and on the other hand, definition of observational strategies and instrumentation gets guidance from modeling efforts to optimize the use of mission resources.

The dissertation consists of Summary and nine original scientific publications. Publications 1 to 7 address the development of new atmospheric science payloads for exploration missions to Mars and Titan, a Saturnian moon. Actual and planned missions included are the Mars-96 Program and its Small Surface Stations and Penetrators during the years 1988-1996, PPI/HASI onboard the Cassini/Huygens spacecraft to Saturn and its moon Titan in 1989-2005, the MET-P payload onboard the Mars Polar Lander in 1997-1999, the BAROBIT instrument for the Beagle 2 lander in 2001-2003, the NetLander Mars Mission in 1997-2001 and the ongoing Mars MetNet Mission, started in 2000. Specifically, Publication 4 reviews the sensor qualification process that facilitated the use of new type of atmospheric sensors at Mars, while Publications 2 and 7, as well as Summary, address the highly successful determination of the Titan atmospheric pressure profile. Publication 8 combines in situ observations and simulations by analyzing Mars Pathfinder measurements with the help of a Martian mesoscale atmospheric model. Finally, in Publication 9 the effect of airborne dust and CO2 on the radiative transfer in the Martian atmosphere is assessed and a new radiative transfer paramerization scheme for the mesoscale model is introduced. Summary gives an overview of the work, provides background information and draws conclusions.

This work has been going on for quite some time. The wide range of planetary projects and missions gives an excellent internal view to the inside of scientific planetary exploration and enables to draw conclusions of profound nature. During the few quiescent periods of time of the hectic project work the scientifically interesting topics of the work were documented in the form of scientific publications. Eventually, this Summary was written in the same fashion.

Helsinki, August 2005. Ari-Matti Harri

LIST OF PUBLICATIONS

The following original publications are part of this thesis.

1. Harri, A.-M., O. Marsal, G.W. Leppelmeier, P. Lognonne, K.-H. Glassmeier, F. Angrilli, W.B.Banerdt, J.P. Barriot, J.-L. Bertaux, J.J. Berthelier, S. Calcutt, J.C. Cerisier, D. Crisp, V. Déhant, S. Di Pippo, D. Giardini, D. Guerrier, R. Jaumann, K. Kumpulainen, Y. Langevin, S. Larsen, M. Menvielle, G. Musmann, J. Polkko, J.P. Pommereau, J. Runavot, W. Schumacher, T. Siili, J. Simola and J. E. Tillman, Network Science Landers for Mars, *Adv. Space Res.*, Vol. 23, No. 11, pp. 1915-24, 1999.

2. Harri, A.-M., B. Fagerstrom, A. Lehto, G.W. Leppelmeier, T. Mäkinen, R. Pirjola, T. Siikonen and T. Siili, Scientific objectives and implementation of the pressure profile instrument (PPI/HASI) for the Huygens spacecraft, *Planet. Space Sci.*, Vol. 46, No. 9/10, pp. 1383-1392, 1998.

3. Harri, A.-M., V. Linkin, J. Polkko, M. Marov, J.-P. Pommereau, A. Lipatov, T. Siili, K. Manuilov, V. Lebedev, A. Lehto, R. Pellinen, R. Pirjola, T. Carpentier, C. Malique, V. Makarov, L. Khloustova, L. Esposito, J. Maki, G. Lawrence, V. Lystsev, Meteorological Observations on Martian Surface: Met-packages of Mars-96 Small Stations and Penetrators, *Planet. Space Sci.*, Vol 46, No. 6/7, pp 779-793, 1998.

4. Harri, A.-M., T. Siili, R. Pirjola, R. Pellinen, Aspects of atmospheric science and instrumentation for Martian missions, *Adv. Space Res.* Vol. 16, No. 6, pp. (6)15-(6)22, 1995.

5. Polkko, J., A.-M. Harri, T. Siili, F. Angrilli, S. Calcutt, D. Crisp, S. Larsen, J.-P. Pommereau, P. Stoppato, A. Lehto, C. Malique and J. E. Tillman. The NetLander Atmospheric Instrument System (ATMIS): description and performance assessment, *Planet. and Space Sci.*, Vol. 48, pp. 1407-1420, 2000.

6. Linkin, V., A.-M. Harri, A. Lipatov, K. Belostotskaja, B.Derbunovich, A. Ekonomov, L. Khloustova, R. Kremnev, V. Makarov, B. Martinov, D.Nenarokov, M. Prostov, A.Pustovalov, G. Shustko, I. Järvinen, H. Kivilinna, S. Korpela, K. Kumpulainen, A. Lehto, R. Pellinen, R. Pirjola, P. Riihelä, A. Salminen, W. Schmidt, T. Siili, J. Blamont, T. Carpentier, A. Debus, C.T. Hua, J.-F. Karczewski, H. Laplace, P. Levacher, Ph. Lognonné, C. Malique, M. Menvielle, G. Mouli, J.-P. Pommereau, K.

Quotb, J. Runavot, D. Vienne, F. Grunthaner, F. Kuhnke, G. Musmann, R. Rieder, H. Wänke, T. Economou, M. Herring, A. Lane, C.P. McKay, A sophisticated lander for scientific exploration of Mars: Scientific Objectives and Implementation of the Mars-96 Small Station, *Planet. Space Sci.*, Vol 46, No. 6/7, pp 717-737, 1998.

7. Mäkinen, T., P. Salminen, A. Lehto, G. Leppelmeier and A.-M. Harri, PPI results from the balloon drop experiment of the HASI pressure profile instrument, *Planet. Space Sci.*, Vol. 46, No. 9/10, pp. 1237-1243, 1998.

8. Savijärvi, H., A. Määttänen, J. Kauhanen, A.-M. Harri. Mars Pathfinder: New data and new model simulations, *Quart. J. Roy. Meteor. Soc.*, Vol. 130, pp 669-683. 2004.

9. Savijärvi, H., D. Crisp and A.-M. Harri. Effects of CO_2 and dust on present-day solar radiation and climate in Mars. (Accepted for publication in *Quart. J. Roy. Meteor. Soc*).

Summary of publications and author's contribution

The work presented in the publications accompanying the Summary has been performed as teamwork. The author's role in producing these papers is driven by his lead position in the planetary projects and missions giving the framework for the original publications of this thesis. The author was the Primary Investigator of the atmospheric science experiment of the NetLander Mars Mission (ATMIS/NetLander), Co-Investigator for the Mars-96 Small Sations, Co-Investigator for the Meteorology package of the Mars polar Lander's payload (MET/MVACS), Co-Investigator for the atmospheric structure instrument of the Huygens probe for Saturn's moon Titan (HASI/Huygens/Cassini), Co-Investigator for the BAROBIT pressure observation device for the Beagle 2 (surface lander of the Mars Express mission) and the lead scientist of the Mars MetNet Mission. The author had a key role in the start-up phases of the above-mentioned projects and missions. He also initiated the MetNet Mars mission and was one of the two initiators of the NetLander mission. These facts are reflected in the contributions described below.

Paper 1 is a basic review paper on the NetLander Mars mission, a network of four geophysical observation stations to be operated simultaneously on the Martian surface for more than one Martian year. The author was one of the initiators of the mission and the leader of the international team during 1997-1998, when the mission was specified. The author has written the paper and his contribution encompassed specification of the overall mission payload with the mission's lead science team and definition of the payload for ATMIS, which is the atmospheric science experiment onboard the NetLander stations.

Paper 2 is a review paper on the Pressure Profile Instrument (PPI /HASI) for the Cassini/Huygens mission to Saturn's moon Titan. The PPI scientific objectives and instrumental implementation are described. The author has written the paper and has defined the observation modes together with the instrument science team. As the manager of the PPI instrument the author has specified the sensor configuration and settled the controversies between scientific requirements and technical constraints with the eventual instrument design as described in this paper. Being one of the Co-Investigators of the HASI experiment the author had a key role also in the review publication (Space Science Reviews) of HASI -experiment by *Fulchignoni et al.* (2002). The author had a similar co-authorship in the *Nature* -journal by *Fulchignoni et al.* (2005) describing the first results of the highly successful HASI / Huygens experiment.

Due to technical reasons these two publications are not part of this thesis.

Paper 3 reviews the meteorological instruments onboard the Mars-96 Mission's Small Stations (two) and Penetrators (two). The scientific objectives and technical implementations of the meteorological sensor packages are described. The author has written the paper and participated in the definition of the scientific objectives as a member of the science team. As the manager of the FMI Mars-96 team the author has specified the sensor configuration and supervised the technical solutions described in the paper.

Paper 4 discusses the basic requirements posed by the Martian atmosphere to instrumentation when performing *in situ* atmospheric science observations. Also the rationale behind Martian exploration is addressed. The author has written the paper. During a period of several years the author developed and controlled the space qualification program for the Barocap®, Humicap® and Thermocap® sensors of the Vaisala Inc., as well as extended the qualification and acceptance test procedures for the missions on the surface of Mars and Titan. Some results of that qualification program are presented and discussed.

Paper 5 describes the scientific objectives and technical implementation of the ATMIS instrument (ATmospheric science and Meteorology Instrument System) being part of the payload of the NetLander Mars Mission. The author has written most of the scientific objectives and background part of the paper and has supervised the instrument development work.

Paper 6 is a review paper on the Mars-96 Mission's two Small Stations with versatile geophysical payloads to be operated simultaneously on the Martian surface for more than one Martian year. The author has written most of the paper. The author's contribution included participation in specification of the overall mission payload with the mission's lead science team, leading the development work of the command and data management system of the Small Station, and participation in the definition of the atmospheric science payload.

Paper 7 describes the balloon testing of the PPI instrument together with the main HASI -instrument. Test results indicated that the PPI would be functioning as expected. The author's contribution was to participate in the test specification and arrangements and to provide the PPI-prototype for the balloon testing. The PPI passed the ultimate test successfully, when it provided observations of excellent quality from Titan's atmosphere in January 14, 2005.

Paper 8 describes new modeling results and their comparison with the surface observations of the Mars Pathfinder spacecraft. The author contributed to the definition of the modeling scheme and especially to the short wavelength radiation scheme development. Paper predicts some boundary layer features to be addressed by the forthcoming Mars missions.

Paper 9 addresses the short wave radiative transfer in the Martian atmosphere and focuses on the important but still insufficiently known effect of airborne dust. The author initiated the process of comparing radiation schemes of several Mars circulation models (including our own model) against results given by JPL's reference line-by-line radiative transfer model, and contributed to the development of the comparison software and the analysis of results. Paper presents model improvements and studies the present cooling effect of Martian airborne dust using delta-two-stream methods.

Contents

Chapter 1

Introduction

1.1 Explorational framework

The *in situ* exploration of the atmospheres of Mars, Venus and Titan, the moon of Saturn, is discussed in this work. The common thread connecting these four members of our solar system is the fact that they all can be considered terrestrial bodies, which have atmospheres having similarities with the atmosphere of the Earth (*Salby*, 1996; *Houghton*, 2002).

In general, planetary exploration is performed by ground-based observations from the surface of the Earth, by sending automatic research probes into the space and into the vicinity of the planetary body under investigation, and eventually by sending probes onto the planetary body and into its atmosphere. *In situ* exploration involves observations performed physically at the very point of investigation, whereas remote observation means performing studies from the outside of the planetary system. Practically *in situ* exploration can be performed by vehicles landing onto a planetary surface, atmospheric balloons, by aircraft and rockets flying in the planetary atmosphere, and also by devices capable of penetrating into the planetary soil. This work focuses on *in situ* observations performed by vehicles landing on the planetary surface.

The evolution of our solar system has resulted in the current situation, where the smaller planets Mercury, Venus, the Earth and Mars having a solid and distinct surface-to-atmosphere interface are closest to the Sun. Further away from the Sun are located the gas giants Jupiter, Saturn, Uranus and Neptune as well as Pluto. Planetary atmospheres seem to have evolved after the solar system was formed. Indications of the evolution of planetary atmospheres have been detected by studying the atmospheres themselves and the surfaces of the planets, where the ancient climate has carved its fingerprints. Thus, planetary atmospheric research opens up new possibilities to enhance our understanding of the atmospheric evolution and climate change of the Earth.

Various solar system bodies are often classified as terrestrial, *e.g.* Mercury, Venus, Mars, the Earth, Pluto, Titan and some other moons of the gas giants like Jupiter's moon Io. This thesis specifically addresses Mars, Venus, Titan and the Earth, because they possess distinct and prevailing atmospheres. From

the atmospheres point of view these four members of our solar system bear close resemblance to each other. They all carry atmospheres sufficiently thick to generate Earth-like atmospheric motions, climate and weather phenomena. Specifically, the Martian atmosphere has similar type of dynamical motions as the Earth due to the fact that the axial tilts and axial rotation periods of these two planets are quite similar. The atmospheres of Titan and the Earth have approximately the same thickness, and both atmospheres are composed mostly of nitrogen. Finally Venus, having a much thicker atmosphere than the Earth, is interesting due to its location in the solar system next to the Earth, and due to the fact that its atmosphere seems to have gone through a runaway greenhouse process. All of these facts enhance the scientific interests of these solar system bodies, and make them highly rewarding targets for planetary exploration.

Planetary atmospheres are vast entities that, understandably, cannot be subjected to controlled experiments, but only observed. The exploration of planetary atmospheres by *in situ* observations is one of the major tools in the pursuit of enhancing our knowledge of the planets. In the atmosphere, this includes *e.g.* observations made by means of aircraft, rocket, radiosonde, balloon floating in the atmosphere, or observation posts that are able to move or are stationed in fixed locations. These in situ observation methods are in use at the Earth.

In the investigations of planetary atmospheres, vehicles landing on the surface of Mars (*Chamberlain et al.*, 1976; *Hess et al.*, 1977; *Soffen*, 1976; *Golombek et al.*, 1999; *Schofield et al.*, 1997; *Squyres*, 2001; *Christensen et al.*, 2005), and slowly descending ballooning experiments in the Venus atmosphere have been used (*Hunten et al.*, 1983; *Koukouli et al.*, 2005). Measurements at the planetary surface are also needed to support the orbital observations for providing the ground truth. Eventually, the data acquired by surface and orbital observations need to be amalgamated to provide the maximal return of the mission.

Observing atmospheric behavior reveals phenomena that may be studied by incorporating into a model the significant physical and chemical processes. Modeling is an indispensable tool to accompany physical observations by providing means to extend the validity range of the observations. On the other hand, the physical observations provide a solid foundation for the models. Modeling is an activity that can be started with very little amount of actual physical observations, and additional observations and improved models working together and supporting each other enhance gradually our understanding. This has been the case initially for the investigations of the atmosphere of the Earth, and during recent decades for exploration of other planetary atmospheres in the solar system.

The rationale behind planetary exploration is primarily scientific curiosity, but making discoveries on planetary science is also always tightly connected to technology development and international collaboration. Eventually, the long-term dream shared by a good number of politicians, and also by various scientists, of performing manned flights to faraway planetary bodies, is also paving the way for planetary exploration. These are highly important factors helping the scientists to gather the required resources to implement ambitious planetary missions. A key issue is also comparative planetology, which aims at enhancing our understanding on the Earth through studying other terrestrial objects.

1.2 Scope of this thesis

The principal theme of this work is the exploration of planetary atmospheres by means of *in situ* missions focusing on investigations performed by payloads operating on the planetary surface. The contextual frame includes the whole palette of planetary exploration including definition of scientific objectives, observational strategies, scientific payload and data analysis, as well as development of technology and simulation models for planetary missions.

This work deals with various planetary missions; the Mars-96 Mission and its Small Stations during the years 1988-1996, PPI/HASI onboard the Cassini/ Huygens spacecraft for Saturn and its moon Titan in 1989-2005, the MVACS payload onboard the Mars Polar Lander in 1997-1999, the BAROBIT instrument for the Beagle 2 lander in 2001-2003, the NetLander Mars Mission in 1997-2001 and the ongoing (started in 2000) Mars MetNet Mission.

Atmospheric modeling and actual physical observations are strongly intertwined. Modeling efforts require observations to give solid background and foundation for the simulations, and on the other hand, the definition of observational strategies and instrumentation needs guidance from modeling to optimize the use of mission resources. A leading theme in this work is the development of atmospheric instrumentation and modeling tools, and the utilization of these tools in the pursuit of planetary atmospheric research.

Introductory background information on the terrestrial planetary bodies and their atmospheres is given in Summary chapters 1 and 2. The physics and essential features of planetary atmospheres, with emphasis on the atmospheric boundary layer are addressed in chapter 3. The various planetary missions and instrumentation serving as a core piece of substance to this work are described in chapter 4. Atmospheric modeling efforts and development of radiative parameterization schemes are presented in chapter 5, which also underlines the symbiotic nature of the link between atmospheric *in situ* observations and modeling. Finally, chapter 6 gathers together the principal conclusions drawn by this work, as well as discusses the future implications and prospects.

Chapter 2

Atmospheres of Mars, Venus, Titan and the Earth

2.1 Facts and similarities

Terrestrial bodies Mars, Venus, Titan and the Earth are shrouded by atmospheres, which are indispensable sections of the planetary system. The atmosphere moderates the thermal structure of the planetary surface, it provides means to transport material and energy between different regions of the planetary surface, and it is also a weathering tool for various processes that modify the surface. The atmosphere of the Earth supports and protects abundant forms of life, and in a similar fashion another planetary atmosphere may also nurture and harbor some kind of life on other planetary bodies.

Mars, Venus and the Earth are often called sister planets for being similar in size, mass, density and volume. Photos indicating the relative sizes of these planetary bodies are depicted in Figure 2.1. All of them have formed at about the same time and have condensed out of the same nebula. However, during the

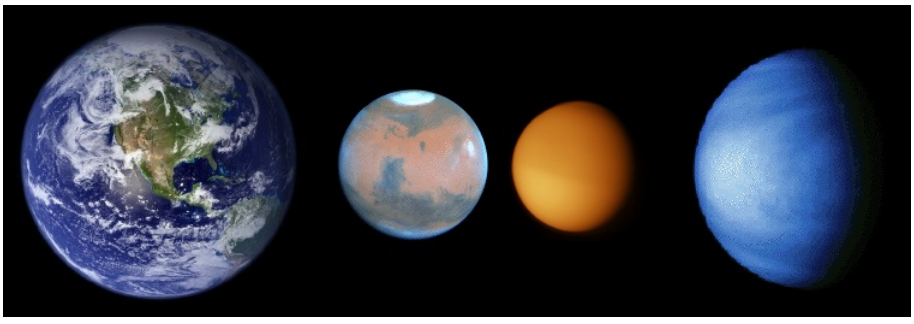

Figure 2.1: Photos of the Earth, Mars, Titan and Venus (from left to right) shown in a composite image illustrating the relative sizes of these planetary bodies.

Parameter	Mars	Mars/ Earth	Titan	Titan/ Earth	Venus	Venus/ Earth	Earth
Mean radius (km)	3390	0.53	2575	0.40	6052	0.95	6371
Density (g/cm^3)	3.93	0.71	1.88	0.34	5.24	0.95	5.515
Mass ($kg/10^24$)	0.642	0.11	0.13	0.02	4.87	0.82	5.97
Eq. surf. gravity (m/s^2)	3.7	0.38	1.35	0.14	8.87	0.91	9.78
Mean surf. pre. (bar)	0.063	0.06	1.5	1.36	92	84	1.0
Mean surf. temp. (K)	214	0.74	94	0.33	740	2.57	288
Atm. CO2 (%)	95.3	-	-	-	96.5	-	0.03
Atm. N2 (%)	2.7	-	94.7	-	3.5	-	78.1
Atm. O2 (%)	0.13	-	5.3	-	-	-	20.9

Table 2.1: Principal planetary parameters of Mars, Titan, Venus and the Earth. Adjacent to each column there is another column with the planetary body parameter value divided by the respective value of the Earth (*Lodders and Fegley*, 1998; *Kieffer*, 1992; *Hunten et al.*, 1983).

solar system formation Mars, Venus, Titan and the Earth were given remarkably different circumstances for their atmospheres to evolve. The principal planetary parameters of Mars, Titan, Venus and the Earth are depicted in Table 2.1.

Venus is located close to the Sun and its atmosphere consists mainly of carbon dioxide. Characteristic features include high surface pressure and temperature (Table 2.1). The main reason behind the high surface temperature is the runaway greenhouse effect caused by the thick atmosphere (*Chassefiere et al.*, 2002).

Mars has approximately the same obliquity of ecliptic to celestial equator as the Earth and the planets rotate around their main axis with similar rates (Table 2.2). This results in the same type of atmospheric dynamics for these planets. This similarity is so strong that the atmospheric simulation models made for Mars utilize the dynamic cores of the models built for the Earth.

These similarities in the atmospheric behavior of Mars and the Earth make Mars an extremely interesting planet from the comparative planetology point of view. Because the Martian atmosphere is practically devoid of water and Mars lacks oceans and vegetation the atmospheric behavior of Mars is less complicated than that of the Earth. Mars can be regarded as being a simplified version of the terrestrial atmosphere with similar dynamics. Accordingly, by investigating the Martian atmosphere we will learn something new from the behavior of our own planet.

Because of being closer to the Sun than the Earth, Venus gets more solar radiation than the Earth. The structure of the Venusian atmosphere, composed largely of CO_2 being a powerful infrared absorber, and having a surface pressure higher than 90 bar, has resulted in a runaway greenhouse effect and hence in an extremely high surface temperature (Table 2.1) of about 740 K. Liquid water is understandably nonexistent on Venus, but the atmosphere contains small amounts of water vapor. The processes leading to the strong greenhouse effect are highly interesting when contemplating the future atmospheric evolution

Parameter	Mars	Titan	Venus	Earth
Obliquity (deg)	25.2	-	177.4	23.5
Sidereal rotation period	24.6 h	16 d	243 d	23.9
Sidereal revolution period	687 d	29.5 yrs	225 d	365.3
Mean solar constant (w/m^2)	589	15	2614	1370
Orbital eccentricity	0.093	-	0.007	0.017

Table 2.2: Planetary parameters affecting significantly to atmospheric conditions on Mars, Titan, Venus and the Earth (*Lodders and Fegley*, 1998).

(*Savijärvi*, 1994) in general, and in particular at the Earth.

When Mars and Venus are considered being sister planets to the Earth, Titan, Saturn's largest moon, is another type of world with a surface pressure of approximately 1.5 bar and surface temperature of about 90 K. Titan is about 10 times further away from the Sun than the Earth thus getting only 1% of the solar irradiation the Earth gets. Titan's atmosphere consists mostly of nitrogen with also methane and various other substances, *e.g.*, Argon, H_2, CO (*Lodders and Fegley*, 1998). Among the planetary bodies only Titan and the Earth have nitrogen-rich atmospheres. This is one the reasons making Titan so interesting. The Titan atmosphere may actually have similar conditions prevailing at Earth before oxygen emerged in the atmosphere.

The early history of Mars and its atmosphere holds an intriguing question, whether the ancient Mars was significantly different from the contemporary Mars. The Martian atmosphere may have evolved to its current state from an initial or intermediate state of atmospheric conditions resembling the conditions prevailing currently on the Earth. Investigations on the evolution of Mars may provide clues also to the understanding of the climate change on the Earth. Analysis and simulations of the atmosphere of the early Mars and Martian climate have been performed by, *e.g.* *Haberle et al.* (1994); *Haberle* (1998); *Kasting* (2002).

Unlike the Earth, Venus, Mars and Titan possess no obvious significant intrinsic magnetic field. Their atmospheres, and ionospheres in particular, interact directly with the solar wind and the surrounding plasma environment enabling the occurrence of various atmospheric erosion processes (*Ledvina et al.*, 2004).

Exploration of the structure, dynamics and evolution of planetary atmospheres is a significant discipline of comparative planetology. Through investigations of various atmospheres we will learn more of the basic underlining principles behind the general behavior of planetary atmospheres. Moreover, we are also likely to learn important lessons on the atmosphere of our own planet, the Earth.

2.2 Mars

The composition of the CO_2-rich Martian atmosphere in its current form (Table 2.1) was established by Viking Lander observations (*Hess et al.*, 1977; *Chamberlain et al.*, 1976; *Hess et al.*, 1972). The average surface pressure at Mars is

approximately 7 hPa. The seasonal pressure variation is about 30%, because the atmospheric carbon dioxide condenses on the polar caps during winter and sublimes back to the atmosphere during summer, as indicated by, *e.g. Sutton et al.* (1978); *Hess et al.* (1979); *Tillman et al.* (1993). The Martian atmosphere is sufficiently thick for forming strong winds beyond 20 m/s (*Murphy et al.*, 1990; *Tillman et al.*, 1994). Also, in some occasions large amount of dust is lifted into the atmosphere to create planet-wide dust storms obscuring the surface from space for the period of a few months (*Tillman et al.*, 1979; *Tillman*, 1988).

Due to similar declination angles and rotation rates the global atmospheric circulation patterns of Mars and the Earth resemble each other, as shown by, *e.g. Santee and Crisp* (1995). A see-breeze type of mesoscale circulation cell occurs over the edge of the Martian polar caps (*Siili et al.*, 1997). The principal contributors to the Martian global atmospheric circulation that have been identified are (*Zurek et al.*, 1992): a Hadley cell between the summer hemisphere tropics to the winter hemisphere subtropics, baroclinic eddies in the winter hemisphere, stationary eddies induced by topographical and other surface variations (*Siili*, 1996), condensation/sublimation flow between the CO_2 polar caps, thermal tides, and other normal mode oscillations as shown by, *e.g. Tillman* (1985).

The Martian atmosphere is thin, and hence it allows a substantial fraction of the incoming solar radiation to reach the surface. The fraction absorbed by the atmosphere is of the order of 5 % to 20 %. This results in the situation, where the atmosphere close to surface is superadiabatic and strong convective mixing prevails (*Larsen et al.*, 2002). On the other hand, in the nighttime strong inversion prevails close to the surface due to the cooling of the surface by thermal radiation. In these conditions knowledge of optical parameters of the atmosphere, surface (*Bell et al.*, 1999), and dust loading as well as H_2O and CO_2 clouds (*Bell et al.*, 1996; *Colaprete et al.*, 2003) are important.

The thin Martian atmosphere creates a weak greenhouse effect raising the surface temperature by a few Kelvin. Hence, Martian average surface temperatures are well below the freezing point of water. The surface temperature varies between the CO_2 condensation temperature at the polar areas up to the summertime low-latitude temperatures up to about 300 K. The diurnal surface temperature variation is of the order of 70 K (*Kieffer*, 1992). Even if during summertime the daytime temperature at low latitudes often rises above freezing, the atmospheric pressure is so low that water exists only in solid or vapor phases. Martian surface pressure measured by Viking Landers is depicted in Figure 2.2 for a period of two Martian years.

Mars and the Earth have approximately the same obliquities and they rotate around their main axis with similar rates (Table 2.2) resulting in the same type of atmospheric dynamics for these planets. A significant cause of differences between the atmospheric boundary layers of Mars and the Earth are due to the fact that the Martian atmospheric surface pressure is only about 1 % of that of the Earth. When combined with the fact that the amount of water vapor is very low, the importance of the atmospheric heat flux in the surface energy budget is reduced. This increases the temperature variation of the surface forcing and the near-surface temperature gradient. Hence the diurnal temperature variation at

Mars is higher than is typically the case on the Earth (Figure 2.3). Furthermore, this results in a thicker daytime atmospheric boundary layer (ABL) than is observed on the Earth. The Martian ABL height may extend to 5 kilometers and beyond in the afternoon. In the nighttime the Martian ABL height is reduced to some hundreds of meters, even only to a few tens of meters (*Tillman et al.*, 1994).

The behavior of the surface layer turbulence and mean flow on Mars is found to obey similar scaling laws as on the Earth (*Tillman*, 1972; *Larsen et al.*, 2002). Utilizing approximations and parameterizations built for the atmosphere of the Earth, and finding them applicable also to the Martian atmosphere, is an essential step in comparing the atmospheric behavior of Mars and the Earth (*Larsen et al.*, 2002).

Small quantities of methane were detected in the Martian atmosphere in March 2004 (*Formisano et al.*, 2004). This finding, when confirmed, is highly significant, because the estimated amount of the detected methane would be destroyed by solar ultraviolet radiation within a few hundred years. Hence, assuming that the methane in the Martian atmosphere is not a transient phenomenon, there should be some process on Mars that is continually producing methane to the atmosphere. This can reasonably be accomplished either by volcanic and hy-

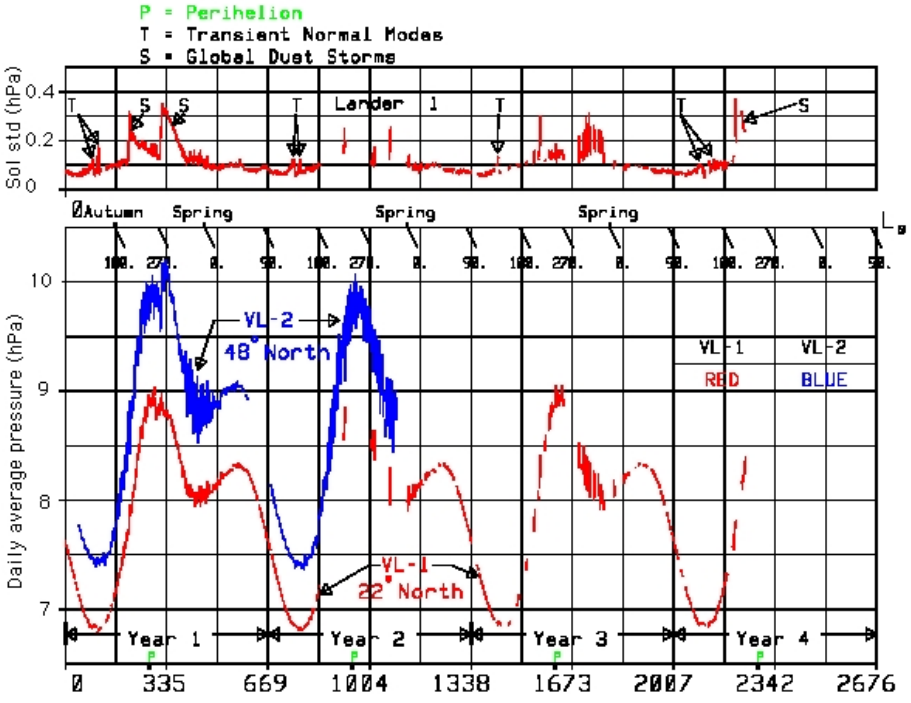

Figure 2.2: Martian surface pressure measured by Viking Landers during four Martian years (*Tillman*, 1994) on the lower panel as a function of sols counted from the landing of Viking Lander 1 (VL-1). The upper panel shows the standard deviation of daily pressure readings.

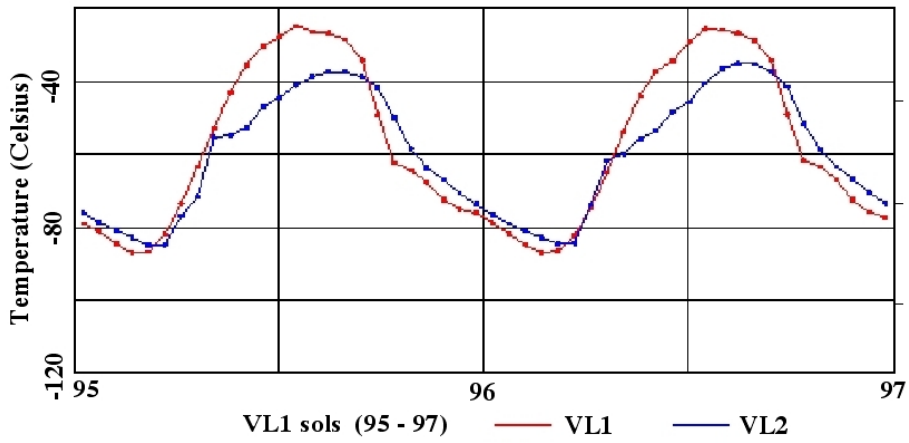

Figure 2.3: Diurnal variation of the Martian atmospheric temperature at an altitude of about 1 meter measured by the Viking Landers during two sols. The sol number represents Viking Lander 1 (VL 1) sols counted from the day VL 1 landed on the Martian surface.

drothermal activity, or subsurface microorganisms. Accordingly, a direct implication is that either Mars is still volcanically active or some biological processes are going on Mars at present. This brings up various cosmological issues on planetary evolution.

2.3 Venus

Venus has a thick atmosphere composed mainly of carbon dioxide with little amount of water vapor (Table 2.1). It is veiled by clouds composing of sulfuric acid droplets. The atmospheric pressure at the surface is about 90 times that of the Earth's at sea-level (*Lodders and Fegley*, 1998). A key Venusian feature is the extremely high surface temperature, about 700 K (Table 2.1). This is principally due to a runaway greenhouse effect caused by the thick and cloudy atmosphere of carbon dioxide, which effectively absorbs infrared radiation. At upper levels of the atmosphere the temperature is colder than that of the Earth. As depicted in Figure 2.4, the Venusian atmospheric temperature diminishes rapidly when the altitude increases. Interestingly, the amount of absorbed solar radiation at Venus is smaller than at the Earth due to the fact that about 80% of the incoming solar radiation is scattered away from the planet by the thick sulfuric acid clouds. This demonstrates the strength of the Venusian greenhouse effect (*Hunten et al.*, 1983).

Venus has a retrograde rotation, unlike the other terrestrial planets. The rotation of Venus is very slow, the Venusian day is 243 Earth days whereas it takes 225 Earth days for Venus to make one full orbit around the Sun (*Hunten et al.*, 1983).

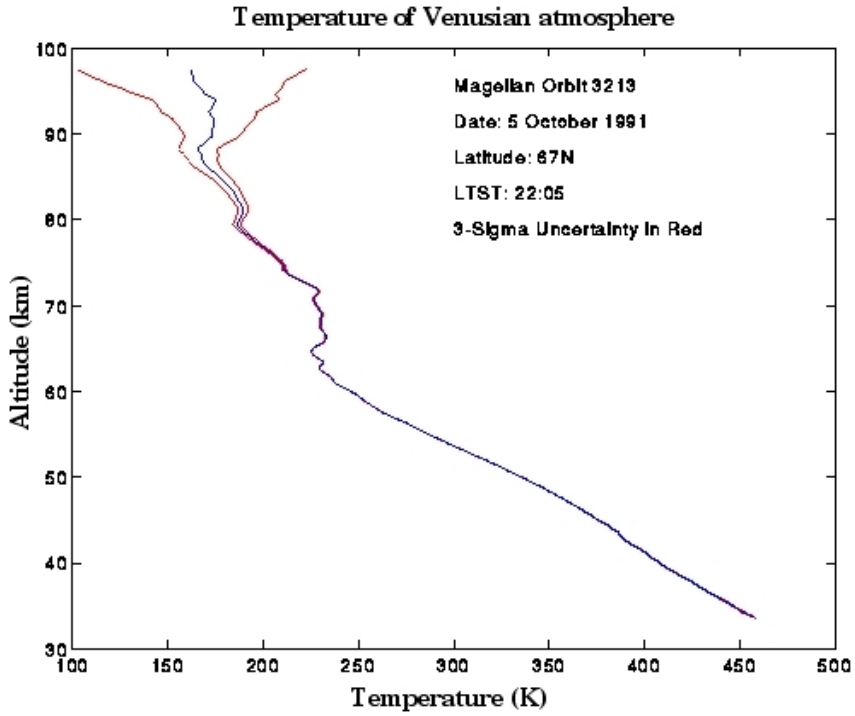

Figure 2.4: Temperature as a function of altitude of the Venusian atmosphere measured by the Magellan spacecraft that during 1990-1994 provided most extensive information of the Venusian surface and also atmosphere (*Jenkins*, 1998).

Due to the high pressure, the atmospheric mass of Venus is about 90 times more than at the Earth. 90% of the Earth's atmosphere is within 10 km of the surface, whereas at Venus this limit is at the altitude of 50 km. The clouds in the Venusian atmosphere extend from about 50 to 70 km and can be divided into three distinct layers. There is a layer of haze below the clouds down to about 30 km and from there down to the surface there are no more clouds or haze layers (*Jenkins*, 1998).

There is a high-speed prograde jet stream above the clouds blowing from the west to the east at the speed of about 300-400 km/h. It is fastest at the equator and slows down when moving toward the poles. At the surface the atmospheric conditions are calm and gentle with wind speeds typically less than 2 m/s (*Hunten et al.*, 1983).

The dense cloud cover of Venus has obscured the surface from remote investigations for a long time. The main cloud layer is about 25 km thick. However, the amount of sunlight penetrating through the clouds makes the daylight at the Venusian surface resemble a cloudy day on the Earth. The atmosphere gets replenished by large-scale volcanic eruptions including sulfur dioxide into the air. In addition to upper atmospheric chemical reactions the volcanic activity produces raw material for the sulfuric acid clouds.

The most successful exploration mission in revealing the Venusian surface was NASA's Magellan radar mapping mission in 1990-1994 (*Jenkins*, 1998). Earlier important missions exploring the Venusian atmosphere and surface were NASA's Pioneer Venus mission (1978), the Russian Venera 15 and 16 missions (1983-1984), which provided a good insight into the atmospheric composition (*Hunten et al.*, 1983). The next link in the chain of Venusian exploration will be ESA's Venus Express, which is to provide first new observations in early 2006 (*Svedhem et al.*, 2005).

The weather patterns of Venus are rather uneventful close to the surface, but highly active and interesting at the upper levels of the Venusian atmosphere. With practically devoid of water, the general atmospheric circulation on Venus (as on Mars) is considerably less complex than the circulation on the Earth. Venus also has a slow rotation rate, which effectively eliminates the Coriolis effect. These two principal factors result in the situation, where the Venusian atmosphere involves a nearly perfect Hadley cell extending from the equator to the poles in both hemispheres. The cause of the super-rotating jet streams is a major remaining mystery of the Venusian atmosphere.

2.4 Titan

Saturn's moon Titan is a sizeable planetary body with an equatorial radius of 2,575 kilometers (*Lodders and Fegley*, 1998). It is the second largest moon in our solar system and bigger than the planet Mercury. Titan is a unique in the sense that in addition to the Earth it is the only planetary body having an atmosphere composed largely of nitrogen. The main planetary and atmospheric facts of Titan are depicted in Tables 2.1 and 2.2. Titan is a cold world veiled by a thick, hazy atmosphere impenetrable by far-away telescopes and imaging devices. The surface pressure at Titan is approximately 1.5 bar and the temperature 90 K. Titan has a synchronous orbit around Saturn and it takes about 16 Earth days for Titan to perform one revolution around Saturn. Hence this is also the length of one Titan day (Table 2.1).

Titan is an especially interesting planetary body for being the only moon in our solar system having a thick atmosphere with clouds, and for being the only solar system body having an Earth-like nitrogen-rich atmosphere. The atmospheric structure of Titan is depicted in Figure 2.5.

The atmospheric structure and composition were for the first time observed by the Voyager radio occultation experiment (*Lindal*, 1983), and were determined accurately by the Cassini/Huygens mission (*Lebreton*, 2005). The temperature profile bulging toward lower temperatures up to 60 km altitude can effectively contain volatiles, *e.g.* methane, at the lower parts of the atmosphere. This results in the possibility of that methane would evaporate from surface to the atmosphere and precipitate (rain) back to the surface. A similar situation is with water on the Earth.

The atmosphere is estimated to be calm at low altitudes and the wind speed increases gradually with altitude up to about 60 km. Above that altitude winds turn much stronger and also significant vertical wind shear is expected to occur (*Bird*, 2005).

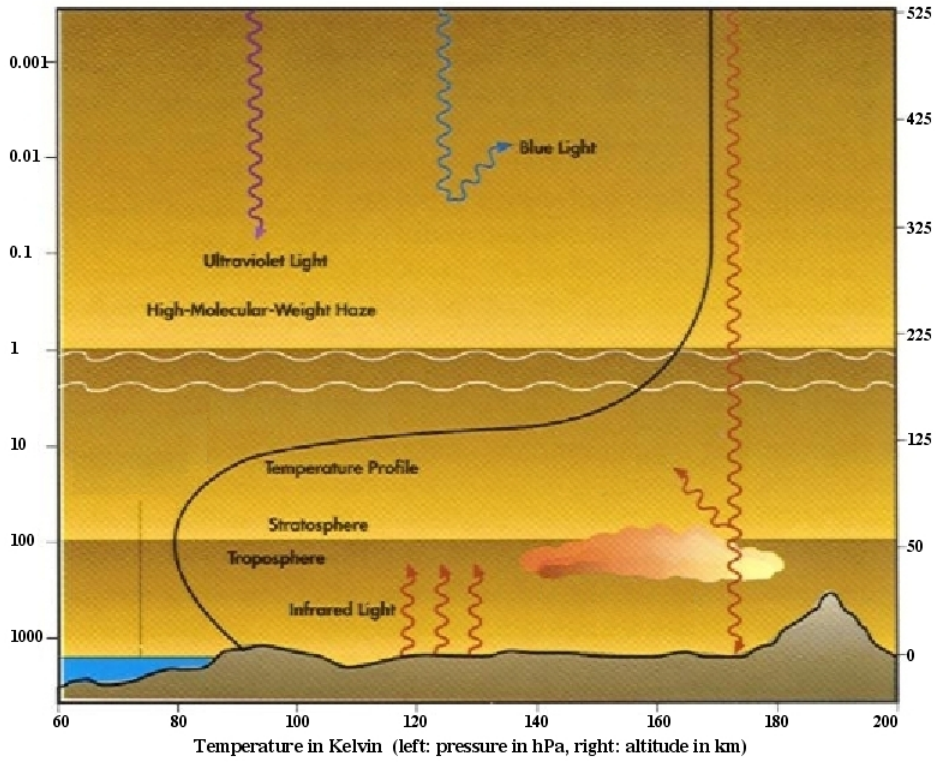

Figure 2.5: The Titan atmospheric sections as well as temperature and pressure profiles (in rough agreement with Huygens observations) with atmospheric constituents and artist's perception of the surface (artwork adapted from an unknown source). The left axis presents pressure in hectopascals (hPa), and the right is altitude in kilometers.

The chemical composition of the extremely cold Titan atmosphere is of great interest, because it may be composed of chemical compounds that are similar to the early days of the Earth's atmosphere before life and oxygen. As on the Earth, the Titan atmosphere is primarily nitrogen, but it also contains methane as well as ethane and other organic compounds forming haze layers in the atmosphere. The heavier compounds float down to the surface and add organic constituents in the icy surface material (*Lebreton and Matson*, 2002).

Titan has practically no intrinsic magnetic field (*Ledvina et al.*, 2004) and therefore external plasma hits directly on the upper atmosphere and ionosphere of Titan. The moon is mostly located inside Saturn's magnetosphere and hence Titan atmosphere interacts with the magnetospheric plasma. Occasionally Titan is also located outside the shelter of Saturn's magnetosphere, and then the atmosphere will interact directly with the solar wind. These interaction processes create complex phenomena involving also mass loss from the Titan atmosphere (*Kallio et al.*, 2004).

Chapter 3

Atmospheric Physics and Observations

3.1 Atmospheric modeling

Planetary atmospheres cannot be subjected to controlled experiments, they can only be observed. Systematic measurements shed light on atmospheric behavior that can be investigated further by modeling efforts. The processes that are thought of being significant to the observed phenomena are included in the models and simulation activity.

The planetary atmospheres have similar physical constraints that are the drivers behind the atmospheric structure and dynamics. They consist of a relatively thin layer of mixed gases around a giant planetary body and are constrained by the surface and the empty space surrounding the planetary system. The atmospheres are constantly subjected to the gravity force of the planetary body and to solar forcing. Solar irradiation creates temperature differences that together with the rotating planetary body and atmosphere cause atmospheric motions.

The planetary atmospheric motions can be governed by equations of motion and continuity, the equation of state of gas, and the first law of thermodynamics (*Holton*, 1992; *Andrews*, 2000). In a generic form this can be formulated as follows:

$$\frac{d\vec{V}}{dt} = -\alpha\nabla p - 2\vec{\Omega}\times\vec{V} + \vec{g} + \vec{F} \tag{3.1}$$

$$-\frac{1}{\rho}\frac{d\rho}{dt} = \nabla\cdot\vec{V} \tag{3.2}$$

$$p = \rho RT \tag{3.3}$$

$$Q = c_v\frac{dT}{dt} + p\frac{d\alpha}{dt} \tag{3.4}$$

where $\vec{V}$ is the flow velocity, ρ the atmospheric density, $\alpha = 1/\rho$, p the atmospheric pressure and T the gas temperature, $\vec{\Omega}$ is the rotation angular velocity,

$-2\vec{\Omega} \times \vec{V}$ is the apparent Coriolis acceleration, $\vec{g}$ the gravitational acceleration, $\vec{F}$ the frictional force, Q the rate of heat energy change, and c_v the specific heat at constant volume (*Holton*, 1992; *Houghton*, 2002).

Various features need to be added to these governing equations to make them better reflect the actual atmospheric behavior. At Mars the principal mechanisms to be added are the effect of dust that is transported by the atmosphere and that is constantly present in the atmosphere at varying amounts, and the CO_2 cycle. At Mars CO_2 is condensing at the poles during the winter and sublimating back to the atmosphere in the summertime. Due to this cycle the atmospheric mass varies by approximately 30 % between Martian winter and summer (*Kieffer*, 1992). At the Earth the water cycle, oceans and vegetation are the main features to be taken into account in the governing equations 3.1- 3.4 (*Holton*, 1992).

Atmospheric modeling incorporates a hierarchy of models and approximations that address in a different fashion the atmospheric volume to be observed or the phenomena to be included in the investigation. Concerning the atmospheric large-scale motion, an important simplification is the geostrophic equilibrium that results in the practical concept of geostrophic motion being approximately valid at Mars and the Earth. This is caused by the relatively high planetary rotation rate of these planets resulting in strong apparent Coriolis force (*Houghton*, 2002; *Andrews*, 2000). On the other hand, Venus is a slowly rotating planet, where the Coriolis effect is not significant and the material acceleration dominates. Therefore the Venusian atmosphere is governed by cyclostrophic equilibrium instead of geostrophic equilibrium prevalent at Mars and the Earth (*Hunten et al.*, 1983; *Houghton*, 2002). Also Titan rotates relatively slowly. Hence it is very likely that Titan atmospheric motions can also be characterized by cyclostrophic equilibrium.

The atmospheric models include various approximations, simplifications and sub-grid parameterization schemes. This requires accurate observations to verify the model assumptions, and on the other hand, the observations require modeling to extend the value of the observations beyond the position and time the observation was performed. This is also demonstrated by Chapter 5 and by Papers 2 and 8.

The subsections below review some key phenomena of planetary atmospheres, and atmospheric boundary layers in particular, to shed light on the requirements and constraints of *in situ* atmospheric observations. The formulation of this chapter gives some guidelines for the development work of the missions and experiments to investigate the atmospheres of planetary bodies. It also gives background information for our modeling efforts presented in Chapter 5.

3.2 Atmospheric boundary layer

The lowest part of the atmosphere is affected by the planetary surface. The effects created by the surface interacting with atmosphere and by the diurnal cycle extend up to a few kilometers above the surface. Within this regime also fluxes of momentum, heat, humidity and aerosols are transported via turbulent eddy motions within a time scale of the order of an hour (*Stull*, 1988). This

region is called the atmospheric boundary layer (ABL). The rest of the atmosphere is often referred to as the *free atmosphere* indicating the fact that it is free of the surface effects.

The generic formulation (equations 3.1 to 3.4) for atmospheric motions also applies to the motions in the atmospheric boundary layer. The main difference is that the frictional forces causing turbulent motions and viscous flow are more significant to the ABL than to the free atmospheric flow (*Holton*, 1992; *Clarke and Hess*, 1973; *Hess*, 1973; *Stull*, 1988).

It is useful to divide the atmospheric parameters in the mean and perturbed parts with overlines (*e.g.* mean flow $\overline{U}$) representing the mean values and the primed parameters (*e.g.* u', perturbed part of flow caused by turbulence and waves) are deviations from the mean value (u' = U - $\overline{U}$) (*Stull*, 1988). Then a set of equations governing the mean variables in a turbulent ABL flow can be presented using the summation notation as follows (*Stull*, 1988)

$$\frac{\partial \overline{U}}{\partial t} + \overline{U}_j \frac{\partial \overline{U}}{\partial x_j} = -f_c(\overline{V}_g - \overline{V}) - \frac{\partial \overline{u'_j u'}}{\partial x_j} \tag{3.5}$$

$$\frac{\partial \overline{V}}{\partial t} + \overline{U}_j \frac{\partial \overline{V}}{\partial x_j} = -f_c(\overline{U}_g - \overline{U}) - \frac{\partial \overline{u'_j v'}}{\partial x_j} \tag{3.6}$$

$$\frac{\partial \overline{q_T}}{\partial t} + \overline{U}_j \frac{\partial \overline{q_T}}{\partial x_j} = S_{qT}/\overline{\rho} - \frac{\partial \overline{u'_j q'_T}}{\partial x_j} \tag{3.7}$$

$$\frac{\partial \overline{\theta}}{\partial t} + \overline{U}_j \frac{\partial \overline{\theta}}{\partial x_j} = -\frac{1}{\overline{\rho} C_p}\left(L_p E + \frac{\partial \overline{Q^*_j}}{\partial x_j}\right) - \frac{\partial \overline{u'_j v'}}{\partial x_j} \tag{3.8}$$

$$\frac{\partial \overline{U_j}}{\partial x_j} = 0 \tag{3.9}$$

$$\frac{\overline{P}}{R} = \overline{\rho}\overline{T_v}, \tag{3.10}$$

where U and V represent horizontal flow velocity components, P is the atmospheric pressure, T_v the virtual absolute temperature, ρ is the density, R the molar gas constant and f_c is the Coriolis parameter ($f_c = 2\omega \sin\phi$, ϕ is latitude and ω=2π radians/day)). The mean geostrophic wind components are defined as $\overline{U}_g = -1/(f_c\overline{\rho})\frac{\partial \overline{P}}{\partial y}$ and $\overline{V}_g = -1/(f_c\overline{\rho})\frac{\partial \overline{P}}{\partial x}$. q_T is the specific humidity, S_{qT} is the net moisture source term. θ is the virtual potential temperature, L_p is the latent heat associated with the phase change of E, and C_p is the specific heat for moist air. Q*is the net radiation.

It is evident in the light of the generalized set of governing equations 3.1 to 3.4 as well as the formulation above (equations 3.5 to 3.10) that to resolve the space and time dependent atmospheric behavior a network of observation posts around the planet is required. The network should operate continuously to properly cover the time scale of the atmospheric phenomenon under investigation.

When investigating atmospheric phenomena with short time scales the time constant of the observations play a key role. Sensor systems with short time constants provide readings for the primed variables (formulation above, equations 3.5 to 3.10) and mean values are allocated for the variables with overlines.

The time scale of the investigated phenomenon dictates the desirable integration time of the *in situ* observations. This applies both to a measurement network and to a single individual observation post.

The ABL plays a key role in the atmospheric dynamics. The principal driver behind the atmospheric motion, the solar radiation, is transported through the boundary layer and is absorbed or reflected at the surface. This process is strongest at Mars, when the airborne dust content is low, and at the Earth during clear sky conditions. Exchange processes of momentum, heat and material are continuously taking place between the surface and the atmosphere.

Eventually the entire troposphere is affected by the ABL characteristics, but this process is slow compared to the processes taking place inside the ABL. It should also be noted that the ABL actually never reaches steady state conditions, but is rather driven by continuously changing solar forcing (*Salby*, 1996).

The exchange processes between the surface and the atmosphere are based on molecular transport and turbulent eddy transport, the latter being a predominant transport process in the ABL. Molecular transport is prevailing in the surface molecular boundary layer just above the surface (few centimeters), where the vertical shear is large, and at very high altitude (>100 km at the Earth) where the density is small. Thus, within the boundary layer the principal mechanism to transport momentum, heat and humidity is the turbulent eddy motion (*Stull*, 1988; *Andrews*, 2000).

One of the most significant features of the ABL is the fact that it is highly efficient in vertical transfer of momentum, heat and mass. This transfer process is a key issue in understanding the ABL as well as the dynamics of the whole atmosphere. Major tasks in the investigation of the ABL include the study of surface fluxes and their variation through the depth of the ABL and of turbulence characteristics (*Garratt*, 1992). The fact that turbulence is relatively abundant in the ABL is one more feature making the ABL distinct from the rest of the atmosphere.

The ABL can be divided into two main layers, the surface layer that is the part of atmosphere touching the surface and assuming about 10% of the full depth of the ABL and the outer ABL layer (Ekman layer) on top of the surface layer. Furthermore, the surface layer is still divided in the lowermost section to roughness sublayer and the inertial sublayer (*Garratt*, 1992).

The depth of the boundary layer varies from a few tens of meters during very stable nighttime ABL conditions up to several kilometers during daytime, when strong convective motions dominate. The ABL is called neutral, if mechanical production of turbulence is dominating over the convective production (*Holton*, 1992).

The vertical fluxes of momentum ($\rho\overline{u'w'}(\mathrm{z})$), sensible heat ($\rho\overline{\theta'w'}(\mathrm{z})$), and buoyancy ($\rho\overline{\theta'_v w'}(\mathrm{z})$) are significant factors in the ABL behavior. They are among the components of the parameterization process needed to simplify the equations governing the turbulent flow of the atmospheric boundary layer. This requires proper scaling parameters, as surface friction velocity u_{*0} (*Garratt*, 1992), which is a key parameter defined as

$$u_{*0}^2 = [\overline{(u'\,w')}_0^2 + \overline{(v'\,w')}_0^2]^{\frac{1}{2}} = -\overline{(u'\,w')}_0, \tag{3.11}$$

where the subscript$_0$ refers to surface level values, u_0', v_0' and w_0' are turbulent velocity components in x, y and z (vertical) directions, respectively.

The simplified form $u_{*0}^2 = -\overline{(u'\,w')}_0$ results when the surface stress (parallel to x-axis) is assumed to be in the direction of the mean wind at the surface.

The behavior of the ABL is very much dependent on turbulence, which is also the driver of the principal atmospheric stress, the Reynolds stress. Mixing of momentum, heat, and also material constituents are driven by turbulent eddy motions. The size of the eddy motions range from roughly the depth of the ABL down to millimeter scale eddies.

The turbulent eddies are brought up by various mechanisms. The surface being heated by the varying solar irradiation causes increased buoyancy and decreased buoyancy when cooled down by infrared radiation e.g. during the nighttime. Wind shear is generated by frictional drag when the air is flowing over the surface. Often the shear becomes turbulent. Also obstacles deflecting the flow may cause turbulent wakes in the vicinity of the obstacle.

The largest eddies are the most intense, because they are generated directly by the surface forcings. The smaller eddies are feeding on the larger ones, which cause eddy-size regions of wind shear. Eventually, the smallest eddies deliver their energy by means of molecular dissipation (*Garratt*, 1992).

When atmospheric observations are being planned the time resolution of adjacent observations dictate the size of the turbulent eddies that may be detected and resolved. The unresolved part of the turbulence must be parameterized, when the observations are used in modeling efforts.

The overall intensity of turbulence and the ratio of the buoyancy and shear production terms of the turbulence kinetic energy are good measures of the atmospheric dynamic stability. When the static stability depends on the vertical gradient of the potential temperature ($\partial\theta/\partial z$), the dynamic stability depends on the ratio between the forced convection and mechanical shear (*Garratt*, 1992). This is measured by the Richardson's number and its flux version R_f (*Garratt*, 1992) as follows

$$R_f = \frac{g}{\theta_v}\overline{(w'\theta')}/[\overline{(u_i'u_j')}\,\frac{\partial\overline{u_j}}{\partial x_j}], \tag{3.12}$$

where θ_v is the virtual potential temperature. When assuming horizontal homogeneity and neglecting subsidence, and after removing the summation indexes R_f turns out as (*Garratt*, 1992)

$$R_f = \frac{g}{\theta_v}\overline{(w'\theta')}/[\overline{(u'w')}\,\frac{\partial\overline{u}}{\partial z} + \overline{(v'w')}\,\frac{\partial\overline{v}}{\partial z}]. \tag{3.13}$$

The gradient version of the Richardson number R_i is often more convenient to use in the form (*Garratt*, 1992)

$$R_i = \frac{g}{\theta_v}\frac{\partial\overline{\theta_v}}{\partial z}/[(\frac{\partial\overline{u}}{\partial z})^2 + (\frac{\partial\overline{v}}{\partial z})^2]. \tag{3.14}$$

The gradient Richardson number (equation 3.14) is widely used as a parameter

characterizing the thermal stability of the of the ABL. The flow is dynamically unstable when the mechanical shear is stronger than the positive buoyant effect trying to damp the turbulent eddy motions (R_i is negative). Experiments have indicated that the flow becomes dynamically unstable when $R_i < 0.25$ and stable when $R_i > 1.0$ (*Garratt*, 1992).

Another important scale parameter characterizing the ABL stability is the Obukhov length L. It is a central parameter in the Monin-Obukhov similarity theory developed for the ABL surface layer (*Garratt*, 1992). It is applied on the Earth and can also be utilized for characterization of the Martian surface layer (*Tillman et al.*, 1994; *Larsen et al.*, 2002). The Obukhov length can be defined in the case, when the buoyant and mechanical turbulence kinetic energy productions are equal, implying that $R_f = -1$. When the main axis is set parallel to the mean wind we get from the equation 3.13

$$(g/\overline{\theta_v})\,\overline{w'\theta'_v} = -(\overline{u'w'})_0 \frac{\partial \overline{u}}{\partial z}. \tag{3.15}$$

When using the gradient form of the wind profile (non-neutral case) $\partial U/\partial z = (u_{*0}/kz)\,\phi_M$ (*Garratt*, 1992), where ϕ_M is the dimensionless wind shear parameter, and the friction velocity relation (equation 3.11) we get from equation 3.15 the height z = -ϕ_M L. At this height the buoyant and mechanical turbulence kinetic energy productions are equal. The scale parameter L is then

$$L = -\frac{\overline{\theta_v} U_*^3}{kg\,\overline{(w'\theta'_v)}_s}. \tag{3.16}$$

The Obukhov length L is an important scaling parameter and especially the term z/L is widely used as a stability parameter when modeling the ABL surface layer. It is one of the primary parameters in the surface layer similarity theory. The z/L parameter is also a convenient variable when describing evolution of the characteristics of turbulent eddy motions. For instance the terms of the turbulent kinetic energy budget and their evolution are often given as functions of the stability parameter (*Garratt*, 1992).

The spectrum of the turbulent eddy motions reveals a spectral gap in the terrestrial atmosphere. Turbulence is intense and abundant both with the periods ranging from a few minutes up to 60 minutes, as well as with the periods longer than 1 hour to a few tens of hours (*Stull*, 1988). Around the period of the order of one hour there is only weak turbulent activity. This spectral gap observed at the ABL of the Earth should be taken into account when defining the *in situ* investigations of planetary atmospheres.

3.3 Stress forcings and dust devils

The atmospheric stresses, the viscous stress, the pressure stress and the Reynolds stress are key elements in the behavior of the atmosphere. They create turbulent motion of the atmosphere and are key elements behind the surface-to-atmosphere exchange processes.

The viscous stress is created by shear in the fluid motion. The motion may be either laminar or turbulent, depending on the intensity of the shear and the viscosity of the fluid. The atmospheric fluids are Newtonian, for which the viscous stress depends linearly on the intensity of the shear.

Turbulent motion of a fluid results in the Reynolds stress, which actually is

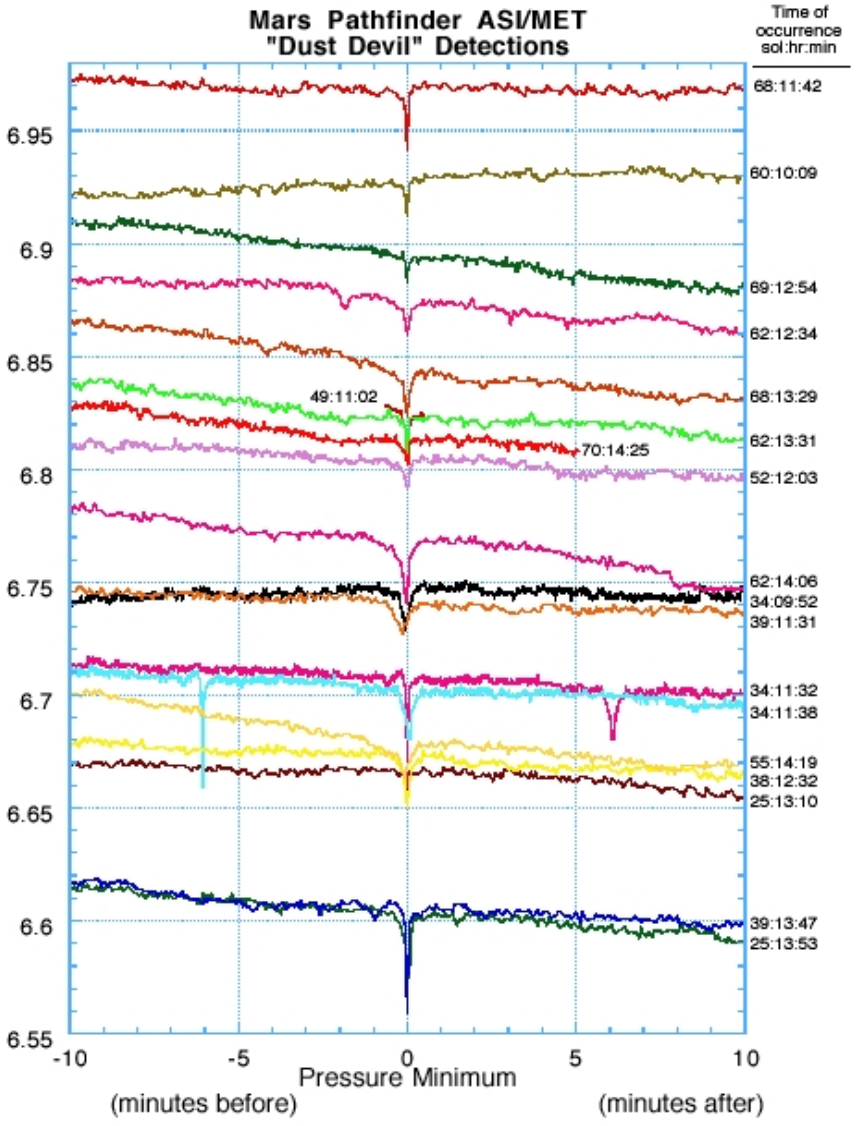

Figure 3.1: Dust devils detected by the Mars Pathfinder. The pressure (in hPa) around the MPF is presented as a function of time (min) before and after the dust devil passes MPF. Pressure drops ranging from 1 to 5 Pascals are clearly visible in the pressure recordings. (*Schofield et al.*, 1997; *Golombek et al.*, 1999; *Ferri et al.*, 2003).

mixing of air parcels with different momentum, and is equivalent to momentum flux. Accordingly, Reynolds stress exists only when the fluid is turbulent (*Salby*, 1996).

Atmospheric pressure is also a type of stress. It acts on fluids at rest, while the viscous stress and the Reynolds stress exist only when the fluid is in motion.

The stress forcings play key roles in the dust devil lifting processes. A dust devil is a small-scale atmospheric feature of whirling motion of air mass that lifts dust and also other light particles into the atmosphere. Dust devils are common on the Earth. On Mars dust devils were detected for the first time when analyzing the Viking mission data. The Mars Global Surveyor finally revealed the frequent occurrence of the dust devils at Mars (*Fisher et al.*, 2005). At Titan and Venus dust devils have not been observed.

Dust devils are local atmospheric phenomena that are often observed in dry terrain conditions on the Earth and on Mars. They are vortices with a warm low-pressure core that appear to be formed in connection to convective plumes. Dust devils move along with the wind, lift surface material (*e.g.* dust on Mars) into the atmosphere and are tilted by the wind shear (*Ferri et al.*, 2003; *Fisher et al.*, 2005). Dust devils play an important role in the evolution of the Martian atmospheric dust-load, which is a key parameter in the behavior of the Martian atmosphere (*Kieffer*, 1992; *Murphy*, 1996).

A dust devil manifests itself by changes in the pressure, temperature and wind at the point of occurrence, as well as decreasing the transparency of the atmosphere due to surface material lifted into the atmosphere. At Mars dust devils also leave visible tracks on the surface (*Fisher et al.*, 2005). At the Earth dust devils have been observed to cause a temperature rise of a few degrees, increased wind speed and change of wind direction due to the whirling motion of air, and updrafts of a few meters per second in the center of the dust devil (*Tratt et al.*, 2003).

Observation results from Mars Pathfinder (MPF) in Figure 3.1 present a series of pressure drops caused by dust devils passing the MPF location (*Golombek et al.*, 1999; *Ferri et al.*, 2003). The behavior of dust devils can be characterized by assuming cyclostrophic balance (*Rennó et al.*, 2000; *Renno et al.*, 2004; *Tratt et al.*, 2003; *Holton*, 1992), where centripetal acceleration equals the pressure gradient resulting in $Mv_t^2/r = RT\Delta p/rp$. When solving for Δp we get

$$\Delta p = \frac{Mv_t^2 p}{RT} \tag{3.17}$$

where R = 8.314 $JK^{-1}mol^{-1}$ is the molar gas constant, M is the molar mass of the atmospheric gas, v_t is the maximal tangential velocity at the edge of the core of the dust devil, T is the gas temperature, p is the atmospheric surface pressure and Δp is the drop in atmospheric pressure caused by the passing dust devil.

From the data given by the Viking Landers and Mars Pathfinder (*Soffen*, 1976; *Golombek et al.*, 1999; *Murphy et al.*, 2002; *Tillman et al.*, 1994; *Ferri et al.*, 2003) we can estimate the tangential velocity v_t to reach at least the velocity between 10 and 20 m/s, even though higher winds than 20 m/s have been speculated to occur on Mars in connection with dust devils (*Rennó et al.*, 2000).

When applying the pressure drop equation 3.17 we find out that with the wind velocity of 10 to 20 m/s the pressure drop should range from 1 to 6 Pascals. This is in perfect agreement with the pressure drops observed by MPF as depicted in Figure 3.1.

This implies that to the resolution of the Martian atmospheric pressure observations should be better than 1 Pascal to resolve dust devils. This matches with the requirements posed for atmospheric instrumentation in some of the earlier Mars missions (Papers 3, 5 4), where requirements were set to be more stringent. Detecting the dust devil on time requires that a fast measurement campaign can be established immediately, when the dust devil is detected. An arrangement using satellite images could also be foreseen to provide early warning for the observation posts on Mars.

3.4 Requirements on Martian investigations

Time-resolved *in situ* Martian meteorological measurements acquired by the Viking and Mars Pathfinder landers and remote sensing observations by the Mariner 9, Viking, Mars Global Surveyor, Mars Odyssey and the Mars Express orbiters have provided the basis for our current understanding of the behavior of weather and climate on Mars. However, the available amount of data is still scarce and a wealth of additional *in situ* observations are needed on varying types of Martian orography, terrain and altitude spanning all latitudes and longitudes to address microscale and mesoscale atmospheric phenomena. Detailed characterization of the Martian atmospheric circulation patterns and climatological cycles requires simultaneous *in situ* atmospheric observations by a network of stations at the Martian surface (*Haberle and Catling*, 1996; *Barnes et al.*, 1993; *Squyres*, 1995; *Harri et al.*, 1999b). The requirements on measurement accuracies of *in situ* atmospheric observations have been discussed by, *e.g. Hess et al.* (1972) and in the papers accompanying this Summary.

To shed more light on the Martian atmosphere an exploration mission should be able to (*Kieffer*, 1992)

- Provide regular observations of the key atmospheric parameters (pressure, temperature, dust load, wind, humidity) on various types of Martian conditions all over the planet;
- Quantify heat, mass, and momentum fluxes as a function of time of sol and season;
- Identify the primary components of general circulation, including the Hadley circulation, thermal tides, stationary Rossby waves, transient baroclinic waves, and the net mass flow associated with the CO_2 cycle;
- Determine interannual climate variability;
- Provide atmospheric vertical profile observations and preferably nested images of the landing environment during the entry vehicle's descent into the Martian atmosphere;

- Discriminate between effects of surface albedo, thermal inertia, slopes, and roughness;
- Identify processes that lift and transport dust (dust devils, dust storms);
- Estimate current rate of aeolian weathering of the surface;
- Monitor surface to atmosphere exchanges of water over diurnal and seasonal cycles.

The implementation of the scientific objectives described above require *in situ* observations as well as remote observations. Practical forms of investigation tools include vehicles landing onto the planetary surface, atmospheric balloons, aircraft and rockets flying in the planetary atmosphere. Also devices capable of penetrating into the planetary soil are significant for providing knowledge of the conditions and behavior of the soil and surface. This information is required for proper determination of exchange processes between the surface and the atmosphere.

The landing vehicles are often split into categories of soft landers, semi-hard landers and hard landers depending on the deceleration and terminal velocity at the time of impact on the planetary surface. At Mars this means that soft landers land gently usually by utilizing retro-rockets in the final phase of the landing, like the Viking landers (*Soffen and Snyder*, 1976; *Soffen*, 1976). Hard landers decelerate their impact speed by impacting on the surface and making the vehicle penetrate into the soil thus halting rapidly the vehicle's speed resulting in high level of deceleration (of the order of tens of thousands of m/s^2). Semi-hard landing vehicle specification falls between the hard lander and soft lander specifications. Typical Martian semi-hard landers are, *e.g.* the Mars Netlander vehicle (Paper 1) and the Mars-96 Small Station (Paper 6) both of which were using the heat shield, parachutes and airbags in the entry, descent and landing phase. The MetNet mission utilizes typical Martian hard-lander vehicles (*Harri et al.*, 2003b) that in the final phase of the landing penetrate into the Martian soil to eventually halt the landing process and to also achieve a proper operational position.

Semi-hard landing vehicles impact on the surface with a moderate deceleration (few thousands of m/s^2 over the time of some tens of milliseconds) and thus provide a practical solution for a planetary surface payload including robust geophysical instruments. That is especially suitable for instrumentation including lightweight sensor systems needed to perform atmospheric science experiments.

Soft landing technology is practical for large payloads with fragile parts, whereas the hard landers provide a platform to take robust science payload to a planetary surface with a high mass efficiency. This is because the more gently a vehicle lands the more mass is needed for the descent and landing systems to decelerate the vehicle's velocity before the impact on the surface.

In situ observations on the planetary surface are imperative for understanding the atmospheres. The principal reasons are:

- Atmosphere to surface exchange processes are decisive for the behavior of the atmosphere, and those processes can only be understood by *in situ* measurements;

- Atmospheric science requires *in situ* surface observations performed simultaneously at several locations for a timeframe of various planetary years to develop synoptic and climatic models. This can practically be achieved by a network of surface payloads distributed through the planetary surface;
- Barotropic component of the atmospheric general circulation can be provided only by in situ observations;
- *In situ* surface observations provide the ground truth for remote observations;
- Various planetary scientific experiments require knowledge of the actual state of the atmosphere, and that can only be obtained by *in situ* observations;
- Atmospheric observations, and in particular *in situ* observations, significantly enhance the science return of practically all planetary experiments, and are also indispensable for the safety of planetary science missions with any type of landing components. The safety of the possible future human landing missions require atmospheric knowledge in such detail that can only be provided by *in situ* observations.

Number of the *in situ* payloads and their locations on the planetary surface play an essential role in the mission planning process, as documented by, *e.g. Grant et al.* (2004). When addressing local and regional scale atmospheric behavior with one or few surface payloads, the observation posts should be located on areas with, *e.g.* variable types of geography, terrain, thermal inertia, altitude, as well as surface materials and albedo. Capturing synoptic and large-scale atmospheric flows and global circulation phenomena requires a number of simultaneously operating observation posts located around the planetary surface. At least of the order of ten to twenty observation posts are required to address planet-wide atmospheric phenomena (*Haberle and Catling*, 1996).

Regardless of the locations and number of observation posts on a planetary surface, remote observations by a satellite orbiting the planet are highly valuable in supplementing the science return of the surface observations. Atmospheric observations through an orbiting satellite cover eventually the whole atmosphere and the planetary surface, and will thus extend the validity of the *in situ* observations beyond the point of the *in situ* measurement. On the other hand, the *in situ* observations give accurate reference values for the remote measurements, whose relatively low accuracy is therefore improved. Hence *in situ* and remote observations utilized together provide a most fruitful and effective combination of mission tools for atmospheric investigations.

3.5 Sensors for planetary atmospheres

When developing payloads for various planetary missions we started to investigate accurate and reliable atmospheric sensor types. After the first set of test runs with various types of sensors we focused our attention to the radiosonde sensors for pressure (Barocap®), humidity (Humicap®) and temper-

ature (Thermocap®) manufactured by the Vaisala Inc. The sensor characteristics are recorded, *e.g.* in Papers 2, 3, 4 and 5.

The operation principle of the Vaisala sensors is based on measuring the sensor capacitance that is changing due to variations of the particular meteorological parameters. The Barocap®, Humicap and Thermocap® sensors are interfaced by similar type of transducer electronics, which saves the instrument mass and decreases complexity when using all these sensors in the same instrument.

The Barocap®, Humicap® and Thermocap® sensors are light, have a weight of a fraction of a gram, and have low power consumption (Paper 4). A significant issue is the fact that these sensors are being produced in large quantities for the radiosonde and other commercial applications by high quality production lines. Accordingly, there is very little variation of characteristics between individual sensors. All this makes these sensors excellent candidates for planetary exploration. That was the rationale behind commencing the sensor qualification procedures.

The sensor qualification program was implemented during the years 1989 - 1993 and it consisted of the environmental stress types to be encountered in a Martian surface mission. As described in Paper 4, during the qualification procedures the sensors were exposed to the following environmental stress test types:

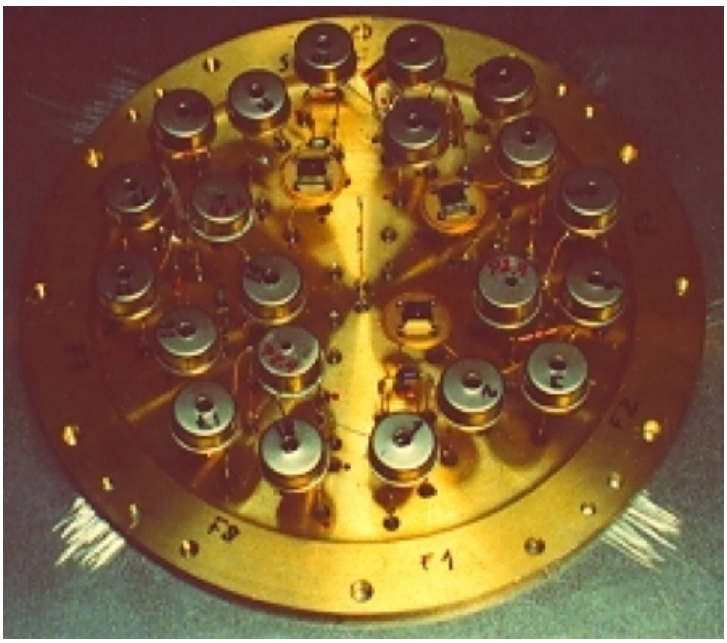

Figure 3.2: One Barocap sensor setup used during the sensor screening tests. The sensor electronics is enclosed in the compartment below the sensors, and the whole assembly is used as the airtight cover for a pressure vessel. Similar type of setups were made use of in both qualification and screening tests of the Barocap and Humicap sensors.

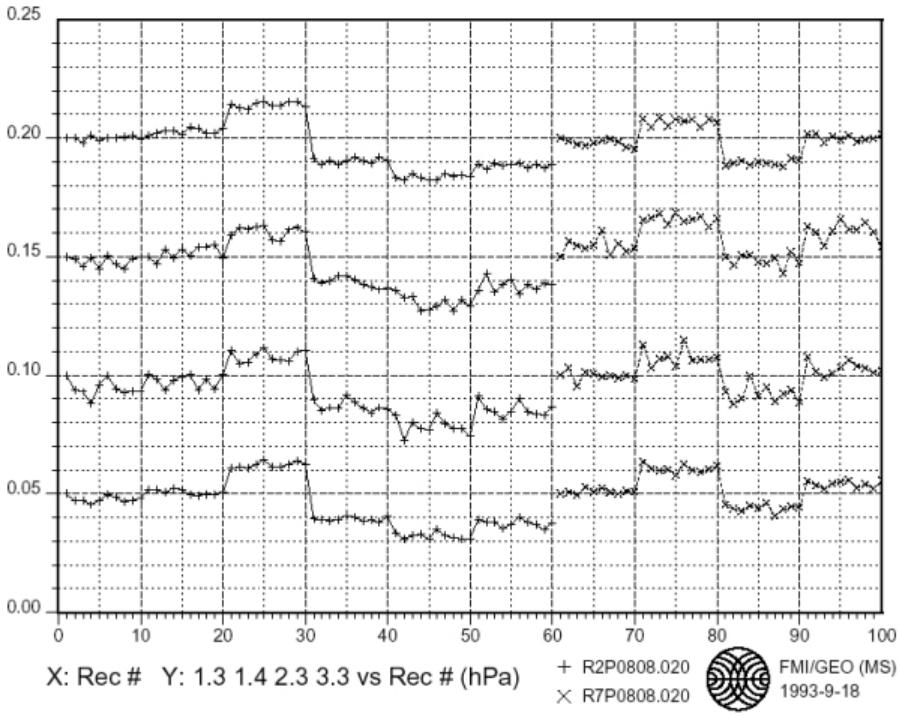

Figure 3.3: A typical response of Barocap® (four different sensors) to sudden stepwise pressure changes of the order of 1 to 3 Pa. The ordinate axis presents the four sensors' output in hPa with an offset of 5 Pa applied to adjacent sensors to make the figure readable. The abscissa is the running measurement number. This test was performed in 253 K temperature (*Harri et al.*, 1993).

- Thermal cycling (between 0°C and -135°C)
- Launch vibrations
- Mechanical impact shocks (up to 500 g)
- Thermal vacuum (+60°C for 7 days)
- CO_2 condensation on and evaporation from sensor surfaces
- Radiation dose (10 kRads for sensors, 60 kRads for electronics).

For the qualification program we procured hundreds of sensor heads. Out of the procured sensors we picked randomly some 5% sample to be used in the qualification tests. The sensors under test were stressed far beyond the specified operating limits on the Martian surface to be sure that the sensors would operate as expected in the Martian environment. Before and after exposing the sensors to environmental stress levels, we performed functional testing to be able to detect if the stress exposure had affected the sensor performance (Paper 4).

In the qualification test setup the Barocap® sensors were attached to the cover of the pressure vessel such that they were facing the interior of the vessel (Figure 3.2). The transducer electronics board was mounted on the other side of the cover to distinguish any possible change in sensor performance from the performance of electronics. The same type of test setups were also used for the humidity sensors (Humicap®s), as well as for the screening tests of both sensor types. Eventually, this turned out not to be practical, and the whole test setup was exposed to the environmental stress treatments. Accordingly, the test results reflected the performance of the chain of the sensor head and transducer electronics.

The qualification process was successful and we could conclude that the performance of Barocap®, Humicap® and Thermocap® sensors was not affected by the environmental stresses the sensors were exposed to (*Harri et al.*, 1993; *Paukkunen and Turtiainen*, 1989). This implied that the sensors were sufficiently robust for the Martian surface conditions. In other words the Barocap®, Humicap® and Thermocap® sensors were qualified for Mars (Paper 4).

After the qualification procedures were successfully accomplished the rest of the sensors in the procured sensor lots were exposed to milder environmental stress levels to screen out those individual sensors that did not have optimal characteristics. Accordingly, in this manner the suitable sensors for our planetary atmospheric missions were firstly qualified and then screened out of the

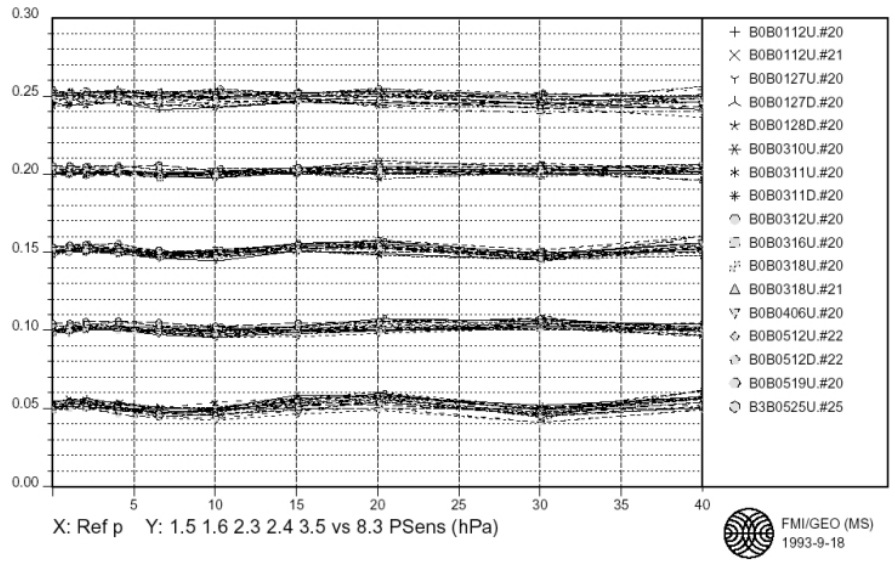

Figure 3.4: Long term stability of 5 Barocap®s during a 5-month period (17 measurement cycles). During the measurements pressure was varied between 0 and 40 hPa in room temperature. The sensor outputs are deviations from the channel 8.3, which served as a transfer standard. The ordinate axis presents the five sensors' output in hPa with an offset of 5 Pa applied to adjacent sensors to make the figure readable (Paper 4).

manufacturing lots.

According to our test runs resolution of the order of 0.1 Pa seems to be feasible for the Barocap sensors. This is also shown by the sensor response curves depicted in Figure 3.3. As a result of the lengthy test process the long term stability of the Barocap®s was better than 0.02 hPa, when measurements had been carried out for 5 months, as presented in Figure 3.4 and in Paper 4.

The Humicap® stability in terms of relative humidity (RH) seems to be better than 2 % RH / year according to our tests in room temperature conditions. The Humicap measurement resolution is better than 0.1 % RH and the accuracy of the order of 1 to 20 % RH, varying with temperature. The Humicap® time constant decreasing with temperature is of the order of 1 min in 233 K and 10 min in 203 K. The Thermocap® long-term stability is better than 0.3 K / 2 years as discussed in Papers 4 and 5.

An interesting issue in our sensor qualification and screening process was the fact that very few individual sensors were eventually discarded. It demonstrates the high quality of the sensor production lines. Hence our original decision to focus on the Vaisala radiosonde sensors proved to be highly rewarding.

Accordingly, we discovered that the pressure (Barocap®), humidity (Humicap®) and temperature (Thermocap®) microsensors manufactured by Vaisala Ltd. are highly suitable for Martian surface expeditions. They are manufactured in quantity enabling a procurement of a large number of sensors, which can then be screened to meet the required criteria. They are especially ideal for planetary missions, where high accuracy and sensitivity, and minimization requirements of mass, dimensions and power are most stringent.

After the qualification process was successfully accomplished the pressure (Barocap(r)), humidity (Humicap®) and temperature (Thermocap®) sensors have been used in a number of planetary missions as described in Papers 1-8 and Chapter 4. These missions have given a further qualification certificate in terms of successfully participating in various space flight equipment. The wonderful success of the Cassini/Huygens mission and the excellent high-quality results of the PPI-device after the 7-year journey in space was an ultimate proof of the suitability of these sensor devices for planetary missions.

3.6 Atmospheric *in situ* observation scenarios

From the point of view of science as well as practical investigation resources it is reasonable to start exploring a poorly known planetary atmosphere, as well as the planet as a whole, first by ground-based and remote sensing observations, and only thereafter with in situ payloads supported by remote observing platforms. In such a fashion the exploration of terrestrial planets has developed. Ground-based observations enabled a proper design of Mariner 4, which performed the first Mars flyby mission in July 1965. Building on that knowledge the next successful Mars flyby by Mariner 6 took place in July 1969. The first spacecraft successfully orbiting Mars was Mariner 9, which mapped about 70 % of the Martian surface and studied the temporal variations of the Martian atmosphere and surface. The first successful landing was the Viking mission including two landers and two orbiters that arrived at Mars in 1975. During

the last decade a wealth of new data was gained by the Mars Pathfinder lander (in 1997), the Mars Global Surveyor orbiter (1996), the Mars Odyssey orbiter (2001), Mars Express (2003) and the MER rovers in 2004 (*Kieffer*, 1992).

As to Titan, it has also been covered by ground-based observations. The first observations of its atmosphere were performed by the Voyager 1 radio science experiment giving a rough understanding of the pressure and temperature profiles as well as of the composition of the atmosphere. Based on these data the experiments onboard the Cassini/Huygens probe were designed. The next set of data on Titan and its atmosphere were gained in early 2005 when the Huygens probe descended successfully in the Titan atmosphere (*Fulchignoni et al.*, 2005; *Zarnecki*, 2005; *Bird*, 2005; *Porco et al.*, 2005).

Ground-based observations of Venus have been abundant for centuries, but the first in situ observations of its atmosphere were performed by Mariner 2 at the end of 1962. The first probe to give *in situ* observations of the Venusian atmosphere was Venera 4. It was followed by additional entry probes until Venera 7 was able to land on the surface of Venus and send data back to the Earth. The first successful landing onto the Venusian surface was followed by various Venera, Pioneer Venus and Vega probes each of them providing small bits of new information on the atmosphere and surface of Venus. Eventually the surface of Venus was mapped with high precision by the Magellan Venus Probe during the years 1990-1994. The most recent information was gained by the Messenger Venus flybys in 2004, and the next observations will be provided by the Venus Express mission in early 2006 (*Svedhem et al.*, 2005)

Some important recommendations can be made when assessing where to invest the resources available for the exploration of planetary atmospheres in the near future, *e.g.* during the next ten years. The Martian atmosphere has been extensively investigated by landing vehicles and various orbiting remote sensing missions. The next step should be a mission with a large number of versatile atmospheric science payloads on the surface operating simultaneously and supported by concurrent orbiter observations of the atmosphere. The mission could preferably be a MetNet type of mission focused on atmospheric science, which would be an optimal mission for today. A general geophysical network science mission (*Chicarro et al.*, 1993) like the NetLander Mission would also be a leap forward from the current understanding of Mars. The NetLander type mission also has the support of a wide planetary science community and hence could be a highly reasonable scenario for the near future.

A network of well-instrumented meteorological payloads would be a good choice also for the Venusian atmosphere. This would be more preferable than sending more individual probes to Venus. This recommendation is likely to be supported by the data to be gained by the Venus Express mission.

The Titan atmosphere was explored by the first *in situ* mission when the Huygens probe descended through the Titan atmosphere in January 2005. After the highly successful Cassini/Huygens probe operations the recommendation on the next type of an atmospheric science mission for Titan is to have one successful mission investigating Titan from orbit and with at least one extensive atmospheric science payload operating simultaneously on the surface. Then comes the time to have a network mission dedicated either to atmospheric science only or to general geophysical network science including an extensive atmospheric

science payload.

3.7 Discussion

The practical forms of *in situ* planetary atmospheric observations are surface components (mobile and non-mobile vehicles) equipped with versatile set of atmospheric instruments, aircraft capable of flying in the atmosphere, radiosondes, balloon-borne payloads and rockets. Lander investigations have a unique advantage, because they are able to provide long-term measurements of the atmosphere, which is of prime importance in determining the long-term trends involving the basic atmospheric features. On the other hand, also alternative forms of *in situ* investigations, *e.g.* laser-based sounding devices, are necessary because they provide *in situ* data on a large volume of the atmosphere, and they are also important in providing data outside the planetary boundary layer as well as on the boundary itself. However, it can be stated that a good strategy to perform *in situ* investigations of planetary atmospheres is to use payloads operating on the planetary surface for a long time. They give a better *in situ* science return on the resource investment than airborne *in situ* investigations. On the other hand, additional observation methods have an important role in complementing the results given by the *in situ* surface payloads.

We suggest that when performed simultaneously, the combined science return of the *in situ* and remote observations is greater than the sum of either of these forms of observations when performed separately, or in an uncoordinated fashion. In practice it means that having a strong remote sensing support for *in situ* observations - for instance in the form of atmospheric sounding payload orbiting the planet - is highly recommendable.

The number of stationary landing payloads on the planetary surface in order to conduct useful atmospheric science depends on the type of investigations planned. On the other hand, there is no drastic threshold level in the number of landers in order for a lander network to provide useful data for large-scale atmospheric investigations provided that there is a strong orbital support in terms of constant atmospheric observations. Even one surface observation post is extremely useful by providing an accurate global pressure reading and enabling local and mesoscale investigations, as well as by giving the ground truth for remote sensing observations. In general it can be stated that the more extensive global atmospheric investigation there is to be performed, the denser network of *in situ* observation stations is needed.

As far as instrumentation is concerned, it appears to be advantageous to procure the key sensor elements in large batches. We did this in 1989 by procuring pressure, temperature and humidity sensors in hundreds and performed separate qualification and acceptance tests on them. Thereafter the sensor performance was monitored at regular intervals. As a result we got sensors that were very good and which we also knew very well. We understood the performance of each sensor head after having tested and monitored them for many years. It should be underlined that additional sensor batches need to be exposed to similar type of qualification and screening tests. Sensors from the batches procured in 1989 were used in the Mars-96, Mars Polar Lander and Beagle 2 mission for Mars as

well as in the Huygens mission to Titan. The same sensors will also be used in some forthcoming planetary missions. Accordingly, with a relatively low procurement price per sensor we got a large number of excellent sensors. The investment on the sensor performance monitoring was modest compared to the vast enhancement of our knowledge on the sensors, which resulted in improved performance.

When defining the scientific objectives of a planetary mission, the available resources and the scientific ambitions of the planned investigation meet at the same trade-off table. The fewer surface observation posts a planned exploration mission includes, the more of the resources allocated to the investigation should be focused on making the scientific payload of the landers most comprehensive.

A specific form of atmospheric exploration is a network of observation posts covering the whole planetary surface. This type of a network would be required for Mars at present (*Haberle and Catling*, 1996) after the atmospheric information provided by Viking Landers, Mars Pathfinder, the MER Rovers and the various scientific satellites orbiting Mars. The network of observation posts around the planet are needed to resolve the space and time dependence of global and large scale atmospheric behavior, as indicated by equations 3.1 to 3.4. The functions of this type of a network cannot be performed by remote sensing observations, because the main requirement is to conduct atmospheric *in situ* observations around the planetary surface simultaneously.

The location of the atmospheric surface observation posts should be chosen based on the scale and focus of the investigation. When studying large scale phenomena and global circulation, the observation posts should be placed on locations with slowly varying surface conditions *e.g.* large plains, large areas with similar type of geographical, optical or thermal properties. In case of focusing investigations on mesoscale and smaller scale phenomena, it would be preferable to select observation locations involving significantly varying properties, like geography, surface albedo, thermal inertia. This would facilitate the determination of the exchange processes between the surface and the atmosphere, and other mesoscale and microscale phenomena on different types of a planetary surface. This knowledge can then be taken into account in the parameterization schemes of atmospheric modeling efforts.

Dust devils play an important role in the evolution of the Martian atmospheric dust-load, which in turn is a key parameter in the behavior of the Martian atmosphere (*Kieffer*, 1992; *Murphy*, 1996). The detection of the dust devils on time is a key issue, because dust devils are moving along with the wind. This requires a fast internal alarm system to start a special campaign measurement mode in case some atmospheric parameters show signs of a dust devil, or the dust devils could be probed ,*e.g.* by a laser-based sounding device. One option could also be the arrangement, where dust devil movements would be followed by analyzing the images taken by Mars orbiting platforms, and the early warning on approaching dust devils could be sent to the observation stations on Mars.

The current level of knowledge of the atmosphere of the planet under investigation plays a major role in the trade-off process between the number of landers, payload complexity and locations. It is reasonable from the point of view of science as well as investigation resources to start exploring a poorly known atmosphere at first by remote observations, and then with few in situ payloads

supported by remote observing platforms. How many is few in this context is then a trade-off between ambition and mission reliability, which then finally brings to the table the resources allocated to the particular investigation. The planetary missions described in this Summary (*e.g.* Mars-96, Huygens, NetLander, MetNet Mission) demonstrate solutions following this strategy.

Chapter 4

In situ planetary surface missions

4.1 Overview

Planetary *in situ* science missions contribute in an indispensable fashion to our knowledge of planets and the solar system. In practice *in situ* exploration is often performed by sending robotic vehicles to land and operate on the planetary surface or to float in the planetary atmosphere. The following sections introduce some of the *in situ* planetary missions and experiments where we have actively participated in the science definition and instrument development. They are mostly exploration missions or projects aiming at Martian research. We also participated in one Venusian atmospheric mission proposal (*Chassefiere et al.*, 2002). The last section of this chapter focuses on our contributions to the highly successful Huygens Mission to the Saturnian moon Titan.

When exploring planetary atmospheres the observation locations play a key role in the implementation of the investigation plans, as discussed in the preceding chapter. Deploying payloads on various types of sites and latitudes poses, however, stringent requirements on the landing vehicle's development as well as on the mission design. When jettisoning landing vehicles from an orbit around a planet, the specified location on the planetary surface can be reached with a higher accuracy than by deploying the vehicles from the planetary trajectory when still approaching the planet. The latter deployment method saves mass, because the mass of the landing vehicles is not part of the assembly that is decelerated and injected to the orbit around the planet. This method has been used by various planetary probes as described in Papers 1 and 6, and by, *e.g. Golombek et al.* (1999).

Deploying surface payloads at high latitudes of, for example Mars, is a challenge for the power supply system. The amount of solar radiation is too low to facilitate an effective solar radiation based energy supply. Power systems utilizing radionuclides are effective in that environment, but their usage is not favored due to the potential radioactive contamination. However, such systems have been used to provide electricity in many planetary probes. To reach, for

example Martian polar caps, radionuclide-based power supply systems appear to be a mandatory choice.

High elevations pose an additional challenge for surface vehicle deployment at planets with a thin atmosphere, as Mars. The higher in altitude the selected landing site the smaller is the atmospheric mass to decelerate the speed of the landing body. This requires that a high fraction of the total mass of the landing vehicle must be devoted to the landing systems. To overcome the various deployment constraints several landing vehicle concepts like hard, semi-hard and soft landing technology can be utilized, as discussed in 3.4 and in the original papers accompanying this Summary. Those papers deal with missions to the terrestrial planets in our solar system. They are either focused on atmospheric research, or central components of the missions cover atmospheric investigations.

4.2 Mars-96 Mission

The Mars-96 mission was an ambitious Martian exploration program encompassing an orbiter to perform remote observations of the Martian atmosphere and surface, two Small Stations, which were semi-hard surface landers, and two penetrators as described in Papers 3 and 6. We had a key role in the Mars-96 mission definition through the leadership of the Small Station feasibility Study (*Korpela et al.*, 1988; *Harri et al.*, 1988). During the mission development phase the responsibility of the command and Data Management System (CDMS) and the meteorological instrument package (MET) rested with us. This included data interface topologies between the scientific instruments and the CDMS as well as the mass, energy and data bandwidth distribution between the science payload and the service systems (*Harri et al.*, 1996). We also developed a part of the MET instrument package for the penetrators (Paper 3).

The landing vehicles, two Small Stations and two penetrators were to separate from the main spacecraft when still on the interplanetary transfer orbit. This jettisoning concept saves fuel mass, but on the other hand it poses more restrictions on the landing site selection than the deployment of landing vehicles from the Martian orbit would do. The Small Stations utilized a heat shield, parachutes and airbags during the entry, descent and landing phase. The station obtained the proper operating position through opening petals (Paper 3). The sequence of the Small Station landing on Mars is depicted in Figure 4.1.

The Small Station was a highly sophisticated piece of equipment. With the total available power of approximately 400 mW the Station supported an ambitious scientific program. The Station accommodated a panoramic camera, an alpha-proton-x-ray spectroscope, a seismometer, a magnetometer, an oxidant instrument, equipment for meteorological observations, and sensors for atmospheric measurements during the descent phase, including imaging by a descent phase camera. The total mass of the Small Station with payload on the Martian surface, including the airbags, was 32 kg (Paper 6).

The fourth stage of the Mars-96 launcher malfunctioned and hence the ambitious mission objectives were never really put on test. However, the state-of-the-art concept of the Small Station worked as a source of inspiration and guidance in the development of the successive NetLander and MetNet missions as described

by Chapters 4.3 and 4.6, and by *Harri et al.* (1999b); *Marsal et al.* (1999); *Harri et al.* (2003b).

The Mars-96 Mission observations on the surface of Mars, combined with data from orbiter instruments would have shed light on the contemporary Mars and its evolution. The specific science goals included exploration of the interior and surface of Mars, investigation of the structure and dynamics of the atmosphere, the role of water and other materials containing volatiles, and *in situ* studies of the atmospheric boundary layer processes.

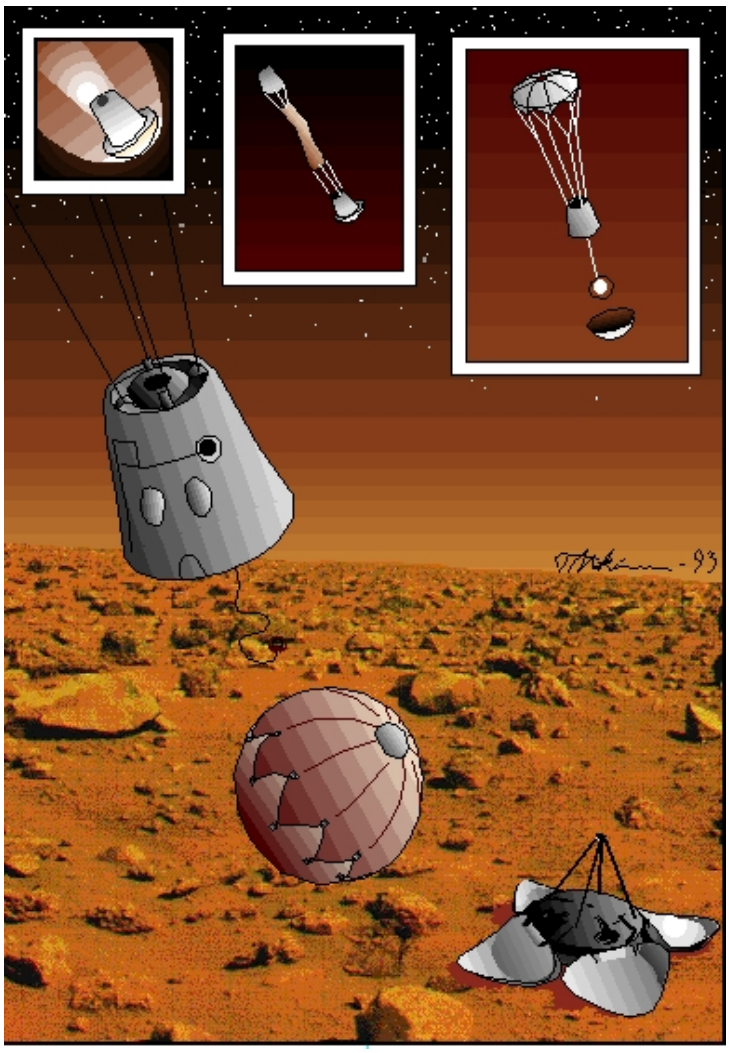

Figure 4.1: Illustration of the Mars-96 Small Station descending onto the Martian surface (artwork by Teemu Mäkinen). During atmospheric entry the Small Station utilizes a heat shield, later on parachutes and finally airbags when impacting on the Martian surface. The proper operating position is gained by opening petals (Paper 3).

The scientific objectives of the *in situ* atmospheric science experiments were defined, and the meteorological equipment of the landing elements of the Mars-96 mission were described with emphasis on the applicability for re-use in forthcoming Mars missions (Paper 3). The climatological cycles and atmospheric circulation, as well as the boundary layer phenomena can be understood thoroughly only if the contribution of *in situ* surface measurements are amalgamated with the remote observations. The Mars-96 mission was to deploy four versatile payloads at four Northern hemisphere sites. The observations of pressure, temperature, wind, atmospheric optical thickness and humidity, as well as pressure, temperature and density measurements during the atmospheric descent were included in the meteorology experiment. Even though the Mars-96 mission was unsuccessful, the objectives and implementation of the meteorology experiment are applicable to forthcoming landing missions to Mars. This applies both to missions having a number of observation sites spread over the surface of Mars, and to single landers or rovers.

The performance of the Mars-96 landing elements was severely constrained by the limited power supply. This prevented us from designing operation schemes where the *in situ* atmospheric observations are performed continuously, as would be needed. Therefore we developed operation modes involving observations performed at regular intervals, as well as burst and campaign modes with high sampling rate practically giving a continuous sampling scheme.

It is particularly challenging to determine the diurnal atmospheric turbulence structure with the available energy constraining the number of observations per sol. To overcome this obstacle, we developed a specific measurement mode where high speed observations are performed continuously for a certain time slot of the sol, and this is repeated the next sol continuing at the local time where the observations were halted on the preceding sol. This procedure enables us to record the diurnal turbulence provided that the diurnal variation of the turbulence structure is small during the sols this observation mode is completed. The longer the high speed observation time per sol we can make, or the smaller the diurnal turbulence structure variation is, the better picture will be obtained from the atmospheric turbulence structure and its diurnal variation.

The Mars-96 Small Station was state-of-the-art equipment that supported a highly challenging scientific program with a total available power of approximately 0.4 W. Had the mission succeeded, it would have placed us in a much better position to define the Mars missions that came later. However, even the Mars-96 development work was indispensable in giving us the experience and insight to define the NetLander and MetNet Mars missions.

4.3 NetLander Mars Mission

The FMI team initiated the NetLander mission to fulfill the scientific objectives missed by the Mars-96 mission. The goal of the NetLander mission was to deploy four landers carrying a geophysical instrumentation payload on the Martian surface. We led the mission definition phase and the feasibility study phase, which resulted in the mission proposal that was submitted to ESA in response to the Mars Express Announcement of Opportunity (*Harri et al.*, 1999a; *Marsal*

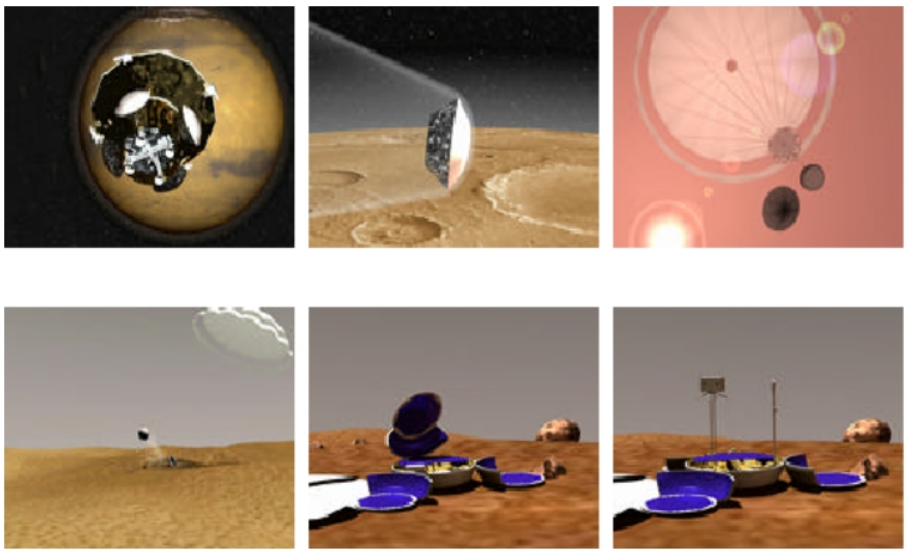

Figure 4.2: The NetLander vehicle speeding through the Martian atmosphere. The vehicle is decelerating by means of a heat shield and parachutes, and the landing impact is absorbed by airbags (artwork by Teemu Mäkinen). The Netlander mission was to include four landing vehicles forming a geophysical observation network (*Harri et al.*, 1999b).

et al., 1998).

We were also responsible for the development of the atmospheric science experiment (ATMIS) carried by the NetLander vehicles as described by *Harri et al.* (1999c), as well as by Papers 5 and 1. The NetLander mission development work made considerable use of the lessons learned during the Mars-96 mission. Later on the NetLander mission took the form of an independent European network science mission to Mars (*Marsal et al.*, 1999).

The NetLander Mission was to be the first planetary mission focusing on the investigations of the interior of the planet and the large-scale circulation of the atmosphere, as well as the ionospheric structure and geodesy, as described by Paper 1 and also by *Marsal et al.* (1999); *Harri* (2001). The investigations were to be performed by surface landers deployed on the Martian surface to conduct simultaneous seismological, atmospheric, magnetic, and geodetic measurements, supported by panoramic images. The payloads also included entry phase measurements of the atmospheric vertical structure, but due to mass optimization reasons this section was eventually descoped from the NetLander payload (*Marsal et al.*, 1998). The scientific data was to be combined with simultaneous observations of the atmosphere and surface of Mars by the Mars Express Orbiter and the Mars Odyssey orbiter that were expected to be functional during the NetLander Mission's operational phase on the Martian surface (*Harri et al.*, 2003a).

The landers were to be separated from the spacecraft and targeted to their

locations on the Martian surface 10 to 20 days prior to the spacecraft arrival at Mars. The entry, descent and landing system included parachutes and airbags. After impacting on the Martian surface the Netlander vehicle was anticipated to bounce several times off the ground and roll over the Martian terrain for some time. This sequence is depicted in Figure 4.2. After halting its motion the vehicle was to wait for a while to allow the parachute to be blown away by the wind. Thereafter the opening petals were to turn the vehicle into the proper operating position and to deploy the instrument booms, as well as to expose the solar panel surfaces to solar radiation. The concept of the Netlander vehicle in its operational position with its instruments deployed is presented in Figure 4.3. During the baseline mission of one Martian year, the communication between the landers and the Earth was planned to take place via a data relay onboard the Mars Express, Mars Global Surveyor and Mars Odyssey orbiters around Mars (*Harri et al.*, 1999b; *Marsal et al.*, 1999).

The NetLander mission was eventually canceled after four years of hectic development work. The final mission goal was never accomplished, but we learned various practical ways of tackling the mission development work. This included, among other things, the optimization of the integration level of the instrumentation and electronics as well as the possibility to optimize the overall payload mass by challenging the importance of a heavy rechargeable battery and the accompanying thermal isolation and heat removal systems. Eventually, the NetLander

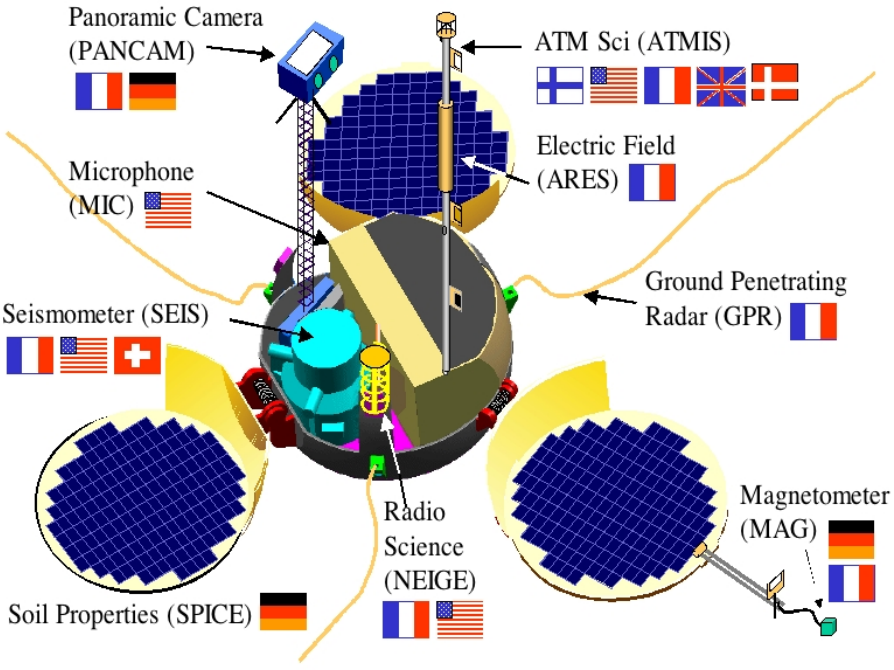

Figure 4.3: Illustration of the NetLander vehicle at the Martian surface (artwork by Teemu Mäkinen). The petals have opened and the scientific payload is indicated with the teams responsible for the instruments (*Marsal et al.*, 1999).

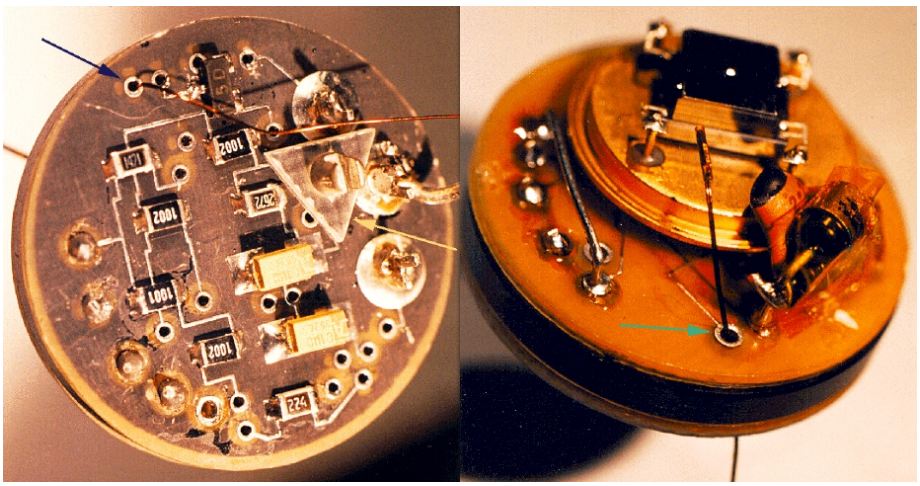

Figure 4.4: Photo of the EGA-P device for the Mars Polar Lander's Evolved Gas Analyzer instrument. The picture shows both sides of the device's electronics board. The diameter of the device's outer envelope was 25 mm and height 15 mm (*Harri et al.*, 1997).

system was implemented with a concept that divided the data management and power distribution responsibilities to the subsystems, *e.g.* to the science instruments. This granted relatively high level of autonomy to the subsystems and simplified the interface control tasks. On the other hand this implied that the amount of required system resources, like overall mass and energy, were higher than in the case where the lander system and subsystems would be more tightly grouped together.

4.4 MET-P and EGA-P for Mars Polar Lander

As part of NASA's Mars Surveyor Program, the Mars Polar Lander (MPL) spacecraft was launched towards Mars in January 1999, carrying onboard the lander and two penetrator probes provided in the frame of the Deep Space 2 (DS2) program (*Smrekar et al.*, 1997). Unfortunately, due to the failure in a descent system, the MPL crashed to the Martian surface on December 3, 1999. We participated in the mission by providing MET-P (device dimensions with housing were mass 45 grams, dimensions 55x45x25 mm) and EGA-P (mass 15 grams, dimensions 15 x Ø 25 mm) miniaturized pressure devices for the lander (*Harri et al.*, 1997). MET-P was part of the Martian meteorological instrument (MET), whereas EGA-P was a support device in the Evolved Gas Analyzer (EGA) instrument. Photos of the EGA-P device are depicted in Figure 4.4.

The MET-P provided data at the health check measurement periods during the interplanetary cruise phase to Mars. The last bits of data were acquired prior to the incident, when the Mars Polar Lander entered the Martian atmosphere. The MET-P data were analyzed on the Earth and the device was found to operate as expected.

The Mars Polar lander was targeted to a southern high latitude site, and was expected to enter the Martian atmosphere directly from the hyperbolic transfer orbit at a velocity of 7 km/s in December 1999 (L_s 257°). It was to make a soft landing on Mars after decelerating by means of atmospheric drag (heat shield), a parachute, and guided propulsion. The two penetrators (Deep Space 2) were released from the MPL prior to the atmospheric entry. The Mars Polar Lander was planned to provide the first surface-based observations in the southern hemisphere of Mars and in the polar regions.

The planned landing time was in late southern (Martian) spring. This is an optimal time for operations at a southern high latitude site, because the Sun is always above the horizon during the time of the primary mission. The environmental conditions are relatively mild and a relatively large amount of solar energy is available. The MPL primary mission was to last only 85 Martian days to optimize the probability of success with the total operational costs. An additional secondary mission (123 days) was to take place during the southern winter, when solar energy supply is low and environmental conditions are harsh.

The MPL was directed to land on a site at 71 S, 210 W, which is at the most equatorward boundary of the south polar-layered deposits. These deposits are of great geological interest. The layers are believed to be composed of ice and dust that has accumulated in the polar region in response to variations in the Martian climate due to oscillations of Mars' orbital and axial elements. The Mars Polar lander carried an integrated payload called Mars Volatiles and Ancient Climate Surveyor (MVACS), which was developed to address the Martian volatiles and climate history (*Paige et al.*, 1998; *Smith et al.*, 2001). The payload instruments and their scientific objectives included

- Surface Stereo Imager (SSI): Multispectral stereo images, Atmospheric column aerosol and H_2O vapor;
- Robotic Arm (RA) / Robotic Arm Camera (RAC): Surface and subsurface sample acquisition; MET wind/temperature sensor deployment; close-up surface and subsurface images;
- Meteorology Package (MET): Atmospheric pressure, wind temperature and surface H_2O vapor concentration;
- Thermal and Evolved Gas Analyzer (TEGA: Abundances of water ice, adsorbed CO_2 and H_2O, and volatile-bearing minerals in surface and subsurface samples.

The MPL was equipped to answer some of the most fundamental questions related to Mars volatiles and Mars climate history. A key feature of the mission was its high-latitude landing site, which makes it possible to address its unique science goals (*Paige et al.*, 1998).

The two Deep Space 2 penetrator-type microprobes had a rigid aeroshell by means of which the microprobe velocity was reduced to approximately 200 meters per second prior to impacting on the surface (*Smrekar et al.*, 1997; *Harri et al.*, 2000). After impact the forebody containing temperature sensors and a water detection device was to penetrate the Martian soil maximally down to 2 meters. The aftbody was supposed to remain on the surface to relay data back

to the Earth via the Mars Global Surveyor spacecraft, which has been orbiting Mars since September 1997. The forebody and aftbody were connected to each other via a flexible cable for communications purposes. The Microprobe mass at the point of atmospheric entry was about 6 kg.

The DS2 atmospheric entry system was designed such that the heat shield is passively aligned to the right position prior to peak heating even if the system is tumbling upon atmospheric entry. The probes utilized a 1-cascade system concept that did not include jettisonable aeroshells. The probes were to carry the aeroshells to the surface where they shatter on impact. This reduces the number of tests required to demonstrate their design, and thus greatly reduces mission costs.

The Mars Polar Lander and the DS2 microprobes failed to reach their final objectives, but they provided valuable experience for mission definition as well as for descent systems development. Our MET-P device provided high-quality data at the health check measurement periods during the interplanetary cruise phase to Mars, and thus demonstrated the performance of the device. The experience we gained by participating in the Mars Polar Lander mission also contributed significantly to the practices of developing miniaturized instrumentation like the MET-P and EGA-P. And this experience was capitalized in subsequent science missions like the NetLander, Beagle 2 and MetNet missions to Mars.

The Mars Polar Lander aimed at investigating the Martian polar regions, specifically the southern pole. Polar regions play a central role in the inflow of atmospheric mass into the polar CO_2 caps and back to the atmosphere, and in other atmospheric phenomena. The importance of atmospheric investigations at the Martian polar regions and investigation goals are discussed, *e.g.* by *Clifford et al.* (2000).

4.5 BAROBIT onboard Beagle-2 Mission

The Mars Express mission, successfully launched toward Mars in June 2003, carried a surface component, the Beagle 2 lander (*Pullan et al.*, 2004). Unfortunately, the Beagle 2 vehicle was destroyed when landing on the Martian surface on December 25, 2003. We participated in the Environmental Sensor Suite (ESS) (*Towner et al.*, 2004) of the lander by providing the BAROBIT pressure device. The BAROBIT (dimensions 30 x 30 x 10 mm, mass 15 grams) is a derivative of the MPL EGA-P device addressed in Chapter 4.4. The Beagle 2 lander prototype with its petals opened is shown in Figure 4.5.

The ESS was designed to investigate the environmental conditions at the landing site. The sensor suite was planned to measure air temperature at two heights, surface level pressure, wind speed and direction, saltated grain momentum, UV flux (diffuse and direct at five wavelengths), the total accumulated radiation dose and to investigate the nature of the oxidizing environment. The ESS was designed to monitor and characterize the current local atmospheric conditions. The investigations were focused on specific areas of scientific interest identified during previous Mars missions, most notably dust transport and transient phenomena (*Towner et al.*, 2004).

Figure 4.5: The prototype of the Beagle 2 lander, the arrow is showing the BAROBIT location. BAROBIT was a EGA-P type device (shown in figure 4.4) with dimensions of 30 x 30 x 10 mm and 15 grams. The Beagle 2 lander body was 0.7 m in diameter (*Towner et al.*, 2004).

4.6 MetNet Mars Mission

The unfortunate cancellation of the NetLander mission underlined the need of atmospheric *in situ* observations at Mars. While the NetLander and Mars-96 missions targeted a wide range of geophysical science disciplines, there remained a need for a mission that would focus more directly the atmospheric science objectives. To that end the MetNet mission concept was developed.

We initiated a new type of atmospheric science mission for Mars. The MetNet Mars Mission is to deploy a network to the Martian surface consisting of some tens of atmospheric science observation posts. This type of a network will enable simultaneous *in situ* observations all over the Martian surface. The network is designed to operate for several Martian years, which facilitates detailed characterization of the Martian circulation patterns, boundary layer phenomena, and climatological cycles. The payload and landing vehicle development work benefits significantly from the experience gained during Mars-96, NetLander, Mars Polar Lander and Mars Express missions. We developed concepts of designing highly integrated packages of space science instruments and system devices

during the Mars-96 Mission, and thus enhanced our experience in the course of the subsequent missions. The currently ongoing MetNet mission is being developed in collaboration between the Finnish Meteorological Institute (FMI), the Babakin Space Center (BSC) and the Russian Space Research Institute (IKI) as described by *Harri et al.* (2003b).

The mission endeavors to develop an extensive atmospheric science payload onboard a landing vehicle that requires fewer pyrotechnical commands and less mass in the entry, descent and landing system (EDLS) than the traditional parachute-based EDLS (*Harri et al.*, 2003b, 2004b). The EDLS is depicted in Figures 4.6, 4.7 and 4.8. Additionally, the vehicle and payload are designed to survive hard landing on the Martian surface. The mass optimization target is approached from both the EDLS and the payload design. To survive the hard impact the payload will be densely integrated without easy-to-use disassembling capability, which will give mass savings. Optimizing the total mass to payload mass ratio requires that the payload design and manufacturing processes must be performed in a unified fashion, essentially by one design team.

The novel idea behind the MetNet landing vehicles is to use state-of-the-art inflatable entry and descent systems instead of rigid heat shields and parachutes

Figure 4.6: Two MetNet vehicles being separated from the spacecraft. Separation takes place before reaching the Martian orbit to save fuel mass (*Harri et al.*, 2003b).

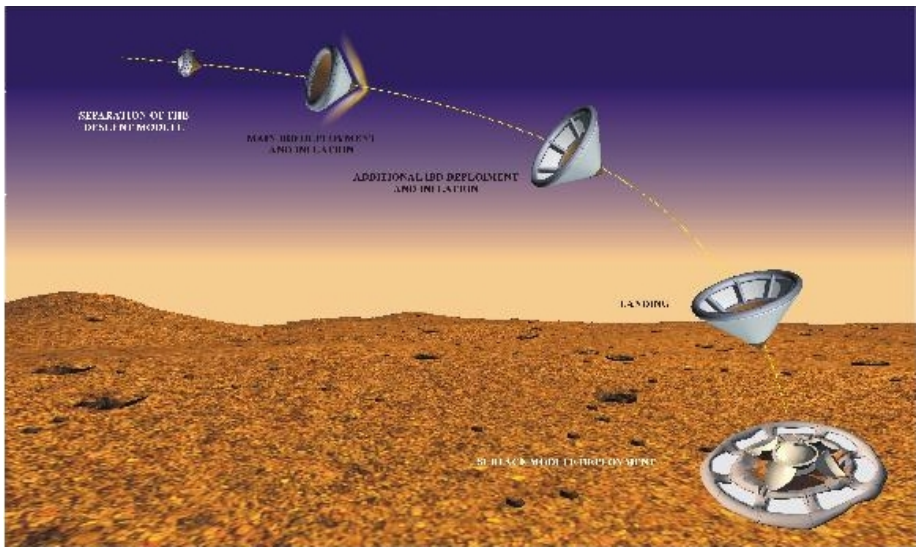

Figure 4.7: Entry, descent and landing scenario of the MetNet landing vehicle based on inflatable structures. The specified maximum impact shock on the Martian surface is 500g. The vehicle obtains proper operations attitude through penetrating into the Martian soil, which also serves as one deceleration mechanism (*Harri et al.*, 2003b)

that earlier semi-hard planetary landing devices have used. This way the overall reliability is increased due to diminished number of pyrotechnical devices, the ratio of the payload mass to the overall mass is optimized, and more mass and volume resources are spared for the science payload. This semi-hard landing vehicle using inflatable descent system structures is called the Mars Meteorological Lander (MML).

The scientific payload of the MetNet Mission encompasses separate instrument packages for the atmospheric entry and descent phase and for the surface operation phase. For the descent phase an imager, accelerometers and devices for free flow pressure and temperature observations are envisaged. At the Martian surface the MML will take panoramic pictures, and perform measurements of pressure, temperature, humidity, wind direction and speed, as well as atmospheric optical depth.

The scope of the MetNet Mission is eventually to generate the observation network over the course of several years. This is possible due to the fact that the MML lifetime is designed to be a few years. Hence the network can be established and expanded by sending MMLs to Mars using launches in successive launch windows. This strategy also mitigates the risk of losing the network by one single launch failure. The first real mission step is to have a MetNet Precursor Mission with a few MMLs deployed to Mars. Partnership discussions are being conducted with other space organizations.

The MetNet development work has been going on since autumn 2001. Initially, five different entry, descent and landing system scenarios were investi-

gated. One of them was the traditional parachute-based system, the rest of the analyzed concepts were based on using inflatable structures to decelerate the vehicle descending into the Martian atmosphere (*Pichkhadze and Linkin*, 2002c; *Pichkhadze et al.*, 2002). Figure 4.9 presents the MetNet vehicle in the form it assumes just prior to impacting on the Martian surface. The chosen concept for the MML entry, descent and landing system is composed of the following systems and units (*Pichkhadze and Linkin*, 2002a):

- Surface module that finally stays at the Martian surface;
- Rigid section of front aerodynamic shield;
- Inflatable heat protection section;
- Main inflatable decelerating device (IBU) with gas generator and load-bearing elements;
- Additional IBU with gas generator;
- Forebody with shock-absorbing system.

As a result of detailed studies in 2001 - 2002 the chosen descent system scenario was found to be feasible for Martian exploration. The capabilities of the system parts were examined by numerical simulations. In 2002 - 2004 the new descent system prototype was manufactured (*Pichkhadze and Linkin*, 2002b, 2003) and

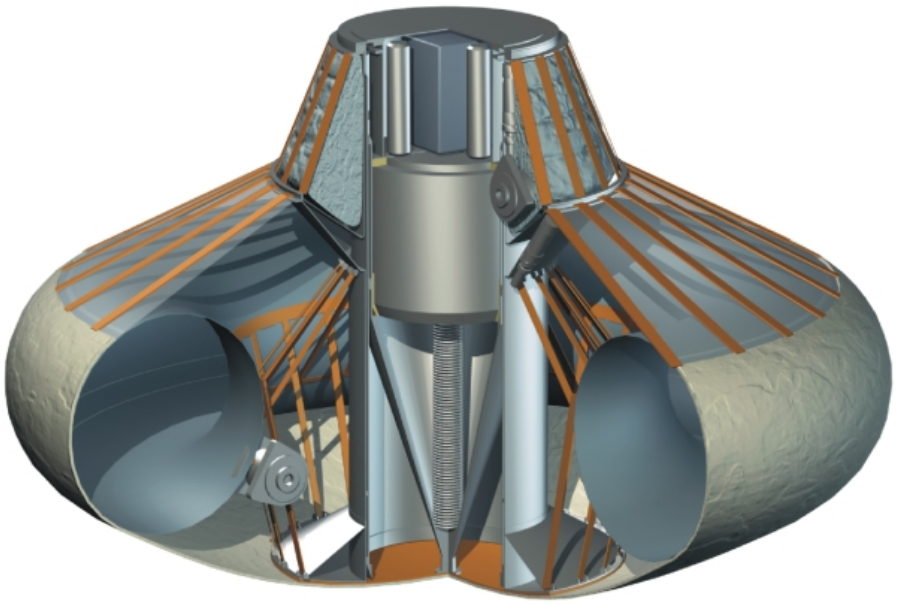

Figure 4.8: MetNet vehicle in the entry configuration. The inflatable heat shield with the diameter of 1.0 m has been coated with an ablative material for thermal protection (*Harri et al.*, 2003b).

Figure 4.9: MetNet landing module in the configuration prior to the landing impact on the Martian surface. The diameter of the torus-shaped main decelerating structure is 200 cm, and the height of the penetrating body in front of the module is 87 cm (*Harri et al.*, 2003b).

key parts were exposed to environmental tests to qualify the design for the conditions the system will encounter during the entry into the Martian atmosphere. The tests were successful and demonstrated the applicability of the developed MetNet concept for Mars (*Terterashvili et al.*, 2003; *Rogovskaya et al.*, 2003)

At present the MetNet prototype has been developed and the critical subsystems have successfully passed the proper environmental and functional tests. Currently a suborbital test launch by a Russian SS-19 missile is under preparation to test the descent systems. This test will take place in 2005: the test prototype will be launched into space and made re-enter the atmosphere of the Earth with the same velocity and entry angle with which the probe will eventually enter the Martian atmosphere. A photo of the MetNet prototype with FMI MetNet team is depicted in Figure 4.10.

The individual MetNet vehicle (MML) deployment to the Martian surface takes place in the following fashion (*Harri et al.*, 2003b):

- Spacecraft is targeted and the MML is separated when still on the approaching path to Mars; this is more economical than jettisoning the MML from Martian orbit.

- Autonomous flight to Mars (from a few days up to some weeks).

- Entry into the Martian atmosphere. The inflatable heat shield is deployed at the Mach number (M) of approximately 29. At this phase the vehicle speed is reduced from supersonic speed to subsonic speed.
- The additional inflatable deceleration structure is deployed when the speed is reduced to $M \cong 0.8$. By means of this device the speed of the landing vehicle is reduced to about 70 m/s by the time the vehicle reaches the Martian surface.
- Impact onto the Martian surface (maximal deceleration 500g over the time of 50 ms) and penetration into the soil thus obtaining a proper operating attitude.
- Systems start-up and checkout.
- Scientific investigations program.

The overall reliability of the developed MML concept using a two-cascade approach was found to be 1.7 times more reliable than the traditional parachute -based landing concept. The mass gain seems to be only of the order of 10% when compared to the parachute -based landing system (*Pichkhadze and Linkin*, 2002a).

Figure 4.10: Prototype of the MetNet entry vehicle has been fabricated and all the key descent systems have been exposed to the entry conditions. This figure shows the MetNet prototype with FMI MetNet team from left: P. Makkonen, H. Lappalainen, B. Fagerström, and A.-M. Harri.

Optimal locations of the MetNet observation posts at the Martian surface depend on the total amount of the network elements as discussed in Chapter 3.7. If the network consists of only a few observation posts, it is worthwhile to either create a small local network or to place the posts on different types of terrain and latitudes. This would encompass differences in altitude, latitude and type of surface. In all cases we should place observation posts also on the locations, where observations were previously performed by the Viking Landers and the Mars Pathfinder. This would enable us to compare the current atmosphere at those sites to the atmospheric conditions prevailing earlier. This would be especially interesting at the Viking Lander sites, where observation records of several Martian years are available. Repeating atmospheric observations at those sites now could even facilitate climatological investigations.

Access below the Martian surface provides the MetNet mission with some unique opportunities for studying the Martian soil. We hope to look for the presence of subsurface water by means of a water ice detection device mounted at the front part of the penetrating vehicle body. Also, we envisage studying the thermal conductivity of the soil by measuring the rate at which the probes cool down after impact. To accomplish this, temperature sensors have to be mounted on the forebody structure.

If the number of observation posts is of the order of 20 or more we can already create a global network (*Haberle and Catling*, 1996). If the number of observation posts would significantly exceed 20 it is possible to create a global network including a section were the observation post density is remarkably higher than elsewhere. This dense section would be placed on an area of particular interest from the atmospheric science point of view, *e.g.* in the vicinity of expanding and retreating polar caps, Hellas region or Valles Marineris.

The MetNet mission will be an excellent tool for enhancing our understanding of the Martian atmosphere. Having a network of *in situ* instrument payloads all over the Martian surface operating simultaneously is what the scientific community has dreamed of for decades. This can now be realized using the MetNet concept.

The MetNet mission is currently taking its shape and the mission development organization is being put together. The first mission step is to have a MetNet Precursor Mission with a few MMLs deployed to Mars slated for launch in 2009 or 2011 (*Harri et al.*, 2004a).

4.7 PPI/HASI for Titan

The Huygens entry probe was developed to study the atmosphere and surface of Saturn's largest moon Titan. It is a very interesting planet-sized moon that has a thick nitrogen-rich and chemically active atmosphere. The Huygens probe carried instrumentation capable of conducting detailed in-situ observations of the physical properties, chemical composition and dynamics of the atmosphere and local characterization of the surface. It is a highly sophisticated robotic laboratory carrying six scientific instruments. Huygens is the element contributed by ESA to Cassini/Huygens (*Lebreton and Matson*, 2002; *ESA*, 2005), the joint NASA/ESA/ASI dual-craft mission to the Saturnian system.

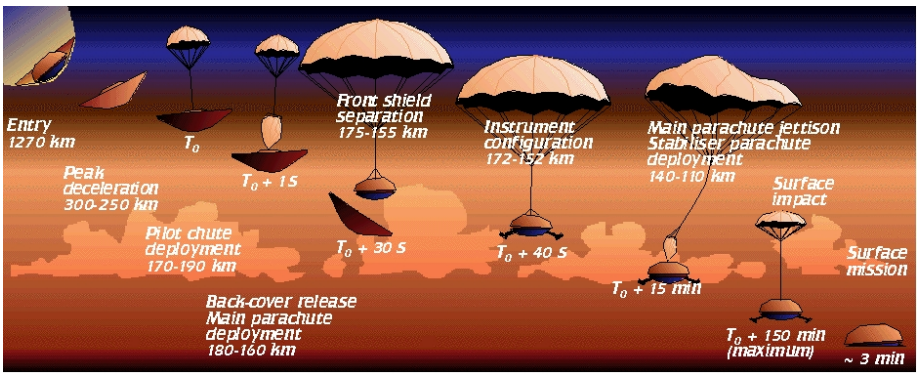

Figure 4.11: Artist's depiction of the Huygens probe's descent in the atmosphere of Titan (artwork by Teemu Mäkinen). The deceleration rate was adapted such that the probe reached the ground a few minutes before the Cassini spacecraft vanished beyond the horizon.

The Cassini/Huygens launch occurred on 15 October 1997 during the primary launch window. Huygens was dormant during the long interplanetary journey. The probe was activated about every 6 months for an in-flight checkout to verify and monitor its health and to perform a periodic maintenance and calibration of the payload instruments. After an interplanetary journey of about 7 years, the spacecraft arrived at Saturn in late June 2004, when a trajectory maneuver placed it in orbit around Saturn. The Huygens probe was targeted to Titan and released from the Cassini Orbiter on December 25, 2004. During the 3-week coast phase Huygens was powered off with the exception of a timer unit that awakened the probe before its parachute-assisted journey through Titan atmosphere, as depicted in Figure 4.11.

The Huygens mission was successfully executed on January 14, 2005. The descent took place during 2.5 hours consisting of a fierce entry into Titan's atmosphere followed by more gradual descent through the atmosphere by means of three parachutes. After impacting on the surface Huygens continued observations planned to go on as long as the batteries and other system devices survived. Throughout the descent phase Huygens transmitted data continuously to the Cassini spacecraft. The Huygens mission was eventually terminated after 30 minutes of observations at the surface, when Cassini went beyond the horizon and the radio contact was lost. Thereafter Cassini relayed the Huygens data back to the Earth (*Lebreton and Matson*, 2002). After the Huygens active mission was over the Cassini spacecraft continued its nominally 4-year mission to explore the Saturnian system (*Matson et al.*, 2002; *ESA*, 2005).

The Cassini Orbiter will perform altogether 45 targeted close flybys of Titan, collecting data about the moon. The detailed set of *in situ* observations acquired by the Huygens probe and the global data set to be gathered by Cassini will provide a unique file of information that will substantially increase our knowledge of Saturn's largest moon, Titan.

Cassini will perform detailed observations of Saturn's atmosphere, magneto-

sphere, rings, and moons. It will also make a complex tour around the other satellites of Saturn helped by gravity-assisted orbit changes. It will also explore the dynamic interactions between the magnetosphere, the solar wind, Saturn and its satellites (*Matson et al.*, 2002).

The Huygens probe carried onboard the Huygens Atmospheric Structure Instrument (HASI) when entering the Titan atmosphere. During the 2.5-hour descent into Titan's atmosphere HASI observed a comprehensive set of variables encompassing pressure, temperature, density and atmospheric electricity (*Lebreton and Matson*, 2002). The Pressure Profile Instrument (PPI) provided by the Finnish Meteorological Institute (FMI) recorded the Titan atmospheric vertical pressure profile. A photo of the PPI flight unit prior to delivery is presented in Figure 4.12.

The HASI experiment was divided into four subsystems: accelerometers (ACC); deployable booms system (DBS); the stem (STUB) carrying the temperature sensors, a Kiel probe pressure sampling inlet, an acoustic sensor, and the data processing unit (DPU). Scientific measurements were performed by four instruments: the accelerometers (ACC), the temperature sensors (TEM), the Permittivity, Wave and Altimetry package (PWA), and the Pressure Profile Instrument (PPI) as described by *Fulchignoni et al.* (2002). In addition to the proper space instrument tests the HASI instrument performance was also verified by several balloon flights in the atmosphere of the Earth as presented in Paper 7 and in *Fulchignoni et al.* (2004). The principal sections of PPI are:

- Sensor boom extending out of the Huygens main body,
- Kiel probe with pitot tube at the end of the sensor boom
- Pressure hose conveying the pressure signal from the Kiel probe to the

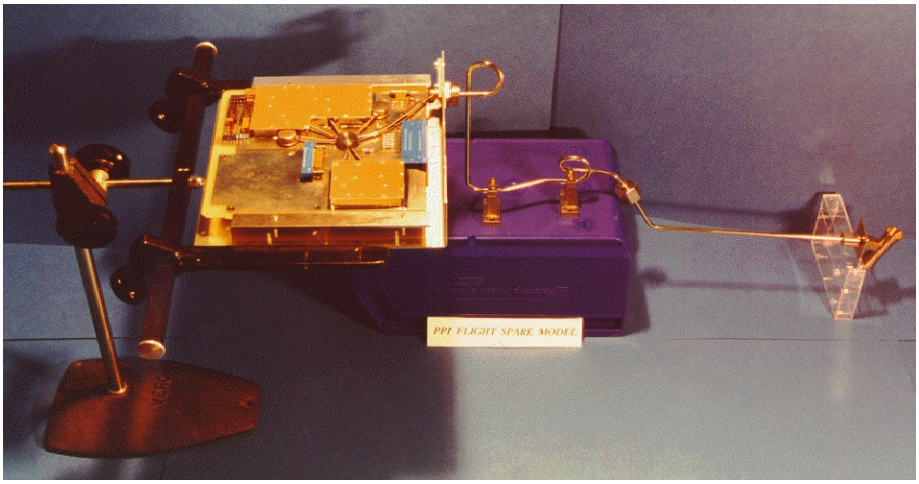

Figure 4.12: The flight unit of the Pressure Profile Instrument (PPI) prior to being delivered to the HASI/Huygens system tests. In its eventual location at the Huygens probe the last 20 cm of the pressure pipe in the right of the figure extends outside the probe.

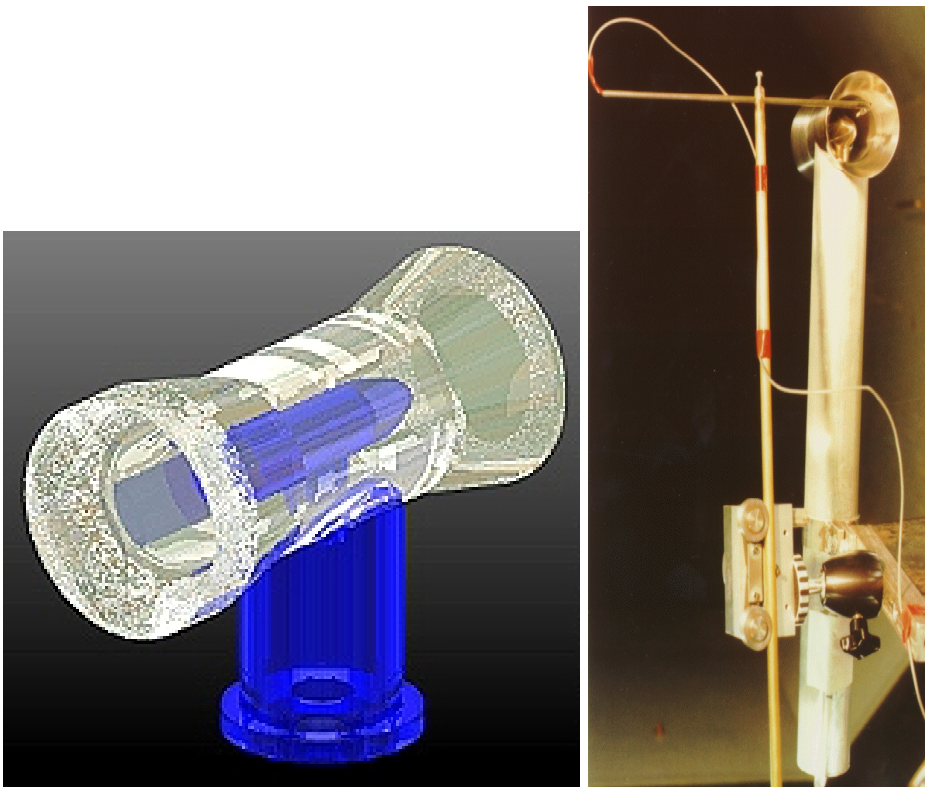

Figure 4.13: The pressure profile instrument's pitot tube was surrounded by a Kiel-type tube, by means of which the PPI is insensitive to the varying angle between the pitot tube's main axis and the streamlines. The internal structure of the Kiel-type pitot tube is depicted on the left pane (image created by T. Mäkinen), whereas the right pane photo is taken at the wind tunnel tests.

pressure sensors and

- Pressure sensors (Barocap®) and the associated sensor and system interface electronics inside the Huygens body.

The decision to measure total pressure instead of static pressure was based on the fact that during the descent in the Titan atmosphere the static pressure varies significantly in the proximity of the Huygens probe. Figure 4.14 presents the simulated strongly varying pressure coefficient and streamline fields around the descending Huygens probe (*Hoffren et al.*, 1992). The direct measurement of the free flow static pressure would have required positioning of the static pressure measurement head of the order of 1 meter away from the Huygens probe. This was not feasible from the system resources point of view. Therefore we had to measure the total pressure, which is invariant around the descending probe (*Laine et al.*, 1991).

Detailed analysis of the measurement concept and the final decision to measure the total pressure instead of the free flow static pressure was based on aerody-

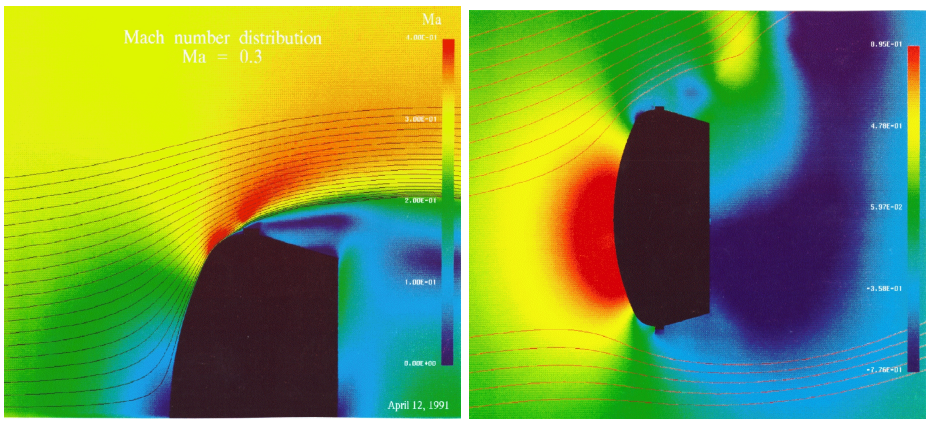

Figure 4.14: Simulated pressure coefficient C_p and streamlines of the flow around the descending Huygens probe. The left panel describes the situation at Mach number 0.3 with zero angle of attack, the right panel at 0.6 M (10° angle of attack) (*Laine et al.*, 1991; *Hoffren et al.*, 1992).

namic simulations (*Siikonen et al.*, 1990; *Siikonen*, 1991). They were performed for the airflow around the Huygens probe and in the vicinity of the tip of the sensor boom (*Laine et al.*, 1991; *Hoffren et al.*, 1992; *Kivekäs*, 1992). The results were verified by extensive wind tunnel tests (*Renko et al.*, 1992).

During the descent in the Titan atmosphere the attack angle of the Huygens probe was constantly changing. Hence a pitot tube alone would not give a reliable pressure reading. By using the Kiel probe the total pressure reading is insensitive to the angle between the streamlines and the Kiel probe up to 45° (*Renko et al.*, 1992). The PPI pitot tube surrounded by a Kiel-type tube is depicted in Figure 4.13.

The PPI used pressure sensors with three different sensitivities to cover the pressure range of 0..180 kPa. The sensor technology was inherited from a concept that has been applied in earlier space and terrestrial applications. The PPI instrument concept was successfully tested along the whole Huygens probe payload by a special balloon test session simulating the actual Huygens mission as described in Paper 7 and by *Fulchignoni et al.* (2004).

The primary scientific objective of the PPI instrument was to determine the vertical ambient pressure profile of the atmosphere of Titan during the Huygens descent. The PPI measurements started at the altitude of 160 km at Mach number of about 0.6 and continued a few minutes beyond the impact to the Titan surface. To obtain the Titan atmospheric pressure profile, a thorough amalgamation of all the HASI data was carried out. Moreover, data from the altimeter, the wind experiment, and the surface science package were used (*Bird*, 2005; *Zarnecki*, 2005; *Lebreton*, 2005). The profiles of atmospheric pressure, density, temperature, and the mean molecular weight were obtained via iterative means for each data point along the descent trajectory as described in Paper 2 and by *Fulchignoni et al.* (2005):

$$\begin{cases} \rho & = -\dfrac{2ma_s}{C_D A V_r^2} \\ \dfrac{dp}{dz} & = -g(z)\rho(z) \\ T(z) & = \dfrac{p(z)\mu}{R\rho(z)} \end{cases} \tag{4.1}$$

where ρ is the atmospheric density, m is the probe mass, a_s is the acceleration along the path of the Huygens probe, C_D is the drag coefficient, A is the cross-sectional area of the probe, V_r is the probe speed relative to the atmosphere, p is the atmospheric pressure, g is the acceleration of gravity, z is the altitude from the surface of Titan, T is the atmospheric temperature, μ is the mean molecular weight, and R is the gas constant.

The lower part of the Titan atmosphere is too thick for the ideal gas approximation to be valid throughout the atmosphere. Therefore, when generating the atmospheric profile using equation 4.1, a more accurate approximation will be obtained by using the real gas approach as pointed out by *Mäkinen* (1996).

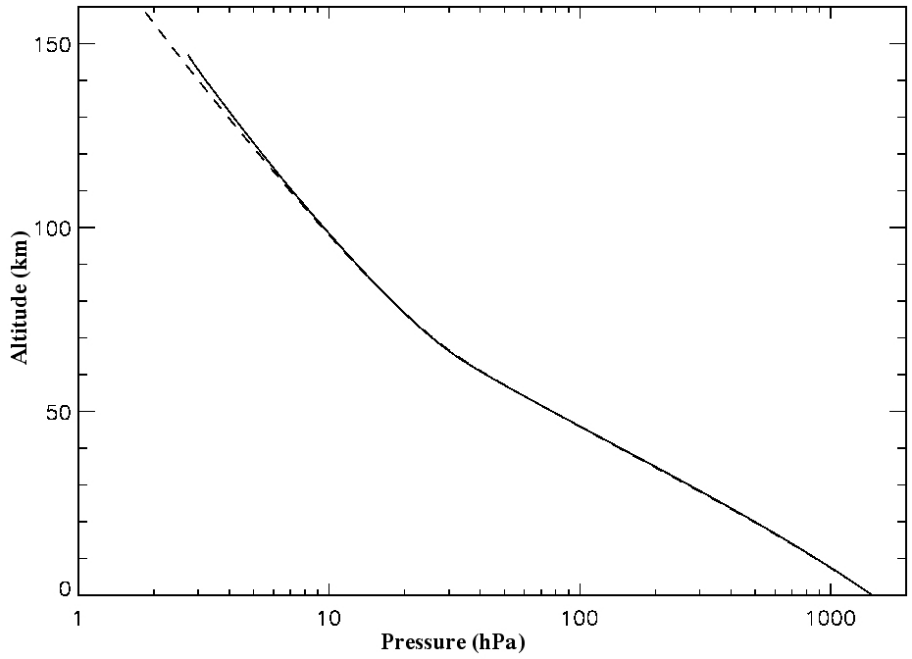

Figure 4.15: The Titan atmospheric pressure (in hPa, abscissa) as a function of altitude (in km, ordinate) measured by the PPI /HASI instrument (solid line) during the descent of the Huygens probe as a result of the first order data analysis of the PPI measurements in the Titan atmosphere (figure by PPI-team). The nominal pressure profile provided by the Titan atmospheric engineering model (*Yelle et al.*, 1997) differs from the actual values by a few per cents (dashed line).

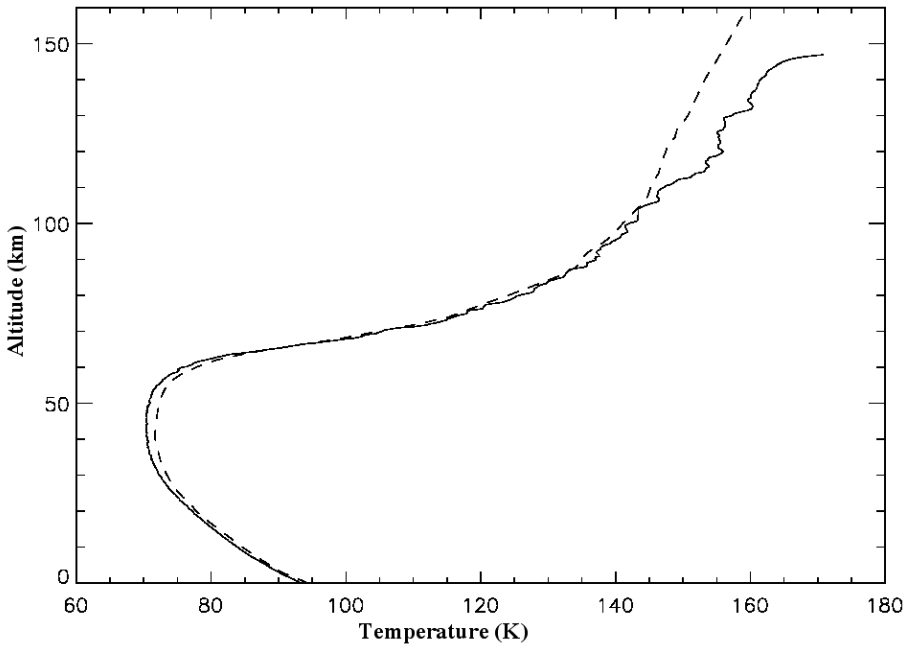

Figure 4.16: The Titan atmospheric temperature (in Kelvin, abscissa) as a function of altitude (in km, ordinate) measured by the TEM /HASI instrument (solid line) in the Titan atmosphere (figure by PPI-team). The temperature profile by the Titan atmospheric engineering model (*Yelle et al.*, 1997) differs from the actual values by a few per cents (dashed line) (*Fulchignoni et al.*, 2005).

When the Huygens probe moves through the Titan atmosphere it is surrounded by a flow-induced pressure field, where the local static pressure differs from that of the undisturbed atmosphere. A non-dimensional pressure coefficient is defined as

$$C_p = \frac{p - p_\infty}{q} = \frac{p - p_\infty}{\frac{\kappa}{2} p_\infty M^2} \tag{4.2}$$

where p is the local pressure, p_∞ the undisturbed static pressure, q the kinetic pressure, κ the specific heat ratio and M the Mach number.

If at some location $C_p \approx 0$, the static pressure could be measured directly by a static pressure probe as it is done on aircraft, *e.g.*, for altimetry purposes. As shown by our numerical simulations above, in the case of the PPI instrument $C_p \neq 0$ at the pressure tap location, and hence the measured pressure p_m is contaminated by the flow and must be corrected as follows:

$$p = p_\infty + C_p q \tag{4.3}$$

At low Mach numbers ($M < 0.2$) the stagnation pressure coefficient $C_p = 1$ with good accuracy; at higher Mach numbers the stagnation pressure coefficient

is greater than unity. Thus, lacking a location where C_p stays low enough to make the correction unnecessary, measurement of total pressure and correcting it for kinetic pressure will lead to a smaller uncertainty in the determination of atmospheric pressure. The implementation of this approach was presented in the first part of this section.

The measured total pressure has to be converted into the desired static pressure using either the correction formula (4.3) or the relation (*Laine et al.*, 1991)

$$p_\infty = p(1 + \frac{\kappa - 1}{\kappa} M^2)^{-\frac{\kappa}{\kappa - 1}} \tag{4.4}$$

The Mach number has to be known to make the correction possible. In the case of PPI the Mach number (M) will be provided by the Huygens velocity profile and the speed of sound measurements performed by the Huygens surface science package instrument (*Laine et al.*, 1991; *Hoffren et al.*, 1992). The Mach number correction will be appreciable at the beginning of the measurement cycle, at high altitude, when the speed of the spacecraft is still relatively high. At low speeds in the denser lower regions of the atmosphere the correction is negligible.

The PPI and the whole HASI instrument performed excellently throughout

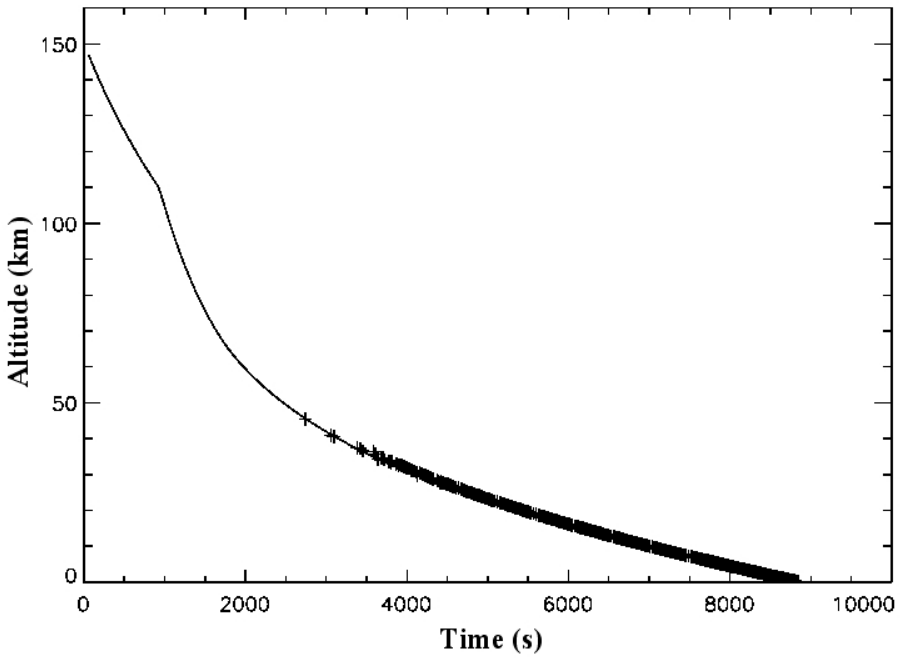

Figure 4.17: Altitude (km, ordinate) of the Huygens probe during its descent in the Titan atmosphere as a function of time (s, abscissa) determined by using the PPI observations and hydrostatic balance assumption (solid line), and direct observations (crosses) of the altimeter (figure by PPI-team). This demonstrates the high level of correlation of the HASI instrument results.

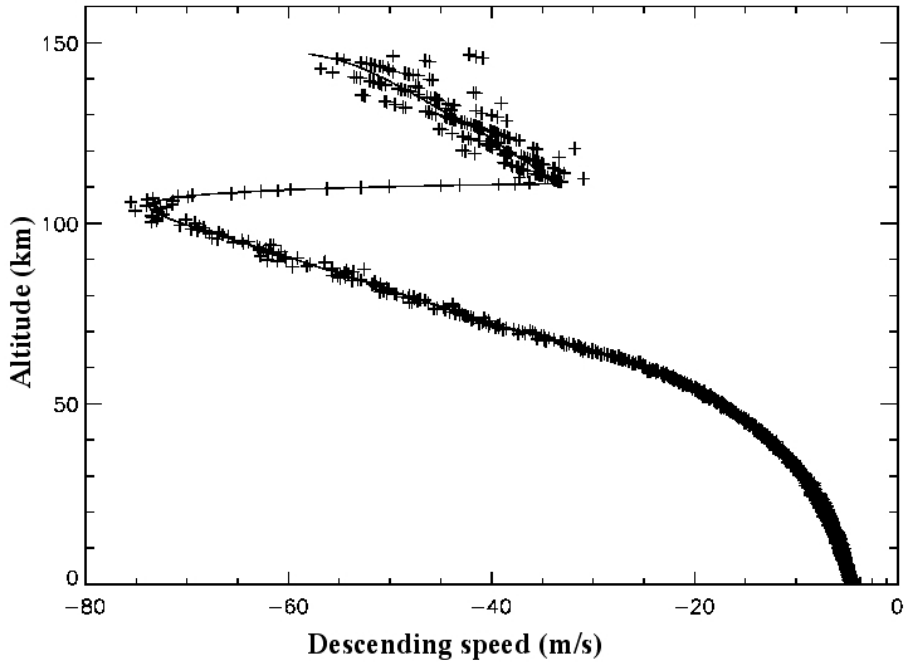

Figure 4.18: The Huygens probe's descending speed (m/s, abscissa) as a function of altitude (km, ordinate) constructed by using only PPI data (figure by PPI-team). During the last 45 km the speed profile is identical with the profile calculated from the radar altimeter measurements shown by crosses.

the Huygens probe descent into Titan's atmosphere. The descent took about 140 minutes after which the probe impacted on the surface with a speed of about 4.5 m/s. The first results of the Titan's atmospheric profile are presented among the other HASI experiment results by *Fulchignoni et al.* (2005) (*Ferri et al.*, 2005). The surface pressure on Titan was discovered to be 1.47 bar. The vertical pressure profile recorded by PPI corrected the engineering pressure profile (*Yelle et al.*, 1997) with a few per cents as shown in Figure 4.15. Similar profiles for Titan atmospheric temperature are presented in Figure 4.16.

All the six PPI pressure sensors measuring the total pressure through the Kiel-type pitot tube gave the same pressure profile well within the one percent accuracy window. The two pressure sensors measuring the internal pressure of the Huygens probe gave pressure readings delayed by the venting hole between the Huygens and the ambient environment. The internal pressure approached the outside pressure, when Huygens altitude and speed were reduced. At the surface the internal pressure and ambient pressure coincided as expected.

We determined the altitude of the Huygens probe during its descent in the Titan atmosphere using the PPI observations and the hydrostatic balance assumption. We compared the calculated results with the direct observations of the HASI altimeter and found that they matched to a few per cents. The results are presented in Figure 4.17. These first results already demonstrate the high level

of correlation of the HASI instrument observations.

The speed of Huygens relative to the Titan atmosphere was also obtained by iterative means using the pressure differences to get the vertical velocity profile. This was used to calculate the static pressure from the total pressure readings. The new pressure profile was used for calculating a more accurate value for C_D, which was then used to give a new speed profile. The iteration resulted in the velocity profile depicted in Figure 4.18. The deployment moment of the main parachute can be seen as a sudden speed increase. The speed of the Huygens probe during the last 50 km of the descent was measured by the HASI radar altimeter and those measurements coincided with the speed profile calculated using the PPI observations.

Due to the weak solar forcing on the surface of Titan the lower atmosphere was expected to be relatively calm. That was demonstrated to be the case by the observations of Huygens wind experiment showing that winds on Titan are weak on the surface and increase slowly with altitude up to approximately 60 km (*Bird*, 2005; *Flasar et al.*, 2005). The winds are blowing in the direction of Titan's rotation.

At the altitudes higher than 60 km the Huygens wind observations revealed large variability of the wind velocity. The highest wind speed (100 m/s) was observed at the altitude of 120 km. Large variations in the Huygens wind experiment may be due to strong vertical wind shear resulting in turbulent motions. This is indicated also by the PPI/HASI data, which exhibit signatures of turbulent motions (*Fulchignoni et al.*, 2005).

4.8 Discussion

The level of integration of the instrumentation affects the total mass of a planetary probe. Mass savings can be achieved by centralizing services (e.g. data preprocessing, power distribution and conversion, data management, data processing and packaging) required to operate the interface between the spacecraft system and science payload. On the other hand, making the spacecraft system to implement the interface and data processing services moves the spacecraft-to-payload interface closer to the sensing system level, which tends to make the system-to-payload interface more complex and more laborious to manage. Hence, when maintaining the same level of system reliability, the overall costs tend to be higher in a centralized system than in a case where payload has more autonomy. This increase in cost decreases as the experience of the participating teams increases. This was demonstrated by the Mars-96 Small Station Mission (Papers 3 and 6), PPI/HASI (Paper 2), NetLander Mission (Papers 1 and 5), and the MetNet mission (*Harri et al.*, 2003a).

PPI/HASI was an excellent example of a successful project, where mass savings requirement forced us to create a centralized system with very little autonomy given to the sensor systems provided by separate teams. In order to maintain a high level of product assurance, the number of project and interface management and control expenses were high, especially because the participating teams were relatively inexperienced and had not worked together before. However, this approach enabled implementation the HASI experiment within the

mass allocation given by the spacecraft.

The NetLander mission clearly required a rechargeable battery and its associated thermal support system. The battery needed an effective isolation system to keep it warm during most of its time at the Martian surface, and then a heat removal system to convey out the excess heat, especially during the cruise phase in space. For a planetary atmospheric science mission it would be of utmost benefit in terms of saving system resources to implement the mission without a special heating and thermal insulation system for the payload. This is not possible with a general geophysical planetary *in situ* payload like that onboard NetLander, which requires a sizeable energy storage during nighttime and needs significant amounts of energy buffering capacity for data transmission. The case is different for a simplified *in situ* atmospheric science payload like the MetNet payload, which gives a wonderful atmospheric science return consuming only a fraction of the power and bandwidth resources allocated to the NetLander mission. Hence a MetNet-type mission could be accomplished without a chemical battery, which is the main subsystem requiring heating. The battery can be replaced by state-of-the-art capacitors capable of buffering sufficient amount of energy for buffering the peak power functions during the relatively short data transmission periods. This would release more mass and volume to be allocated to the science instruments and would increase the ratio of the mass of the science instruments to the overall mass. Hence more scientific observations and results could be expected in return of the invested mission expenses.

The missions and experiments described in this chapter demonstrate distinctly, how the Barocap®, Humicap® and Thermocap® sensors can effectively be used for exploration of planetary atmospheres. The sensors were utilized in the exploration of the atmospheres of Mars and Titan, as described by Papers 1-6. The Barocap® pressure sensor system was also part of our proposed expedition to explore Venusian atmosphere. The proposal included an atmospheric descent probe and balloon flotilla with our Barocap® sensor system (APTIV) for pressure observations in the upper atmosphere (*Chassefiere et al.*, 2002).

The practical forms of in situ planetary atmospheric observations are surface components (movable and non-movable vehicles), aircraft capable of flying in the atmosphere, radiosondes, balloon-borne payload and rockets. Given these possible means of investigations the landers are certainly extremely useful, because they are able to provide long term measurements of the atmosphere. However, other forms of experiments are necessary because they provide data on large atmospheric volume, and they are also important in giving data outside the planetary boundary layer as well as on the boundary itself. Concerning the future Mars missions it is worth contemplating the following mission elements:

In the atmospheric boundary layer (ABL) the vertical profiles of pressure, temperature, humidity and density and their diurnal cycles are functions of latitude, season, and variation of atmospheric constituents, *e.g.* dust loading at Mars. The characteristics of the boundary layer, *e.g.* turbulence, depend on the atmospheric vertical profiles (Chapter 3 and 5) and hence it would be recommendable to include atmospheric instrumentation for the descent phase in all planetary *in situ* probes. For Titan this was implemented by the Huygens probe, which was practically a slowly descending atmospheric sounding device. For Venus the atmospheric structure and profiles were recorded by every exploration probe

(*Hunten et al.*, 1983). As to Mars, there exist only two daytime and one nocturnal vertical *in situ* profiles of density, pressure, wind, and temperature (*Seiff and Kirk*, 1977; *Seiff*, 1993; *Schofield et al.*, 1997). The MetNet mission will measure the atmospheric profiles during the descent phase and should crucially expand the *in situ* database of Martian atmospheric structure. It would be important that any forthcoming planetary *in situ* exploration vehicle would carry onboard also instrumentation for the atmospheric structure.

A planetary landing vehicle utilizing a retrievable balloon attached to a tether would be highly rewarding means to investigate the planetary boundary layer. The atmospheric science payload accommodated onboard the balloon would carry out important soundings of the lower part of the ABL, and could discover the diurnal as well as seasonal cycles of the atmospheric vertical profiles and structure. This type of an experiment should be implemented within a reasonable mass budget that would impose technological challenges. However, a retrievable balloon carrying an atmospheric sounding instrumentation would make a significant contribution to our understanding of, *e.g.* the Martian atmosphere.

Chapter 5

Modeling the Martian atmosphere

5.1 Overview

Detailed and comprehensive observations of planetary systems are scarce. Therefore modeling atmospheric processes in some simplified form has been extensively utilized in planetary research. Martian atmospheric simulations including various parameterization schemes have been indispensable to the understanding of the atmospheric physics and dynamic processes of Mars (*Holton*, 1992).

Analysis and science return of atmospheric *in situ* observations are significantly enhanced by modeling efforts. Modeling results also guide the instrumentation development by predicting atmospheric phenomena and conditions. Vice versa, any type of modeling activity requires actual observations to give the realistic frame for the model as well as to validate the model results. In Paper 8 we simulated atmospheric conditions at the landing site of the Mars Pathfinder (MPF) lander, and compared the model results with the *in situ* MPF observations (Chapter 5.2).

The atmosphere of Mars is thin and therefore its response to local radiative forcing is strong when compared to that of the Earth's troposphere. Airborne dust and also the water vapor give significant contributions to the radiative fluxes (*Savijärvi*, 1995, 1999). Thus models of the Martian atmosphere should have fairly accurate radiative transfer (RT) algorithms (*Santee and Crisp*, 1993). This is specifically important for the net radiative flux at the surface, which is the main driver for the surface temperature evolution, since the surface turbulent fluxes are small due to the thin atmosphere (*e.g. Savijärvi* (1991a,b); *Haberle and Houben* (1991). However, the accuracy of the RT schemes has not been rigorously tested in many cases as reference calculations have been rare. To that end we established a set of atmospheric reference conditions to compare our model's atmospheric radiation scheme for the lower Martian atmosphere with least-compromise reference line-by-line calculations (*Crisp*, 1990; *Santee and Crisp*, 1993, 1995).

In Paper 9 we defined a few test cases of Martian atmospheric conditions. For those cases we performed accurate radiative line-by-line (LBL) calculations to understand the effects of atmospheric carbon dioxide and the airborne dust (Paper 9, Chapter 5.3). We also used the radiative scheme of our mesoscale model (Paper 9) with the same atmospheric conditions to get radiative fluxes and heating rates over the atmospheric profile generated by our radiative scheme. This enabled us to improve the radiative transfer parameterization scheme of our model as described in Paper 9 and in Chapter 5.3. The improved radiative transfer scheme was also implemented in our model used in Paper 8. In our calculations we have divided the frequency band into a short wavelength or solar domain (SW, 0.2 - 4 μm) and a long wavelength or thermal domain (LW, 4-200 μm).

As a further development, the accurate line-by-line calculations were used as a frame of reference to an intercomparison campaign. This included inviting various operating global circulation modeling teams to compare their radiative transfer schemes to the results of the accurate line-by-line calculations. The first results of this ongoing effort were presented by *Savijärvi et al.* (2001). This intercomparison activity is discussed in Chapter 5.4.

5.2 Analyzing the Pathfinder data

The Mars Pathfinder spacecraft (MPF) landed on Mars on July 4, 1997, and was operational for about three months. It sent back to the Earth thousands of images, mineralogical data as well records of atmospheric pressure, wind and temperature (*Rieder et al.*, 1997). The main objective of MPF was to demonstrate proper performance of some key technologies and concepts for future missions to Mars. The MPF payload included an atmospheric science instrument that operated through the MPF lifetime on the Martian surface and also recorded the atmospheric structure during the descent phase (*Seiff et al.*, 1997; *Schofield et al.*, 1997).

The MPF temperature records consisted of observations at three levels, 0.52, 0.77 and 1.27 m above the surface. The pressure sensor was located inside the lander, and the wind observation was made at the altitude of about 1.3 m above the surface at the end of the MPF boom (*Schofield et al.*, 1997).

We compared the results of our one-dimensional high-resolution Martian ABL model described in Paper 8 and by *Savijärvi* (1991b) with the Mars Pathfinder lander sol 3 observations, including the latest wind speed estimates (Paper 8). The model's radiation scheme has been validated against line-by-line scheme results in typical Martian conditions as described in Paper 9. Our model is structured as follows (*Savijärvi*, 1991b, 1995)

$$\frac{\partial u}{\partial t} = f(v - v_g) + \frac{\partial}{\partial z}(K_m \frac{\partial u}{\partial z}) \tag{5.1}$$

$$\frac{\partial v}{\partial t} = f(u - u_g) + \frac{\partial}{\partial z}(K_m \frac{\partial v}{\partial z}) \tag{5.2}$$

$$\frac{\partial \theta}{\partial t} = \frac{\partial}{\partial z}(K_h \frac{\partial \theta}{\partial z}) - \Pi \frac{1}{c_p \rho} \frac{\partial}{\partial z} R_{net} + \Pi \frac{L}{c_p}(C - E) \tag{5.3}$$

$$\frac{\partial q}{\partial t} = \frac{\partial}{\partial z}(K_h \frac{\partial q}{\partial z}) - (C - E) \quad (5.4)$$

$$\frac{\partial q_i}{\partial t} = \frac{\partial}{\partial z}(K_h \frac{\partial q_i}{\partial z}) + (C - E). \quad (5.5)$$

The model simulations predict the evolution of the potential temperature θ, the specific humidity q, the water ice mixing ratio q_i and the horizontal wind components u, v. The radiation is taken into account by the R_{net}-term of $\frac{\partial \theta}{\partial t}$ in equation 5.3, where R_{net} is the net radiation effect of upwelling and downwelling long wavelength (LW, thermal) and short wavelength (SW, solar) radiation. The Coriolis parameter is f, u_g, v_g are geostrophic wind components and ρ the atmospheric density. K_m and K_h are mixing coefficients, C the condensation of water vapor into ice, E sublimation of ice into water vapor, and L the latent heat of sublimation. $\Pi = (p_s/p)^{(R/c_p)}$, where p is atmospheric pressure, p_s pressure at the surface, R is gas constant and c_p the specific heat at constant pressure. The potential temperature θ is related to Π by $\theta = T/\Pi$.

The model radiative schemes for both long wavelength and short wavelength domains were validated and improved by comparing model simulations with accurate line-by-line calculations (Papers 8 and 9).

Our model addresses turbulence through the Monin-Obukhov method (Chapter 3.2) for the lowest layer and above it through a mixing length approach (Paper 8). The model predicts the evolution of energy balance at the surface, where thermal diffusion in the soil is handled through a five-layer Crank-Nicholson scheme. Our model is further described in Papers 8 and 9 and by *Savijärvi* (1991b, 1995).

The wind and atmospheric temperature observations of MPF show distinctive variability due to convective turbulence during the daytime, when there apparently is a strong superadiabatic temperature gradient near the surface. Night-time wind and temperature measurements indicate relatively steady atmospheric conditions with a reversed inversion-type temperature gradient. Our model simulates these features and all the observed magnitudes well except that the strongest low-level temperature gradients given by the model are smaller than the observations (Paper 8). This may be due to a model deficiency, or may be caused by MPF solar panels and other structures, which may disturb the thermal environment and the wind flow field in the vicinity of the lander.

The principal atmospheric heating mechanism near the ground appears to be direct ground-emitted thermal radiation absorbed by the principal atmospheric constituents CO_2 water vapor and dust. In spite of strong convective turbulence during daytime, in the lowest 100 meters of the atmosphere turbulence has a reverse role of cooling the near-surface air. This seems to be the case at all times except just after sunrise, when turbulence mixing is at its minimum and the surface is only slightly warmer than the atmosphere next to the surface. This interesting feature can be explained by the thin Martian atmosphere (Paper 8).

In general the heating and cooling rates of the lower part of the atmosphere are dictated by a sensitive balance between convergence and divergence of the downwelling and upwelling thermal fluxes. A smaller contribution to the daytime heating rate is given by solar heating primarily due to absorption by airborne dust. These results demonstrate the distinct need for accurate radiation

schemes for quantitative atmospheric simulations. Improvement of radiative parameterization is discussed in the following chapter 5.3.

The sensible-heat flux profiles reach a maximum at around the 50 m height and not at the surface (Paper 8, figure 7). This is due to the fact that the atmospheric temperature evolution exhibits a reverse role of turbulence as discussed above and in Paper 8.

Because moisture does not have a strong daytime internal source on Mars, the daytime latent-heat flux profiles are more conventional. According to our results (Paper 8, Figure 8), the night-time relative humidity reaches 100% at 0200 LT near the surface. As a result radiation fog forms and grows up to the height of 80 m by 0600 LT. Moisture is transformed into fog-ice and is also deposited on the surface as thin frost, as has been verified also by imaging instruments of Viking landers and MPF (*Tillman et al.*, 1979; *Higuchi*, 2001). The frost and fog-ice sublimate rapidly after sunrise, and the ABL profiles of the water vapor mixing ratio remain well mixed during the daytime.

The wind speed profiles indicate inertial oscillation and a low level jet at 0600 LT with a steep wind shear across the night-time surface temperature inversion. The daytime wind profile is well-mixed while the night-time wind exhibits a quasi-logarithmic surface layer below 10 m.

Atmospheric radiation, temperature profiles and turbulence are strongly intertwined in the Martian ABL. This generates interesting feedbacks in the atmospheric phenomena, *e.g.* in the structure of local thermals and dust devils that are known to be common on Mars. This is further discussed by *Maattanen and Savijarvi* (2002). Understanding of the structures and physical mechanisms of these phenomena requires high model resolution in both the vertical and horizontal dimensions as well as efficient sub-grid parameterization schemes for radiative and turbulent processes.

5.3 Improving radiative schemes

5.3.1 Overview

The Martian atmosphere is relatively thin and hence the role of radiative transfer in transporting heat within the atmosphere is highly significant (*Savijärvi*, 1991a). Implementing detailed radiative transfer schemes in atmospheric simulations requires so much computer power and labor that such schemes cannot be conveniently implemented in operational models. Therefore various simplifying parameterization schemes are used in all state-of-the-art operational Martian atmospheric models. This situation is continuously changing as better simulation tools and more computation power becomes available. Therefore the parameterization schemes have become more and more detailed, but the need for improvement, validation and intercomparison remains.

Radiative transfer schemes can be effectively improved by comparing the output of the parameterization schemes with more accurate reference calculations, such as spectral line-by-line calculations. Hereafter we call the simulation model implementing those calculations a spectrum resolving transfer model (SRM) as

described in Paper 9. Performing more accurate reference calculations with a minimal amount of simplifications results in computer-intensive and time consuming line-by-line calculations to produce the desired reference results. Making use of such calculations requires a set of well defined atmospheric conditions that can be used as reference cases. Then the accurate SRM calculations are performed for all of the reference cases. Thereafter the same calculations are performed with the atmospheric models, and the results are compared with the SRM calculations. This in turn enables improvement of the model parameterization schemes.

To summarize, our aim was to validate and improve the radiative transfer parameterization of the Martian atmospheric mesoscale model of the University of Helsinki (UH model), and also to compare the usefulness of the parameterization schemes of some operational Martian atmospheric 3D models (Chapter 5.4). To accomplish that, we defined a set of reference cases with varying Martian atmospheric properties and performed SRM calculations for those cases. We then evaluated and compared the results given by the SRM calculations and the Martian atmospheric models.

5.3.2 Atmospheric reference cases

The atmospheric conditions used as reference cases for this investigation utilize the diurnally and globally averaged thermal structure based on data from Mariner 9 IRIS (*Santee and Crisp*, 1992; *Formisano et al.*, 2001) observations acquired during late southern summer ($L_s = 340 - 350°$), as described in Paper 9. The atmosphere is resolved into 36 fixed altitude levels. The vertical grid is dense near the surface in order to resolve the boundary layer. The surface pressure is 6.0 mb and the surface air temperature is 210.0 K.

The mixing ratios of radiatively active trace gases include CO_2, O_3, CO and O_2 with constant mass mixing ratios of 0.953, 3.8×10^{-4}, 9.5×10^{-4}, and 2.0×10^{-8}, respectively (Paper 9).

The average precipitable water content in Mars is about 10 μ m. Adopting that value and assuming a vertically constant relative humidity of 27%, the H_2O mass mixing ratio profile can be obtained. In order to avoid supersaturation in the cold upper levels we used a constant relative humidity instead of a constant H_2O mass mixing ratio (which would be 6.25×10^{-5}).

The surface emissivity varies spectrally in the SRM but yields a broadband value of about 0.96. A ground temperature of 210.0 K is assumed, *i.e.* there is no discontinuity between the air and ground temperatures across the interface.

The dust visible optical depth values at the surface are 0 (*i.e.* no dust), 0.3 (typical low value during the two Martian years of the Viking surface observations), 0.6 (nominal Mars Pathfinder values), 1, and 5 (representing moderate and severe dust storm conditions, respectively). The dust is well-mixed, with altitude-dependent particle number densities specified by a relationship of the form $q(z) = q_o$exp(0.01 (1-exp(-z/H))), where H is the scale height of the atmosphere (*Conrath*, 1975). Optical depths of other cases can be obtained by scaling these values by a constant factor (Paper 9)

For this intercomparison, the dust size distribution was defined by a stan-

dard two-parameter gamma distribution with an effective cross-section-weighted mean radius of 1.6 μm (*Tomasko et al.*, 1999). At wavelengths longer than 1 μ m, the wavelength-dependent complex index of refraction was taken from *Ockert-Bell et al.* (1998). At shorter wavelengths, values were derived from the Mars Pathfinder observations (*Tomasko et al.*, 1999).

5.3.3 SRM calculations

All line-by-line calculations were performed for the reference cases, which are described in Section 5.3.2 and in Paper 9. The calculations solve the following basic radiative transfer equation (*Stamnes et al.*, 1988; *Liou*, 1992)

$$\mu \frac{dI(\tau,\mu,\phi,\nu)}{d\tau} = -I(\tau,\mu,\phi,\nu) + S(\tau,\mu,\phi,\nu). \tag{5.6}$$

where I denotes the radiance, τ is the column-integrated vertical optical depth, measured from the top of the atmosphere downwards, θ is the zenith angle, μ is the cosine of the zenith angle, and ϕ is the azimuth angle. The source term, S, is defined by

$$\begin{aligned} S &= \frac{\omega(\tau,\nu)}{4\pi} \int_0^{2\pi} d\phi' \int_{-1}^{1} d\mu' P(\tau,\Theta,\nu) I(\tau,\Theta,\nu) \\ &\quad + [1-\omega(\tau,\nu)] B[\nu, T(\tau)] \\ &\quad + \frac{\omega(\tau,\nu)}{4\pi} F_\odot(\nu) P(\tau,\Theta_\odot,\nu)\, exp(-\tau/\mu_\odot) \end{aligned} \tag{5.7}$$

where $\omega(\tau,\nu)$ is the single scattering albedo, $P(\tau,\Theta,\nu) = P(\tau,\mu,\phi,\mu',\phi',\nu)$ is the scattering phase function, $B[\nu,T(\tau)]$ is the Planck function at wavenumber ν, and temperature $T(\tau)$. $F_\odot(\nu)$ is the solar irradiance at the top of the atmosphere (*Stamnes et al.*, 1988; *Crisp*, 1986, 1990; *Liou*, 1992; *Santee and Crisp*, 1993, 1995). Numerical integration of the radiative transfer equation gives the radiance field that eventually is used to obtain the radiative fluxes.

Simplifications of the radiative transfer equation are convenient as they reduce the calculation time and in that way speed up the turn-around time of the modeling results. However, making simplifications requires verification that the errors produced are at an acceptable level for the specific investigation. Intercomparison tests with results of least-compromise calculations provide an excellent means for evaluating the performance of the model parameterizations of the radiative transfer schemes.

We performed the least-compromise line-by-line calculations using radiative transfer algorithms that had been developed for investigations of the atmospheres of Mars, Venus and Neptune (*Crisp*, 1986; *Crisp et al.*, 1986; *Meadows and Crisp*, 1996). The algorithms utilize multi-level, spectrum-resolving multiple scattering models for resolving the wavelength dependence of the atmospheric and surface optical properties and the atmospheric radiation field. The

computer programs Discrete Atmospheric Radiative Transfer (DART) and the Spectral Mapping Atmospheric Radiative Transfer (SMART) were used in this study (*Meadows and Crisp*, 1996). DART and SMART utilize a multi-level, multi-stream, discrete ordinate algorithm, DISORT (*Stamnes et al.*, 1988) to generate altitude- and angle-dependent solar radiances at each wavelength.

DART performs a monochromatic multiple scattering calculation with a fine spectral grid to produce a wavelegth-dependent solar spectrum. The spectral grid is sufficiently fine to resolve the spectral variability associated with near-infrared line absorption and UV pre-dissociation and electronic bands of gases, as well as the wavelength dependence of the optical properties of airborne particulates and the surface.

The SMART model performs the same tasks as the DART, but SMART employs high-resolution spectral mapping methods (*Meadows and Crisp*, 1996) to decrease the required computational resources. The DISORT computer code provides solutions to the monochromatic equation of radiative transfer in plane parallel, scattering and absorbing atmospheres.

DISORT was chosen for this application because of its speed and accuracy, and because a well-documented, numerically stable code was readily available (W. Wiscombe, personal communication, 1992). Optical properties ($\delta\tau$, ω, P) are assumed to remain uniform throughout each layer. When 4 or more streams are used, these methods usually produce angle-dependent monochromatic radiance errors no larger than 1% for clear, cloudy, and aerosol-laden atmospheres. These errors were considered acceptable for this investigation.

DART produces the most reliable results, as it uses all available information about the atmospheric and surface optical properties, and using a minimum number of approximations. Its main drawback is the fact that it requires a lot of computational resources.

SMART generates a high-resolution, angle-dependent solar radiance spectrum through using a spectral mapping algorithm employing a user-defined binning criterion to identify all spectral grid points that have optical properties that remain similar at all levels of the atmosphere and at the surface.

Comparisons between SMART and DART indicate that even though spectral mapping methods can reduce the number of monochromatic calculations needed in broad spectral intervals by about a factor of $\sim$80, they rarely introduce radiance errors larger than 2% in spectral intervals wider than 1cm^{-1}. The spectral mapping algorithm adds some computational overhead, but this approach still reduces the computing time required for broad-band solar and thermal calculations in scattering, absorbing atmospheres by factors ranging from 40 (4 streams) to 80 (32 streams). SMART therefore provides the accuracy and efficiency needed for sensitivity studies, even on a global scale, but it still does not provide the computational speed needed for routine use global atmospheric circulation models (GCM).

The atmospheric solar fluxes and the heating rates are essential in the studies of the atmospheric optical properties. The net downward solar flux at each level can be described as

$$F^n(z) \quad = \quad F\downarrow(z) - F\uparrow(z). \tag{5.8}$$

The spectrally-resolved radiances obtained at each atmospheric level with approximately uniform radiative properties were integrated over the lower and upper hemispheres using Gaussian quadrature method to obtain the upwelling and downwelling radiative fluxes. The wavelength-dependent fluxes were then integrated over the shortwave (0.2 – 5 μm) and longwave (5 – 200 μm) wavelength domains to produce the solar and thermal radiative fluxes (Paper 9).

The value of $F^n(z)$ at the top of the atmosphere is the total solar flux absorbed by the planetary surface and atmosphere. The net atmospheric flux, $F_a^n(z) = F^n(z) - F^n(z = z_0)$, is obtained by subtracting the net solar flux at the surface from the net flux at each atmospheric level.

The heating rates can be calculated by

$$Q = -\frac{1}{\rho c_p}\frac{\partial F^n}{\partial z} = \frac{g}{c_p}\frac{\partial F^n}{\partial p}, \tag{5.9}$$

where ρ is density, c_p is the specific heat at constant pressure for air, and g is the gravitational acceleration (*Liou*, 1992; *Holton*, 1992)

The global averages of fluxes and heating rates can be obtained using the values calculated for various solar zenith angles. The globally-averaged net atmospheric flux ($\overline{F_a^n}(z)$) and heating rate ($\overline{Q}(z)$) are defined by

$$\overline{F_a^n}(z) = \frac{1}{2}\int_0^1 F_a^n(\mu, z)d\mu \tag{5.10}$$

$$\overline{Q}(z) = \frac{1}{2}\int_0^1 Q(\mu, z)d\mu. \tag{5.11}$$

Globally-averaged fluxes and heating rates can be reliably derived using calculations for 8 discrete solar zenith angles (*Crisp*, 1990; *Santee and Crisp*, 1993).

5.3.4 Scientific outcome and model improvement

We introduced a framework of reference cases to compare radiation schemes of Martian atmospheric models, as described above in Chapter 5.3.2. Long wavelength flux calculations performed with a spectrum-resolving model (SRM) indicated that in a dust-free CO_2 atmosphere water vapor, even in the small average amounts observed in Mars (precipitable water vapor of about 10 μm, has a significant impact on the long wavelength radiative transfer. It increased the downward long wavelength fluxes by 15 percent and LW heating rates by 25 percent compared to the case without water vapor at all (Paper 8). This was the case with other trace gases (ozone, oxygen and carbon monoxide) included as well as without them. The other trace gases did not show a strong signal in the long wavelength fluxes at their normal, global-average column concentrations. Hence they can be excluded from the radiative parameterization improvement process as a first approximation.

Long wavelength fluxes and heating rates for pure CO_2 atmospheres were generated using two spectral line databases (HITRAN and HITEMP) for CO_2. The resulting difference in the SRM results (the line data uncertainty) was non-zero

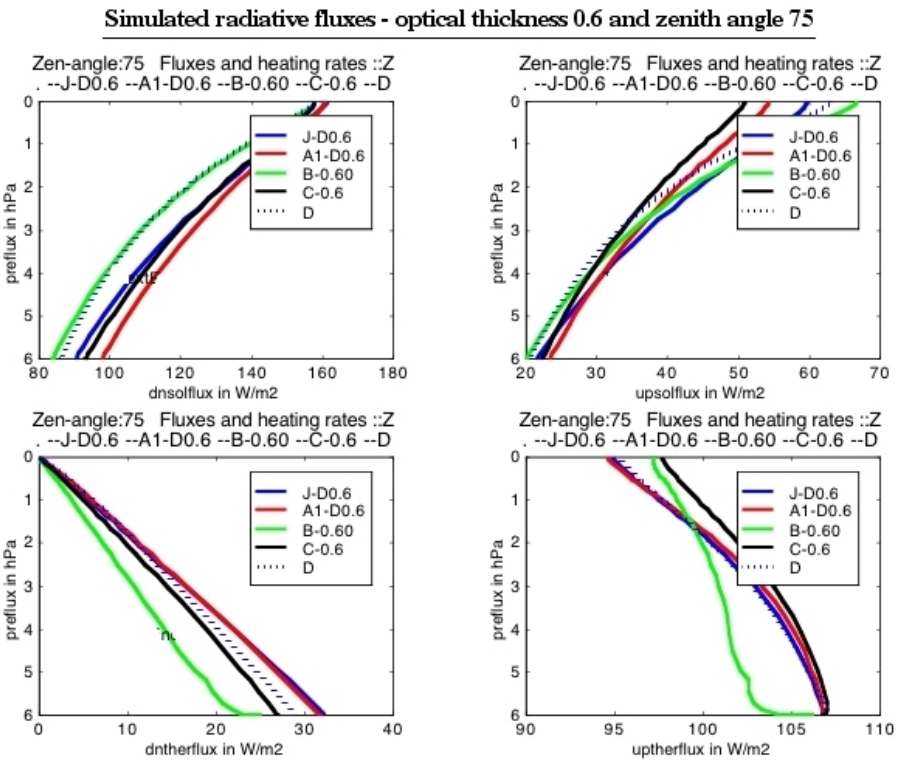

Figure 5.1: Simulated radiative fluxes in the Martian atmosphere with dust-induced optical thickness of 0.6 and the solar zenith angle of 75 degrees from the vertical direction. 'J' refers to SRM calculations, 'A' refers to our model (Paper 9) and the other data are produced by Martian atmospheric global circulation models participating in the intercomparison campaign. Upper frames: solar fluxes (SW, W/m^2) as functions of atmospheric pressure (ordinate axis, hPa), left panel is downwelling flux and right panel upwelling flux. Lower frames: thermal fluxes (LW, W/m^2) as functions of atmospheric pressure (ordinate axis, hPa), left panel is downwelling flux and right panel upwelling flux.

but not significant, and hence we used the somewhat less extensive database, HITRAN (*Newman and Taylor*, 2002). Clouds were not considered at this stage.

In addition to water vapor, airborne dust appears to be another important trace constituent in the long wavelength domain. Including a visible optical depth of 0.3 increased the downward LW flux at the surface by 41 percent from the dust-free value, while a dust optical depth of 1 (weak dust storm conditions) increased the downward LW flux by 111 percent. The upward LW fluxes decrease with increasing dust load while the long wavelength cooling rates increase strongly in the lower atmosphere. Visible dust optical depths near unity appear to roughly double the gaseous greenhouse effect on present-day Mars.

In intercomparison with the SRM calculations, the University of Helsinki Mars model original ('old') emissivity broadband LW scheme proved reasonable in

the no-dust case. Some refinements we made improved it such that it did not differ from the SRM by more than $\pm 0.3 Wm^{-2}$ for down-, up- and net fluxes at any level. Dust was included via the grey approximation (Paper 9). This seems to be a valid assumption, provided that the dust absorptivity coefficients are optimized separately for the downwelling and upwelling fluxes. For the shortwave (solar) domain the main results were (Paper 9).

- CO_2 absorbs about 1 % of solar radiation producing a modest heating rate of 4-5 K / day in the lowest 10 km.
- Trace gases are insignificant at the short wave domain for radiative transfer
- Airborne dust reduces the downwelling short wave radiation significantly and upwelling somewhat less.

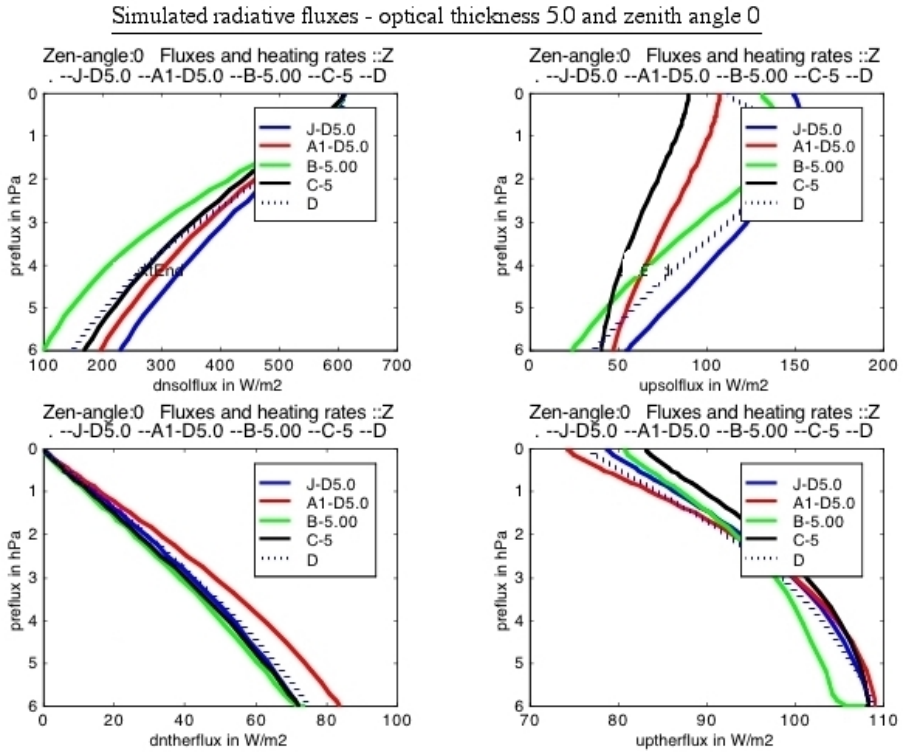

Figure 5.2: Simulated radiative fluxes in the Martian atmosphere with dust-induced optical thickness of 5.0 and the solar zenith angle of 0 degrees from the vertical direction. 'J' refers to SRM calculations, 'A' refers to our model (Paper 9) and the other curves are produced by Martian atmospheric global circulation models participating in the intercomparison campaign. Upper frames: solar fluxes (SW, W/m^2) as functions of atmospheric pressure (ordinate axis, hPa), left panel is downwelling flux and right panel upwelling flux. Lower frames: thermal fluxes (LW, W/m^2) as functions of atmospheric pressure (ordinate axis, hPa), left panel is downwelling flux and right panel upwelling flux.

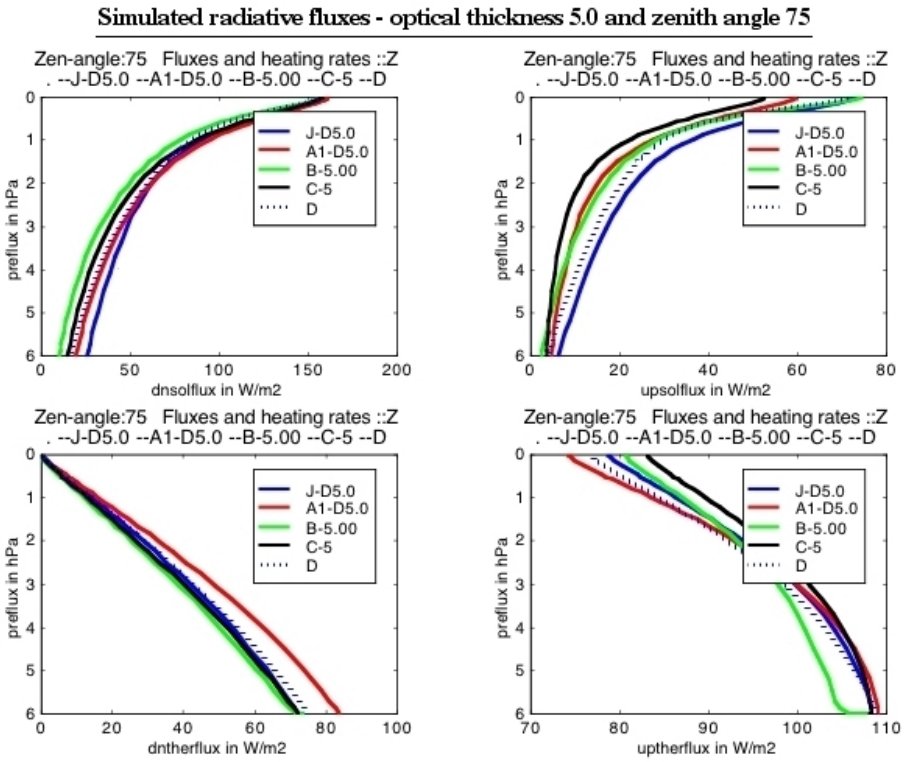

Figure 5.3: Simulated radiative fluxes in the Martian atmosphere with dust-induced optical thickness of 5.0 and the solar zenith angle of 75 degrees from the vertical direction. 'J' refers to SRM calculations, 'A' refers to our model (Paper 9) and the other curves are produced by Martian atmospheric global circulation models participating in the intercomparison campaign. Upper frames: solar fluxes (SW, W/m^2) as functions of atmospheric pressure (ordinate axis, hPa), left panel is downwelling flux and right panel upwelling flux. Lower frames: thermal fluxes (LW, W/m^2) as functions of atmospheric pressure (ordinate axis, hPa), left panel is downwelling flux and right panel upwelling flux.

5.4 Intercomparison campaign

Investigations of the Martian atmosphere requires combining the concurrent knowledge of atmospheric processes with the data flow from the recent and ongoing Mars missions. Several research teams are working on that by utilizing Martian atmospheric simulation models, which use parameterization schemes differing from each other.

The effect of airborne dust and water vapor is strong in the thin Martian atmosphere. This imposes stringent requirements on the radiative transfer (RT) algorithms of the models of the Martian atmosphere. To test the accuracy of the RT schemes, we initiated a campaign to compare the atmospheric radiation schemes for the lower Martian atmosphere.

We introduced a set of reference cases for Martian atmospheric conditions with profiles for temperature, pressure, dust optical depth (*Conrath*, 1975; *Ockert-Bell et al.*, 1998), water, CO_2, O_3, CO and O_2 as described in Paper 9 and Chapter 5.3. The reference cases are based on a diurnally and globally averaged thermal structure derived from Mariner 9 IRIS observations acquired during late southern summer. Computationally expensive reference simulations were performed by applying a spectrum resolving (line-by-line multiple scattering) model, SRM, to give the least-compromise base for comparisons.(Crisp 1986, Meadows and Crisp 1996). By using fixed reference conditions we introduced an intercomparison framework to enable atmospheric modeling teams to compare their modeling results with the reference line-by-line calculations, and to improve their models.

We called for Martian atmospheric modeling groups to participate in the radiative parameterization scheme comparison effort. As a result five different Mar-

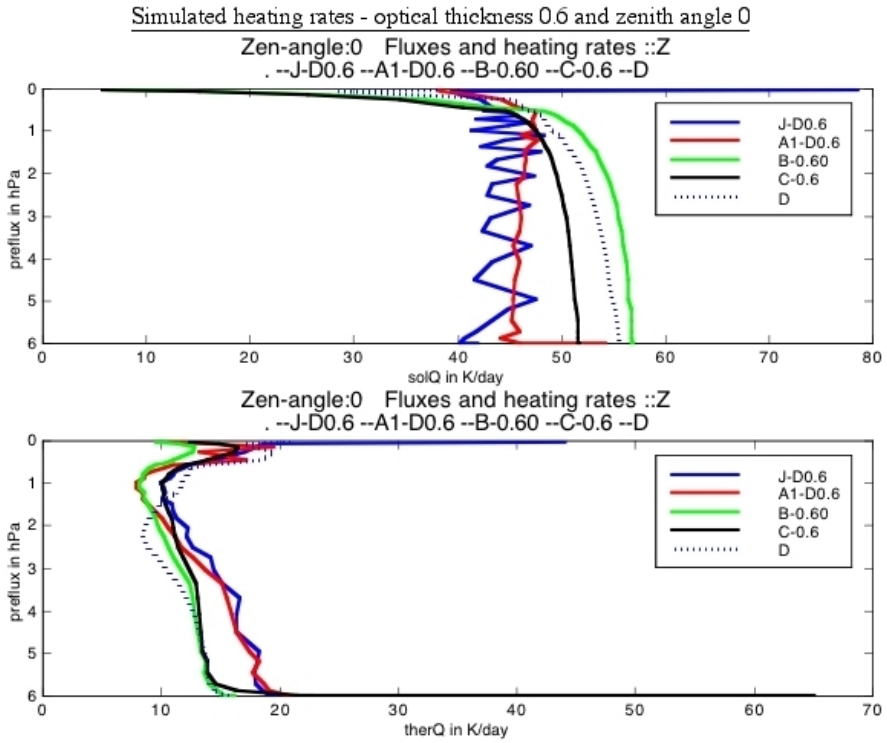

Figure 5.4: Simulated heating rates (K/day) as a function of altitude (served by atmospheric pressure on the ordinate axis, hPa) with dust-induced optical thickness of 0.6 and the solar zenith angle of 0 degrees from the vertical direction. Solar heating rate (K/day) in the upper frame, thermal heating rate in the lower frame. 'J' refers to line-by-line calculations, 'A' refers to our model (Paper 9) and the other data are produced by existing Martian atmospheric global circulation models. Note that the SRM calculations exhibit saw-like structure due to coarse binning of the dust profile.

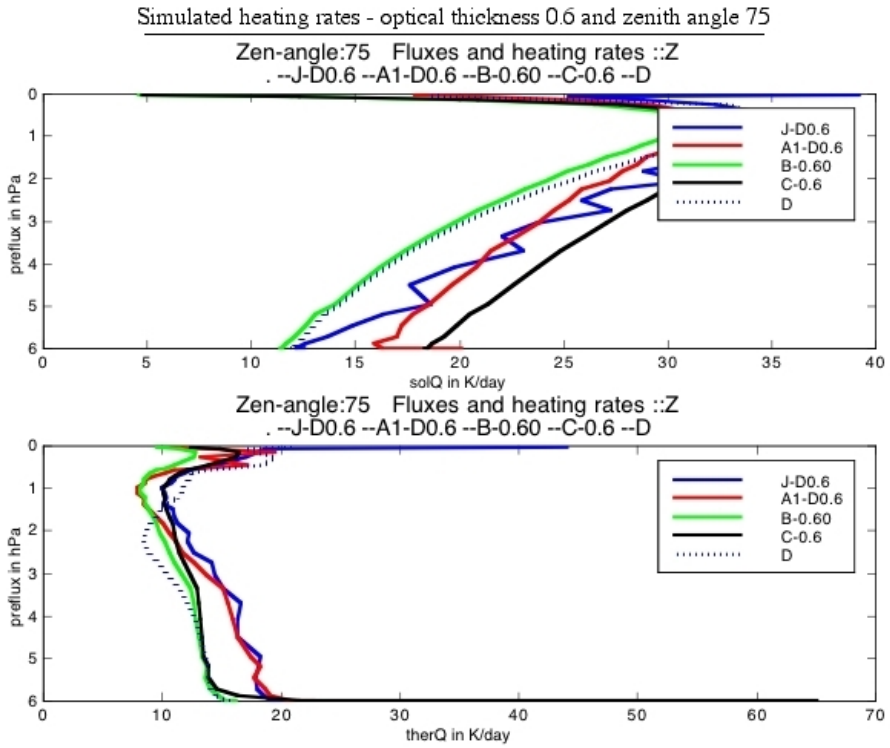

Figure 5.5: Simulated heating rates (K/day) as a function of altitude (served by atmospheric pressure on the ordinate axis, hPa) with dust-induced optical thickness of 0.6 and the solar zenith angle of 75 degrees from the vertical direction. Solar heating rate (K/day) in the upper frame, thermal heating rate in the lower frame. 'J' refers to line-by-line calculations, 'A' refers to our model (Paper 9) and the other data are produced by existing Martian atmospheric global circulation models. Note that the SRM calculations exhibit saw-like structure due to coarse binning of the dust profile.

tian atmospheric model groups joined our intercomparison campaign including the three leading Martian global circulation modeling groups.

Our Martian radiative parameterization intercomparison campaign resembles the International Comparison of Radiation Codes for Climate Models, ICRCCM (*Ellingson and Fouquart*, 1991; *Ellingson et al.*, 1991). The ICRCCM led to many improvements in the Earth GCM radiation codes. Our intercomparison framework is a step toward that direction for Mars.

The first results of this intercomparison campaign were presented by *Savijärvi et al.* (2001). Improving the radiative parameterization of our own model is described in Paper 9, and in Paper 8, where the improved parameterization schemes were applied to our investigations at the Mars Pathfinder landing site.

Simulations with the four Martian atmospheric global (GCM) and mesoscale models were performed for the reference atmospheric conditions to produce

radiative upwelling and downwelling fluxes (W/m^2) and heating rates with varying solar zenith angle (at least with 0° and 75° zenith angle). Both fluxes and heating rates were determined separately for long wavelength or thermal (LW, 4-200 μm) and short wavelength or solar (SW, 0.2 - 4 μm) domains.

At the long wavelength domain the line-by-line (LBL) calculations were performed with two spectral line databases (including CO_2 H_2O and other trace gases): HITRAN (*Newman and Taylor*, 2002; *Rothman et al.*, 1998) and HITEMP that has got more accurate CO_2 data. The results with a slightly more accurate HITEMP database showed that the downward long wavelength radiation was increased by about 1% compared to the SRM calculations using the HITRAN database. This small increase is likely to be due to the contribution of numerous weak CO_2 lines that are not as rigorously included in the HITRAN database. Accordingly, it is a clear result justifying for us to use the somewhat lighter HITRAN database.

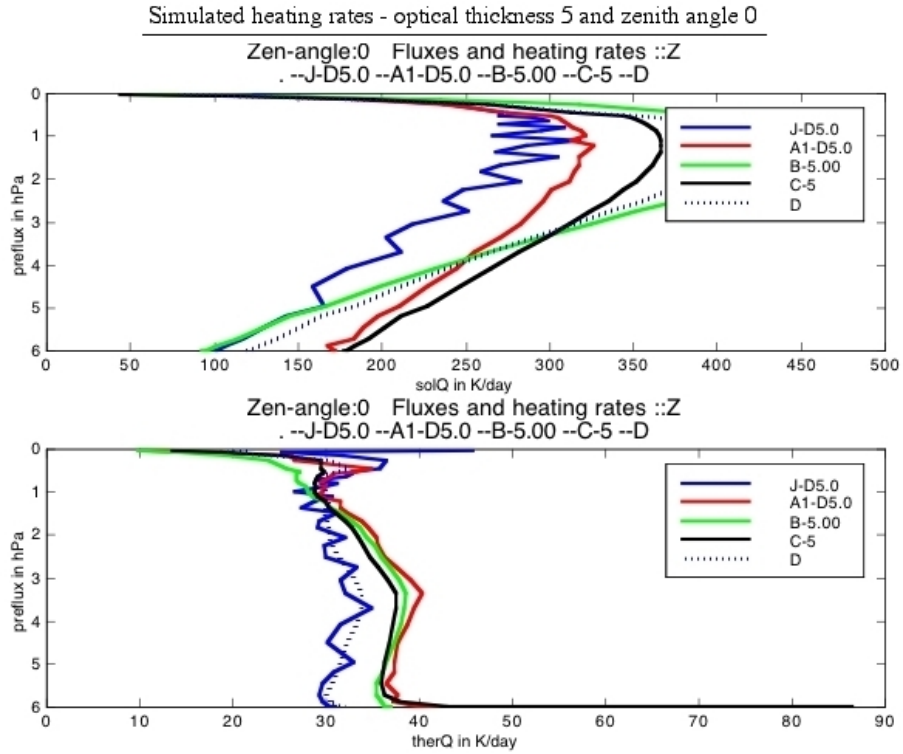

Figure 5.6: Simulated heating rates (K/day) as a function of altitude (served by atmospheric pressure on the ordinate axis, hPa) with dust-induced optical thickness of 5.0 and the solar zenith angle of 0 degrees from the vertical direction. Solar heating rate (K/day) in the upper frame, thermal heating rate in the lower frame. 'J' refers to line-by-line calculations, 'A' refers to our model (Paper 9) and the other data are produced by existing Martian atmospheric global circulation models. Note that the SRM calculations exhibit saw-like structure due to coarse binning of the dust profile.

According to the SRM calculations water vapor increases downward long wavelength radiation by even 15%, hence the water vapor is clearly required to be part of the radiative parameterization schemes. Other trace gases had negligible effects resulting in the conclusion that CO_2 and H_2O are the only atmospheric constituents needed in the long wavelength domain.

Some of the simulated flux density profile results of the intercomparison test series are depicted in Figures 5.1, 5.2 and 5.3. The simulations were performed including the atmospheric constituents CO_2 dust and water vapor, but no other trace gases. The flux profiles are plotted separately for thermal and solar domains. They include results of the SRM calculations and the four Martian atmospheric models participating in the intercomparison. Figures 5.4, 5.5 and 5.6 present the heating rates.

In the long wavelength domain the models under investigation produced results close to SRM flux profiles and heating rates. The deviations between the models, and the SRM calculations were of the order of or less than 10 per cents (Paper 9). Accordingly, in the first order, the long wavelength parameterizations seem to be satisfactory. This is demonstrated by Figures 5.1, 5.2 and 5.3.

In the short wavelength domain the SRM calculations showed that all trace gases, including water vapor, had negligible effects. The key player in the radiative schemes in the long wavelength domain, in addition of CO_2 is airborne dust. Some models investigated produced 10 to 30% higher dust heating than the SRM (Figures 5.4, 5.5 and 5.6). Modifications correcting the parameterization have already been made by some of the modeling teams participating in the campaign. The cause of the deviations can be attributed to differences in dust optical properties, and it requires further analyses.

5.5 Discussion

A few improvements and refinements were introduced to our model's rapid radiative transfer parameterization scheme by intercomparisons with the line-by-line calculations, as described in Paper 9. The new parameterization scheme was already made use of in nucleation studies at Mars by *Määttänen et al.* (2005). Some of the refinements can also be introduced into other radiative transfer schemes of Martian atmospheric models, and even for those of the Earth.

Although thin fog, ice clouds and CO_2 clouds have been observed on Mars, they are not included in the comparisons at this stage. The next feature to be included could be ice clouds and fog at the surface. Another addition that is certainly needed in the reference conditions of the intercomparison campaign is the temperature discontinuity between the surface and the air just above the surface.

Nighttime and daytime conditions have already been added in the SRM calculations, and they will be introduced shortly in the public set of reference conditions. Also, we should add into the set of reference conditions more variation in water vapor contents to include dry, semi-dry and wet cases.

Enhancing the current knowledge of the Martian atmospheric processes as well as interpretation of the data flow from the recent and ongoing Mars missions re-

quires extensive modeling activity to support the investigations and conclusions drawn from the observations. Our work demonstrates that radiative processes play a key role in this task, and underline the importance of accurate radiative parameterization schemes in the Martian atmospheric models. This is also well understood by the international Martian atmospheric modeling community that has participated in our ongoing intercomparison.

Chapter 6

Concluding remarks

6.1 Summary and conclusions

Planetary atmospheres moderate the environmental conditions at the planetary surface, transport material, and also shelter the surface of the planets against electromagnetic and particle radiation coming from space. In the case of the Earth, the atmosphere also harbors life. Investigating planetary atmospheres is crucial in our pursuit of enhancing our understanding of the planets.

In situ observations of planetary atmospheres are essential means in the investigations of planetary bodies. However, complementary atmospheric observations from an orbit around the planet, and even remote observations from the Earth, performed simultaneously with in situ observations always increase the scientific return of *in situ* observations.

The performance of the miniaturized atmospheric instrumentation systems developed by the FMI team for various Martian missions seems to be adequate to discover new features of the Martian atmosphere and to meet the scientific challenges posed by the mission requirements. This is indicated in Chapter 4 and in Papers 3, 1, 5 and 4.

The excellent quality of the instrumentation was highlighted by the PPI instrument onboard Cassini/Huygens, and by the MET-P device in the Mars Polar Lander (4). The MET-P device provided high-quality data at the health check measurement periods during the interplanetary cruise phase to Mars, and thus demonstrated its performance (Chapter 4).The data were analyzed on the Earth and the device was found to operate as expected.

The performance of the Pressure Profile Instrument (PPI) instrument developed by the FMI team for the Huygens Mission to Saturn's moon Titan enabled discovering various new features of the Titan atmosphere. This is discussed in Chapter 4 and in Papers 2, 7 and by *Lebreton* (2005). The measurement system included three sensor sections optimized for three different pressure ranges. Extensive aerodynamic simulations demonstrated that instead of static pressure the total pressure should be measured. The free flow static pressure is then calculated from the observed total pressure readings. To make the PPI instrument insensitive to the varying inclination angle between the total pressure probe

and the flow field, an optimized Kiel -probe was designed to surround the total pressure probe. These design solutions were supported by wind tunnel test results and by numerical simulations as indicated in Chapter 4.7 and Paper 2. The final outcome of the PPI was excellent as described by *Fulchignoni et al.* (2005). The first PPI results provided a slight correction to the known pressure profile of the Titan atmosphere as presented in Chapter 4.

To enhance our understanding on the Martian atmosphere, we proposed and managed the development work of two new scientific planetary missions, the NetLander Mission and the MetNet Mission. The NetLander Mission, which ultimately was abandoned after four years of hard development work, was a general geophysical mission to deploy four landing vehicles on the Martian surface. The mission organization included all major space agencies and planetary research institutes from more than ten different countries. Each lander was to carry an extensive atmospheric science payload as presented in Papers 1 and 5.

We initiated and specified the MetNet Mission making use of a new type of platform for Mars, which encompassed a scientific payload optimized for Martian atmospheric investigations. The mission is currently being developed under our management and is preparing for a precursor mission to Mars as depicted in Chapter 4.6.

Radiative transfer plays a key role in the behavior of the Martian atmosphere. The radiative short wave parameterization scheme for the UH Mars mesoscale model was improved as described in Paper 9. The improved parameterization adopted worked nicely when modeling the atmospheric conditions at the Mars Pathfinder site in Paper 8. That modification was the first step in the intercomparison campaign to improve radiative parameterization schemes of Martian atmospheric models using accurate line-by-line calculations as a reference frame (Chapter 5.3 and Paper 9).

Investigations of the Martian atmospheric boundary layer require proper instrumentation for the characterization of the dust aloft in the atmosphere. The significance of dust to radiative parameterization schemes and then to the atmospheric behavior and climate was clearly demonstrated by the model runs presented in Papers 9 and 8 comparing the *in situ* observations of the Mars Pathfinder with numerical simulation results.

We simulated the atmospheric conditions at the Mars Pathfinder (MPF) landing site with our vertical high-resolution Martian atmospheric boundary layer (ABL) model (Paper 8). We compared our results with MPF sol 3 observations, including the latest wind speed estimates. The wind and atmospheric temperature observations of MPF show distinctive variability due to convective turbulence during daytime, when there apparently is a strong superadiabatic temperature gradient near the surface. The night-time wind and temperature measurements indicate relatively steady atmospheric conditions with a reversed inversion-type temperature gradient. Our model simulates these features and all the observed magnitudes well except that the strongest low-level temperature gradients given by the model are smaller than the observations (Paper 8). The principal atmospheric heating mechanism near the ground appears to be direct ground-emitted thermal radiation absorbed by the principal atmospheric constituents CO_2, water vapor and dust. Turbulence has a reverse role of cooling the near-surface atmosphere (the lowest 100 m). This seems to be the case at all

times except just after sunrise, when turbulence mixing is at a minimum and the surface is only slightly warmer than the atmosphere next to the surface. This interesting feature can be explained by the low surface pressure of the Martian atmosphere (Paper 8).

We initiated an intercomparison campaign, where we called for Martian atmospheric modeling groups to participate in our radiative parameterization scheme comparison effort. As a result five different modeling groups joined our campaign including the three leading Martian global circulation modeling groups. The atmospheric conditions introduced as reference cases of this investigation utilized the diurnally and globally averaged thermal structure based on data from Mariner 9 IRIS observations acquired during late southern summer ($L_s = 340 - 350°$), as described in Paper 9. We performed the least-compromise line-by-line calculations using radiative transfer algorithms that had been developed for investigations of the atmospheres of Mars, Venus and Neptune (*Crisp*, 1986; *Meadows and Crisp*, 1996). Modifications correcting the parameterization were already made by some of the modeling teams participating in the campaign. The need for these corrections was very likely attributable to differences in dust optical properties, which still requires further analyses, which, together with the intercomparison campaign, are currently going on.

A starting point and a common thread behind the planetary missions forming the frame of this work is the sensor technology we have developed for various space missions (Papers 1, 2 and 3). The sensor systems are based on the meteorological sensors of the Vaisala Inc. We performed environmental and functional testing for a few sensor manufacturing lots. After successful qualification test results we screened out the individual sensor heads to take out any non-suitable ones, as indicated, *e.g.* in Paper 4 and Chapter 3.5. This process resulted in the conclusion that the procured manufacturing lots of Vaisala Barocap®, Thermocap® and Humicap® sensors were qualified for the requirements of the semi-hard landing Mars-96 mission, as well as qualified for the Martian surface environmental conditions.

Our experience clearly shows that it is advantageous to make use of sensor components procured in large manufacturing lots and perform the qualification and screening tests for the procured lots. By this approach, with a relatively low original procurement price per sensor we obtained a large number of excellent sensors as a result of our own test procedures. We got a large number of qualified sensor components that we also knew very well. We understood the performance of each sensor head after having tested and monitored them for many years. This was demonstrated by the sensor instruments we have provided for various missions (Chapter 4). The investment in the sensors performance monitoring was modest compared to the vast enhancement of our knowledge on the sensors, which resulted in improved performance and higher science return.

In situ observations of atmospheric parameters at the Martian surface are critical in our understanding of the local as well as global atmospheric behavior. Surface momentum and heat fluxes on the Martian surface, as well as the surface-to-atmosphere exchange processes in general, play significant roles in the development of the atmospheric boundary layer. Hence long-term observations at varying types of terrain occurring at regular intervals are needed to get even a rough understanding of the atmospheric behavior. This was also underlined

by the analysis in Chapter 5 and by the model runs in Papers 8 and 9.

In addition to the atmospheric science as such, atmospheric in situ observations are currently also needed for other types of exploration of any planetary body. Atmospheric observations significantly enhance the science return of practically all planetary missions. This was clearly demonstrated in the course of the planetary missions that form the basis of this work.

Atmospheric science and knowledge of the climate are also indispensable for the safety and success of planetary science missions with any type of landing components. The main thing is the landing process itself, which can be seriously jeopardized by the local weather conditions at the landing site. Recent studies have demonstrated that surface winds stronger than 25 m/s can take place on some Martian sites like Valles Marineris (*Toigo and Richardson*, 2003) that actually would be of utmost interest for geophysical and geochemistry sciences. In particular, for possible planetary manned missions the landing safety is obviously a primary issue.

Knowledge of weather and climate of the planetary body to be explored is also needed when defining the mission scientific objectives and operations. Transport of planetary material and erosion processes are significant issues when assessing the optimal payload complex, landing site and operations scenario for any type of planetary mission. Hence each planetary exploration probe should carry onboard an extensive *in situ* atmospheric science payload to enhance our knowledge on the planetary atmospheres and to assist any other scientific planetary investigations.

At present the terrestrial atmospheres are quite well characterized in general terms. This does not, however, mean that we understand their behavior and evolution to a sufficient degree. A multitude of reasons for additional planetary atmospheric investigations remains ranging from pure scientific curiosity to far-reaching questions on general comparative planetology, planetary climate change, as well as the search for life. The pursuit of planetary atmospheric exploration is well justified and is in near future likely to bring up epoch-making scientific findings.

6.2 Future aspects and related discussion

During the past decade planetary exploration has been focused on Mars, even though missions to other planets have also been performed and initiated. It is likely that Mars missions will continue to have a central role for many years to come. NASA's Mars Exploration program extending beyond 2010 includes two launches to Mars in every launch window opening at 26-month intervals. ESA has the successful Mars Express mission in place orbiting Mars and has got plans for the ExoMars mission slated for launch in the timeframe of 2009 to 2011. An extremely interesting possible future mission is the Finnish-Russian joint MetNet mission to deploy a meteorological observation network on the Martian surface. The MetNet mission is at present heading toward a test launch, and additional partners to join the effort are being sought. In addition, Russia and Japan have their own Mars exploration plans. The ongoing planetary exploration programs also include various new *in situ* surface missions.

Planetary exploration requires significant resources in terms of manpower, relatively expensive gadgetry and also state-of-the-art mission technology. Therefore it is obvious that collaboration is the means for small organizations to contribute in the field of planetary exploration. This fact manifests itself nicely when looking at the latest planetary missions, *e.g.* Mars Odyssey, Mars Express, MER Rovers and Cassini/Huygens. As a good example of the power of collaboration, the Finnish Meteorological Institute (FMI) has also been successful in participating in various planetary missions, where its participation has been adapted with the available resources. This is demonstrated by FMI's share in the Mars-96 and Netlander Missions, Cassini/Huygens, Mars Polar Lander (MPL), the MetNet Mars Mission and Mars Express. Accordingly, collaboration provides small organizations with the means to utilize their own resources in a highly productive fashion.

FMI has developed small scale contributions for the Mars Polar Lander (MPL), Cassini/Huygens and Mars Express Missions, as well as been part of the initiation process of other planetary missions (Mars-96, NetLander, Mars MetNet) giving large scale system level contributions (e.g. CDMS) to those missions. The failure of the Mars-96 Mission showed also the dark side of investing a good portion of the available resources in a single misssion. On the other hand, being responsible for major systems for the Mars-96 and NetLander Missions served also as a forced learning experience making the FMI organization to grow up to and meet the challenges posed by complex international space programs. This experience also indirectly helps to surmount the less complex difficulties encountered in any type of smaller scale contribution to a scientific space mission.

Based on the planetary projects and missions utilized in this work (Papers 1-8) it can be stated that to maximize the science return a small organization like FMI should rather distribute its resources in small contributions to various missions than to invest everything in one large participation in one or a few missions. This would mitigate the risks of mission and instrument failures affecting the science return of a small organization's investment. On the other hand, if a science organization wants to get a profound view of the mission development processes and in particular how to make the scientific objectives prevail in the mission planning sequence, the only way is to make sizeable system level contributions to individual missions. By now FMI has operated in such a way with excellent results.

For planetary atmospheric science mission it would be of utmost benefit in terms of saving system resources to make the mission without a special heating and thermal insulation system for the payload. When compared with a general geophysical planetary in situ payload the atmospheric science payload requires much less energy, data bandwidth, mass and volume, and the peak power requirements are lower. Hence the mission could be accomplished without a chemical battery, which is the main subsystem requiring heating. The battery can be replaced by the state-of-the-art capacitors capable of buffering sufficient amount of energy for peak power functions during the short data transmission periods.

The benefits of manned missions to other planets of our solar system have been under discussion in the space exploration community for decades. When as-

sessing all the scientific, technological, and political objectives behind space exploration it is extremely difficult to find a clear answer. When the resources needed for a manned mission are summoned up one could draw the conclusion that the scientific outcome does not support manned missions. Current estimates suggest that with the cost of a manned mission to Mars up to 1000 robotic missions like Mars Pathfinder could be implemented. A global network science mission like the NetLander Mission, or MetNet Mission focusing on the atmospheric science, would totally explode our knowledge of the Martian atmosphere. For the science, one manned mission to Mars could not do very much more than a few robotic missions could do. With planets further away than Mars this relation would be even more disadvantageous for manned missions.

Accordingly, exploration of planetary atmospheres can be accomplished more economically by robotic missions than by manned missions. With improved technology this gap may even be wider. On the other hand, the political and technological ambitions behind manned missions may result in increased budgets also for space exploration in general. In that case, science community certainly would also advocate manned missions.

When looking even further into the future, it is possible to envisage a concept of a multitude of very small landing vehicles serving as atmospheric observation posts distributed all over a planetary surface (*e.g.* the MetNet Mission). This high density network of atmospheric observations would be complemented by multiple small rovers and crawlers carrying out scientific measurements, and using some stationary vehicle as a source of energy and data bandwidth. The moving vehicles would also drill holes in the ground to take soil samples for analysis. Payload platforms would also move aloft in the atmosphere by using, *e.g.*, free flying balloons, aircraft or gliders, tethered balloons to extend the *in situ* investigations of the atmosphere up to the top of and even beyond the boundary layer. Some roaming devices could collect samples of the Martian deep soil, surface and atmosphere in sealed containers and place the containers in some specific locations, where the samples would be retrieved by sample return missions.

The new Mars landers are very likely to have mobility, or carry small rovers onboard. The Mars Pathfinder already had one. A combination of a lander and a small rover working in the neighborhood of the stationary lander would be very practical from general geophysical investigations point of view. The concept of the rover using the lander as a service center for energy, computation power, data transmission capability is also a highly attractive scenario.

Mars, Titan, Venus and the Earth have a lot in common. By studying the present state of the planets we may be able to infer the past, and thus may be able to better understand the past or predict the future of the Earth. The chain of planetary exploration will receive additional links in years to come. Inspiring technical inventions and scientific discoveries will be made. From the planetary science point of view this is highly rewarding, and it may also prove to be of utmost importance to our understanding of the Earth and its future.

Acronyms

ABL Atmospheric Boundary Layer

APTIV Pressure device for the upper part of the Venusian atmosphere in the proposed Lavoisier balloon flotilla mission to Venus

ATMIS Atmospheric Structure and Meteorology Instrument System - the atmospheric science part of the NetLander payload

AU Astronomical Unit. Mean distance between Earth and Sun.

BAROBIT Pressure measurement device onboard the Beagle 2 lander of the Mars Express mission

CNES Centre National d'Etudes Spatiales. The French space agency.

DART A computer program utilizing the DISORT algorithm to generate altitude- and angle-dependent spectral solar radiances as a solution to the radiative transfer equation

DISORT A multi-level, multi-stream, discrete ordinate algorithm for solving the radiative transfer equation (*Stamnes et al.*, 1988)

ESA European Space Agency

EGA-P Housekeeping pressure device of the EGA instrument onboard the Mars polar Lander

FMI/GEO Finnish Meteorological Institute/Geophysical Research Division

FMI Finnish Meteorological Institute

GC General Circulation

GCM General Circulation Model

GEO Geophysical Research Division

HIRLAM High Resolution Limited Area Model. The Nordic/Dutch/Spanish operational high-resolution weather forecasting model.

HUT Helsinki University of Technology

IMEWG International Mars Exploration Working Group

IR InfraRed.

LIDAR Light Detection And Ranging

MET-P Pressure device of the MVACS payload onboard the Mars Polar Lander that arrived at Mars in December 1999, but failed to land safely.

MGCM Mars General Circulation Model

MGS Mars Global Surveyor. First spacecraft in the NASA Mars Surveyor programme.

MMCM Mars Mesoscale Circulation Model

MOLA Mars Orbiter Laser Altimeter. A LIDAR instrument onboard MGS to determine accurately the Martian topography (*Zuber et al.*, 1992).

MPL Mars Polar Lander. A Mars Surveyor programme mission due to land in the southern polar region in December 1999. Payload includes the Mars Volatiles and Climate Surveyor payload onboard the Mars Polar Lander (MVACS) and an upward-looking Light Detection And Ranging (LIDAR).

MVACS Mars Volatiles and Climate Surveyor payload onboard the Mars Polar Lander

NASA National Aeronautics and Space Administration

PBL Planetary Boundary Layer

PPI Pressure Profile Instrument onboard the Huygens/Cassini probe for Titan

SMART Performs the same tasks as the DART program, but SMART employs high-resolution spectral mapping methods to decrease the required computational resources

TDL Tunable Diode Laser. An atmospheric composition instrument using laser sounding techniques.

UH University of Helsinki

VL Viking Lander

VO Viking Orbiter

Bibliography

Andrews, D. G., *Introduction to Atmospheric Physics*, Campridge University Press, 2000.

Barnes, J. R., J. B. Pollack, R. M. Haberle, C. B. Leovy, R. W. Zurek, H. Lee, and J. Schaeffer, Mars atmospheric dynamics as simulated by the NASA Ames General Circulation Model, 2, transient baroclinic eddies, *J. Geophys. Res.*, *98*, 3125–3148, 1993.

Bell, J. F., III, W. M. Calvin, M. E. Ockert-Bell, D. Crisp, J. B. Pollack, and J. Spencer, Detection and monitoring of H_2O and CO_2 ice clouds on Mars, *J. Geophys. Res.*, *101*, 9227–9237, 1996.

Bell, J. F. I., M. J. Wolff, T. C. Daley, D. Crisp, P. B. James, S. W. Lee, J. T. Trauger, and R. W. Evans, Near-infrared imaging of Mars from HST: surface reflectance, photometric properties, and implications for MOLA data, *Icarus*, *138*, 25–35, 1999.

Bird, M. e. a., First results from the Huygens Doppler Wind Experiment., *Science*, 2005.

Chamberlain, T. E., H. L. Cole, R. G. Dutton, G. C. Greene, and J. E. Tillman, Atmospheric measurements on Mars: the Viking meteorology experiment, *Bull. Amer. Meteor. Soc.*, *57*, 1094–1104, 1976.

Chassefiere, E., et al., The Lavoisier mission : A system of descent probe and balloon flotilla for geochemical investigation of the deep atmosphere and surface of Venus, *Adv. Space Res.*, *29*, 255–264, 2002.

Chicarro, A. F., et al., Marsnet phase-A study report, *Tech. Rep. SCI(93)2*, European Space Agency, 1993.

Christensen, P. R., et al., Mars Exploration Rover candidate landing sites as viewed by THEMIS, *Icarus*, *176*, 12–43, 2005.

Clarke, R. H., and G. D. Hess, On the appropriate scaling for velocity and temperature in the planetary boundary lauyer, *J. Atmos. Sci.*, *30*, 1346–1353, 1973.

Clifford, S. M., et al., The state and future of Mars polar science and exploration, *Icarus*, *144*, 210–242, 2000.

Colaprete, A., R. M. Haberle, and O. B. Toon, Formation of convective carbon dioxide clouds near the south pole of Mars, *J. Geophys. Res.*, *108*, 17–1–17–19, 2003.

Conrath, B. J., Thermal structure of the martian atmosphere during the dissipation of the dust storm of 1971, *Icarus*, *24*, 36–46, 1975.

Crisp, D., Radiative forcing of the Venus mesosphere i: Solar fluxes and heating

rates, *Icarus*, *67*, 484–514, 1986.

Crisp, D., Infrared Radiative Trasfer in the Dust-Free Martian Atmosphere, *J. Geoph. Res.*, *95*, 14,577–14,588, 1990.

Crisp, D., S. Fels, and M. D. Schwarxkopf, Approximate Methods for Finding CO_2 15μm Band Transmission in Planetary Atmospheres, *J. Geoph. Res.*, *91*, 11,851–11,866, 1986.

Ellingson, R. G., and Y. Fouquart, The intercomparison of radiation codes in climate models - an overview, *J. Geophys. Res.*, *96*, 8925–8927, 1991.

Ellingson, R. G., J. Ellis, and S. Fels, The intercomparison of radiation codes used in climate models, long wave results, *J. Geophys. Res.*, *96 (D5)*, 8929–8853, 1991.

ESA, ESA Press releases in 2004 to 2005, *ESA Public Outreach System*, 2005.

Ferri, F., P. H. Smith, M. Lemmon, and N. O. Rennó, Dust devils as observed by Mars Pathfinder, *Journal of Geophysical Research (Planets)*, pp. 7–1, 2003.

Ferri, F., M. Fulchignoni, G. Colombatti, J. C. Zarnecki, A. Harri, A. Coustenis, B. Sicardy, and R. Yelle, Huygens ASI Measurements At Titan: A New Insight Of Titan's Atmosphere, *AGU Spring Meeting Abstracts*, pp. A5+, 2005.

Fisher, J. A., M. I. Richardson, C. E. Newman, M. A. Szwast, C. Graf, S. Basu, S. P. Ewald, A. D. Toigo, and R. J. Wilson, A survey of Martian dust devil activity using Mars Global Surveyor Mars Orbiter Camera images, *Journal of Geophysical Research (Planets)*, *110*, 3004–+, 2005.

Flasar, F. M., et al., Titan's Atmospheric Temperatures, Winds, and Composition, *Science*, *308*, 975–978, 2005.

Formisano, V., D. Grassi, N. I. Ignatiev, and L. Zasova, IRIS Mariner 9 data revisited: water and dust daily cycles, *Planetary and Space Science*, *49*, 1331–1346, 2001.

Formisano, V., S. Atreya, T. Encrenaz, N. Ignatiev, and M. Giuranna, Detection of Methane in the Atmosphere of Mars, *Science*, *306*, 1758–1761, 2004.

Fulchignoni, M., et al., The Characterisation of Titan's Atmospheric Physical Properties by the Huygens Atmospheric Structure Instrument (Hasi), *Space Sci. Rev,*, *104*, 397–434, 2002.

Fulchignoni, M., et al., A stratospheric balloon experiment to test the Huygens atmospheric structure instrument (HASI), *Planet. Space Sci*, *52*, 867–880, 2004.

Fulchignoni, M., et al., Titan's Physical Characteristics Measured by the Huygens Atmospheric Structure Instrument (HASI), *Nature*, 2005.

Garratt, J. R., *The Atmospheric Boundary Layer*, Campridge University Press, 1992.

Golombek, M. P., et al., Overview of the Mars Pathfinder Mission: Launch through landing, surface operations, data sets, and science results, *Journal of Geophysical Research*, *104*, 8523–8554, 1999.

Grant, J. A., M. P. Golombek, T. J. Parker, J. A. Crisp, S. W. Squyres, and C. M. Weitz, Selecting landing sites for the 2003 Mars Exploration Rovers, *Planet. Space Sci.*, *52*, 11–21, 2004.

Haberle, R. M., Early Mars climate models, *J. Geophys. Res.*, *103*, 28,467–

28,479, 1998.

Haberle, R. M., and D. C. Catling, A Micro-Meteorological mission for global network science on Mars: rationale and measurement requirements, *Planet. Space Sci.*, *44*, 1361–1383, 1996.

Haberle, R. M., and H. C. Houben, Mars boundary layer simulations: comparison with viking lander and entry observation, in *The Environmental Model of Mars*, pp. 3–6, 1991.

Haberle, R. M., D. Tyler, C. P. McKay, and W. L. Davis, A model for the evolution of CO_2 on Mars, *Icarus*, *109*, 102–120, 1994.

Harri, A.-M., The atmosphere and ionosphere of Mars: a review of the NetLander payload contribution, in *Proceedings of the 2nd NetLander scientific workshop*, p. 13, Laboratoire de Planétologie et Géodynamique Nantes, Université de Nantes, Faculté des Sciences, 2 rue de la Houssinière, 44322 Nantes cedex 3, France, 2001, invited talk.

Harri, A.-M., S. Korpela, K. Kumpulainen, I. Liede, R. Pellinen, and T. Siili, Metegg Surface Station Phase A-2 study report, *Feasibility study*, Finnish Meteorological Institute, 1988.

Harri, A.-M., A. Lehto, K. Lappalainen, P. Salminen, and R. PIrjola, Qualification test report, METEGG sensor candidates in Martian environment, *Test report*, Finnish Meteorological Institute, 1993.

Harri, A.-M., T. Siili, V. Linkin, A. Lipatov, and D. Nenarokov, The Mars-96 small station meteopackage and its observations, *Bull. Amer. Astron. Soc.*, *28*, 1068, 1996, 28th annual DPS/AAS meeting 1996-10-23. . . 26. Poster presentation.

Harri, A.-M., J. Polkko, T. Siili, and D. Crisp, Accurate pressure observations in the Martian southern polar region: MVACS /MET-P, *Bulletin of the American Astronomical Society*, *29*, 970–+, 1997.

Harri, A.-M., A. Lehto, G. Leppelmeier, S. Merikallio, P. Riihelä, W. Schmidt, and T. Siili, NetLander 2005 lander network to Mars, *Final report, ESA/ESTEC contract study 12722/98/NL/JG*, Finnish Meteorological Institute, 1999a.

Harri, A.-M., D. Crisp, and S. Gavit, Exploring Mars by landing vehicles, in *Towards Mars!*, pp. 201–215, Raud Publishing, 2000.

Harri, A.-M., J. Polkko, S. Calcutt, D. Crisp, S. Larsen, T. Siili, and J.-P. Pommereau, ATMIS experiment — overview and current instrument design status, in *Proceedings of the workshop on Mars atmosphere modelling and observations*, edited by M. C. Desjean, F. Forget, M. Lopez-Valverde, and C. Newman, pp. 16–1, Centre national d'etudes spatiales, European Space Agency, Instituto de astrofisica de Andalucia, Laboratoire de meteorologie dynamique / Centre national de recherches scientifiques, University of Oxford, 2003a.

Harri, A.-M., et al., Network science landers for Mars, *Adv. Space Res.*, *23*, 1915–1924, 1999b.

Harri, A.-M., et al., Atmospheric science experiment for Mars – ATMIS for the NetLander 2005 mission, in *The 5th international conference on Mars, Pasadena, CA, USA, 1999-07-18. . . 23*, no. 6074 in LPI Contributions, Lunar and Planetary Institute, Houston, TX, USA, 1999c, poster presentation.

Harri, A.-M., et al., Metnet — the next generation lander for Martian atmospheric science, in *Proceedings of the 54th International Astronautical Congress*, IAC-03-Q.3.b.09, 2003b.

Harri, A.-M., et al., MetNet — a new kind of Martian atmospheric science network, in *International Mars Conference, Ischia, Italy, 19-23 Sept,*, 2004a.

Harri, A.-M., et al., Mars atmospheric science network — METNET, in *Proceedings of the 55th International Astronautical Conference*, IAC-04-IAA.3.7.2.02, 2004b.

Hess, G. D., On Rossby-number similarity theory fo a baroclinic planetary boundary layer, *J. Atmos. Sci.*, *30*, 1722–1723, 1973.

Hess, S. L., R. M. Henry, J. Kuettner, C. B. Leovy, and J. A. Ryan, Meteorology experiments: the Viking Mars Lander, *Icarus*, *16*, 196–204, 1972.

Hess, S. L., R. M. Henry, C. B. Leovy, J. A. Ryan, and J. E. Tillman, Meteorological results from the surface of Mars: Viking 1 and 2, *J. Geophys. Res.*, *82*, 4559–4574, 1977.

Hess, S. L., R. M. Henry, and J. E. Tillman, The seasonal variation of atmospheric pressure on Mars as affected by the South polar cap, *J. Geophys. Res.*, *84*, 2923–2927, 1979.

Higuchi, K., Formation of Frost Layer of Water Ice on Mars, *Icarus*, *154*, 181–182, 2001.

Hoffren, J., T. Siikonen, and P. Kaurinkoski, Navier-Stokes Calculations for the Total Pressure Probe of the Huygens Spacecraft, *Tech. Rep. T-50*, Helsinki University of Technology, Laboratory of Aerodynamics, 1992.

Holton, J. R., *An introduction to dynamic meteorology*, International geophysics series, San Diego, New York: Academic Press, —c1992, 3rd ed., 1992.

Houghton, J. T., *The physics of atmospheres*, 3rd ed. Cambridge University Press, 2002 xv, 320 p. ISBN #0521011221, 2002.

Hunten, D. M., L. Colin, T. M. Donahue, and V. I. E. Moroz, *Venus*, Univ. of Arizona press, Tucson, Arizona, 1983.

Jenkins, J. M., Radio Occultation Studies of Venus' Atmosphere with Magellan, NASA/CR-1998-208215; NAS 1.26:208215, *Tech. rep.*, 1998.

Kallio, E., I. Sillanpää, and P. Janhunen, Titan in subsonic and supersonic flow, *Geophysics Review Letters*, *31*, 15,703–+, 2004.

Kasting, J. F., Greenhouse Models of Early Mars Climate, *AGU Fall Meeting Abstracts*, pp. B345+, 2002.

Kieffer, H. H. e., *Mars*, Univ. of Arizona press, Tucson, Arizona, 1992.

Kivekäs, J., Measurement Accuracies and Mach Number Reconstruction, *Tech. Rep. T-56*, Helsinki University of Technology, Laboratory of Aerodynamics, 1992.

Korpela, S., A.-M. Harri, I. Liede, R. Pellinen, and K. Kumpulainen, Metegg Surface Station Phase A-1 study report, *Feasibility study*, Finnish Meteorological Institute, 1988.

Koukouli, M. E., P. G. J. Irwin, and F. W. Taylor, Water vapor abundance in Venus' middle atmosphere from Pioneer Venus OIR and Venera 15 FTS measurements, *Icarus*, *173*, 84–99, 2005.

Laine, S., T. Siikonen, B. Fagerström, and E. Salminen, Pressure Measurement

of Titan's Atmosphere on the Huygens Probe, *Tech. Rep. T-36*, Helsinki University of Technology, Laboratory of Aerodynamics, 1991.

Larsen, S. E., H. E. Jørgensen, L. Landberg, and J. E. Tillman, Aspects of the atmospheric surface layers on Mars and Earth, *Boundary-Layer Meteorol.*, *105*, 451–470, 2002.

Lebreton, J.-P., Huygens Descent and Landing on Titan: Mission Overview and Science highlights, *Science*, 2005.

Lebreton, J.-P., and D. Matson, The Huygens probe: science, payload and mission overview. Space, *Space Sci. Rev.*, *104*, 59–100, 2002.

Ledvina, S. A., J. G. Luhmann, S. H. Brecht, and T. E. Cravens, Titan's induced magnetosphere, *Advances in Space Research*, *33*, 2092–2102, 2004.

Lindal, G., The atmosphere of Titan - an analysis of the Voyager-1 radio occultation measurements., *Icarus*, *53*, 348–363, 1983.

Liou, K. N., *Radiation and Cloud Processes in the Atmosphere*, 1992.

Lodders, K., and B. Fegley, *The Planetary Scientist's Companion*, Oxford University Press, 1998.

Maattanen, A., and H. Savijarvi, PBL simulations on Mars, *Bulletin of the American Astronomical Society*, *34*, 864–+, 2002.

Mäkinen, T., Processing the HASI measurements, *Adv. Space Res.*, *17*, 217–222, 1996.

Marsal, O., A.-M. Harri, P. Lognonne, and K.-H. Glassmeier, NetLander for Mars Express, *Proposal submitted for ESA as a response of the Mars Express Announcement of Opportunity*, Finnish Meteorological Institute, 1998.

Marsal, O., A.-M. Harri, P. Lognonné, F. Rocard, and J.-L. Counil, Netlander: the first scientific lander network on the surface of Mars, in *Proceedings of the 50th International Astronautical Congress*, IAF-99-Q.3.03, International Astronautical Federation, 1999.

Matson, D., J.-P. Lebreton, and L. Spilker, The Cassini/Huygens Mission: An Overview and Relevant Laboratory Research, *Bulletin of the American Astronomical Society*, *34*, 910–+, 2002.

Meadows, V., and D. Crisp, Ground-based near-infrared observations of the Venus night side: The thermal structure and water abundance near the surface, *J. Geophys. Res.*, *101*, 4595–4622, 1996.

Murphy, J. R., Understanding the Martian dust cycle, *Adv. Space Res.*, *19*, 1289–1290, 1996.

Murphy, J. R., C. B. Leovy, and J. E. Tillman, Observations of Martian surface winds at the Viking Lander 1 site, *J. Geophys. Res.*, *95*, 14,555–14,576, 1990.

Murphy, J. R., S. Larsen, H. Joergensen, and J. T. Schofield, Derivation and analyses of martian surface winds from Mars Pathfinder, *Bull. Amer. Astron. Soc.*, *34*, 863, 2002, poster presentation in the 34th AAS/DPS Meeting.

Määttänen, A., H. Vehkamäki, A. Lauri, S. Merikallio, J. Kauhanen, H. Savijärvi, and M. Kulmala, Nucleation studies in the Martian atmosphere, *J. Geophys. Res.*, *110*, 2005.

Newman, S. M., and J. P. Taylor, Impact of updates to the HITRAN spectroscopic database on the modeling of clear-sky infrared radiances, *Geophysics Review Letters*, *29*, 18–1, 2002.

Ockert-Bell, M., J. I. Bell, J. Pollack, C. McKay, and F. Forget, Absorption and scattering properties of the martian dust in the solar wavelengths, *J. Geophys. Res.*, *102*, 9039–9050, 1998.

Paige, D. A., et al., Mars Volatiles and Climate Surveyor (MVACS) Integrated Payload for the Mars Polar Lander Mission, *LPI Contributions*, *953*, 30–+, 1998.

Paukkunen, A., and H. Turtiainen, METEGG sensor tests at CNES/ INTESPACE - data evaluation support, *Internal test report*, Vaisala Ltd., 1989.

Pichkhadze, K., and V. Linkin, E-8 design documentation for selected concept, *Tech. rep.*, Finnish Meteorological Institute, 2002a.

Pichkhadze, K., and V. Linkin, D-8 models STM and EM manufacturing, *Tech. rep.*, Finnish Meteorological Institute, 2002b.

Pichkhadze, K., and V. Linkin, E-12 manufacturing of small (mini) landing station experimental models and test plan, *Tech. rep.*, Finnish Meteorological Institute, 2003.

Pichkhadze, K., and V. e. Linkin, E-4 concept - a description, *Tech. rep.*, Finnish Meteorological Institute, 2002c.

Pichkhadze, K., V. Linkin, and et.al., E-5 concept - b description, *Tech. rep.*, Finnish Meteorological Institute, 2002.

Porco, C. C., et al., Imaging of Titan from the Cassini spacecraft, *Nature*, *434*, 159–168, 2005.

Pullan, D., M. R. Sims, I. P. Wright, C. T. Pillinger, and R. Trautner, *Beagle 2: the exobiological lander of Mars Express*, pp. 165–204, ESA SP-1240: Mars Express: the Scientific Payload, 2004.

Renko, K., P. Kere, and B. Fagerström, Wind Tunnel Tests of the Two Kiel Type Total Pressure Tubes, *Tech. Rep. T-55*, Helsinki University of Technology, Laboratory of Aerodynamics, 1992.

Rennó, N. O., A. A. Nash, J. Lunine, and J. Murphy, Martian and terrestrial dust devils: Test of a scaling theory using Pathfinder data, *Journal of Geophysical Research (Planets)*, *105*, 1859–1866, 2000.

Renno, N. O., et al., MATADOR 2002: A pilot field experiment on convective plumes and dust devils, *Journal of Geophysical Research (Planets)*, *109*, 7001–+, 2004.

Rieder, R., T. Economou, H. Wänke, A. Turkevich, J. Crisp, J. Brückner, G. Dreibus, and H. Y. McSween, Jr., The chemical composition of Martian soil and rocks returned by the mobile Alpha Proton X-ray Spectrometer: preliminary results from the X-ray mode, *Science*, *278*, 1771–1774, 1997.

Rogovskaya, V., A. Terterashvili, A. Polyakov, and V. Vorontsov, E-13 tests of small (mini) landing station experimental models, *Tech. rep.*, Finnish Meteorological Institute, 2003.

Rothman, L. S., et al., The HITRAN Molecular Spectroscopic Database and HAWKS (HITRAN Atmospheric Workstation): 1996 Edition, *Journal of Quantitative Spectroscopy and Radiative Transfer*, *60*, 665–710, 1998.

Salby, M. L., *Fundamentals of Atmospheric Physics*, Academic Press, 1996.

Santee, M., and D. Crisp, Atmospheric and surface temperatures and airborne dust amounts during late southern summer from Mariner 9 IRIS data, in

Martian Surface and Atmosphere Through Time, pp. 128–129, 1992.

Santee, M., and D. Crisp, Thermal structure and dust loading of the Martian atmosphere during late southern summer - Mariner 9 revisited, *J. Geophys. Res.*, *98*, 3261–3279, 1993.

Santee, M., and D. Crisp, Diagnostic calculations of the circulation in the Martian atmosphere, *J. Geophys. Res.*, *100*, 5465–5484, 1995.

Savijärvi, H., Radiative fluxes on a dustfree Mars, *Contrib. Atmos. Phys.*, *64*, 103–112, 1991a.

Savijärvi, H., A model study of the PBL structure on Mars and the Earth, *Contrib. Atmos. Phys.*, *64*, 219–229, 1991b.

Savijärvi, H., Meteorology of the terrestrial planets, *Surv. Geophys.*, *15*, 755–773, 1994.

Savijärvi, H., Mars boundary layer modelling: diurnal moisture cycle and soil properties at the Viking Lander 1 site, *Icarus*, *117*, 120–127, 1995.

Savijärvi, H., A model study of the atmospheric boundary layer in the Mars Pathfinder lander conditions, *Q. J. R. Met. Soc.*, *125*, 483–493, 1999.

Savijärvi, H., D. Crisp, and A.-M. Harri, Intercomparison of radiation codes for Mars models, in *Abstracts, 8th Scientific Assembly of IAMAS*, p. 143, International Association of Meteorology and Atmospheric Sciences, 2001, oral presentation in Symposium 10, Planetary Atmospheres and their evolution.

Schofield, J. T., J. R. Barnes, D. Crisp, R. M. Haberle, S. Larsen, J. A. Magalhães, J. R. Murphy, A. Seiff, and G. Wilson, The Mars Pathfinder Atmospheric Structure Investigation/Meteorology (ASI/MET) experiment, *Science*, *278*, 1752–1758, 1997.

Seiff, A., Atmospheric winds indicated by motion of the Viking Landers during parachute descent, *J. Geophys. Res.*, *98*, 7461–7474, 1993.

Seiff, A., and D. B. Kirk, Structure of the atmosphere of Mars in summer at mid-latitude, *J. Geophys. Res.*, *82*, 4364–4388, 1977.

Seiff, A., et al., The atmosphere structure and meteorology instrument of the Mars Pathfinder lander, *J. Geophys. Res.*, *102*, 4045–4056, 1997.

Siikonen, T., A Three-Dimensional Multigrid Algorithm for the Euler and the Thin-Layer Navier-Stokes Equations, *Tech. Rep. A-12*, Helsinki University of Technology, Laboratory of Aerodynamics, 1991.

Siikonen, T., J. Hoffren, and S. Laine, A Multigrid LU Factorization Scheme for the Thin-Layer Navier-Stokes Equations, in *17th Congress of the International Council of the Aeronautical Sciences*, 1990.

Siili, T., Modeling of albedo and thermal inertia induced mesoscale circulations in the midlatitude summertime Martian atmosphere, *J. Geophys. Res.*, *101*, 14,957–14,968, 1996.

Siili, T., R. M. Haberle, and J. R. Murphy, Sensitivity of Martian southern polar cap edge winds and surface stresses to dust optical thickness and to the large-scale sublimation flow, *Adv. Space Res.*, *19*, 1241–1244, 1997.

Smith, P. H., et al., The MVACS Surface Stereo Imager on Mars Polar Lander, *Journal of Geohysics Review*, *106*, 17,589–17,608, 2001.

Smrekar, S. E., E. R. Stofan, S. A. Gavit, and G. E. Powell, New Millennium Deep Space Two: The Mars Microprobe Project, in *Lunar and Planetary*

Institute Conference Abstracts, pp. 1343–+, 1997.

Soffen, G. A., Scientific results of the Viking missions, *Science*, *194*, 1274–1276, 1976.

Soffen, G. A., and C. W. Snyder, The first Viking mission to Mars, *Science*, *193*, 759–766, 1976.

Squyres, S. W., The Mars environmental survey (MESUR) mission, *Advances in Space Research*, *15*, 179–, 1995.

Squyres, S. W., The Mars Exploration Rover Project, *AGU Fall Meeting Abstracts*, pp. A9+, 2001.

Stamnes, S., K., C. Tsay, W. Wiscombe, and K. Jayaweera, Numerically stable algorithm for discrete-ordinate-method radiative transfer in multiple scattering and emitting layered media, *Appl. Optics*, *27*, 2502–2509, 1988.

Stull, R. B., *An introduction to boundary layer meteorology*, Atmospheric Sciences Library, Dordrecht: Kluwer, 1988, 1988.

Sutton, J. L., C. B. Leovy, and J. E. Tillman, Diurnal variations of the Martian surface layer meteorological parameters during the first 45 sols at two Viking Lander sites, *J. Atmos. Sci.*, *35*, 2346–2355, 1978.

Svedhem, H., D. McCoy, D. Titov, J. Rodríguez-Canabal, and J. Fabrega, Venus Express Mission Scenario, in *COSPAR, Plenary Meeting*, pp. 1189–+, 2005.

Terterashvili, A., A. Polyakov, V. Vorontsov, A. Ivankov, V. Rogovscaya, and S. Ivankov, Report no.3: Cdr data package for the MML's operating model, *Tech. rep.*, Finnish Meteorological Institute, 2003.

Tillman, J. E., The indirect determination of stability, heat and momentum fluxes in the atmospheric boundary layer from simple scalar variables during dry unstable conditions, *J. Appl. Meteorol.*, *11*, 783–792, 1972.

Tillman, J. E., Marian meteorology annd dust stroms from Viking observations, *Am. Astron. Society/Sci. and Tech.*, *62*, 333–342, 1985.

Tillman, J. E., Mars global atmospheric oscillations: annually synchronized, transient normal-mode oscillations and the triggering of global dust storms, *J. Geophys. Res.*, *93*, 9433–9451, 1988.

Tillman, J. E., Martian annual pressure curve by Viking Landers, *Technical report*, Viking computer facility, Washington University, 1994.

Tillman, J. E., R. M. Henry, and S. L. Hess, Frontal systems during passage of the Martian North polar hood over the Viking Lander 2 site prior to the first 1977 dust storms, *J. Geophys. Res.*, *84*, 2947–2954, 1979.

Tillman, J. E., N. C. Johnson, P. Guttorp, and D. B. Percival, The Martian annual armospheric pressure cycle: years without great dust storms, *J. Geophys. Res.*, *98*, 10,963–10,971, 1993.

Tillman, J. E., L. Landberg, and S. E. Larsen, The boundary layer of Mars: Fluxes, stability, turbulent spectra, and growth of the mixed layer, *J. Atmos. Sci.*, *51*, 1709–1727, 1994.

Toigo, A. D., and M. I. Richardson, Meteorology of proposed Mars Exploration Rover landing sites, *Journal of Geophysical Research (Planets)*, pp. 33–1, 2003.

Tomasko, M. G., L. R. Doose, M. Lemmon, P. H. Smith, and E. Wegryn, Properties of dust in the martian atmosphere from the imager on mars pathfinder,

J.Geophys.Res., *104*, 8987–9008, 1999.

Towner, M. C., et al., The Beagle 2 environmental sensors: science goals and instrument description, *Planet. Space Sci.*, *52*, 1141–1156, 2004.

Tratt, D. M., M. H. Hecht, D. C. Catling, E. C. Samulon, and P. H. Smith, In situ measurement of dust devil dynamics: Toward a strategy for Mars, *Journal of Geophysical Research (Planets)*, pp. 2–1, 2003.

Yelle, R., D. Strobel, E. Lellouch, and D. Gautier, Engineering models for Titan's atmosphere, *Adv. Space Res.*, *ESA SP-1177*, 243–256, 1997.

Zarnecki, J. C., Titan's Atmospheric and Surface Environments as Measured by the Huygens Surface Science Package (SSP), *Science*, 2005.

Zuber, M. T., D. E. Smith, S. C. Solomon, D. O. Muhleman, J. W. Head, J. B. Garvin, J. B. Abshire, and J. L. Bufton, The Mars Observer Laser Altimeter investigation, *J. Geophys. Res.*, *97*, 7781–7798, 1992.

Zurek, R. W., J. R. Barnes, R. M. Haberle, J. B. Pollack, J. E. Tillman, and C. B. Leovy, Dynamics of the atmosphere of Mars, in *Mars*, edited by H. H. Kieffer, B. M. Jakosky, C. W. Snyder, and M. S. Matthews, pp. 835–934, University of Arizona Press, 1992.